1971

Mechanism of the photocycloaddition of stilbene to olefins

Richard Dean Lura
Iowa State University

Mechanism of the Photocycloaddition of Stilbene to Olefins

by

Richard Dean Lura

A Dissertation Submitted to the

Graduate Faculty in Partial Fulfillment of

The Requirements for the Degree of

DOCTOR OF PHILOSOPHY

Major Subject: Organic Chemistry

Approved:

Signature was redacted for privacy.

In Charge of Major Work

Signature was redacted for privacy.

Head of Major Department

Signature was redacted for privacy.

Dean of Graduate College

Iowa State University
Ames, Iowa
1971

TABLE OF CONTENTS

Page

LIST OF FIGURES

LIST OF TABLES

INTRODUCTION

Organic photochemistry can be divided into two classes, studies dealing primarily with product identification or development of synthetically valuable procedures and, the other dealing with the number and type of the reactive states of molecules and obtaining kinetic data for reaction mechanisms. The latter case, mechanistic organic photochemistry, has risen, in the past decade, to a highly sophisticated branch of chemistry.

Cyloaddition reactions have been the subject of much interest in the past years (see REVIEW OF LITERATURE). These studies have discovered several trends in cycloaddition reactions with respect to stereochemistry of addition, and mechanisms. The present study examines the addition of stilbene to olefins. trans-Stilbene has been the subject of numerous studies and the excited states of the molecule are well documented (see REVIEW OF LITERATURE). This thesis describes the mechanism of the addition of trans-stilbene to olefins, with respect to the mechanistic aspects.

REVIEW OF LITERATURE

Stereochemistry of Photocycloaddition Reactions

Photocycloaddition reactions have been the subject of numerous reviews (1 and references cited therein). Only certain aspects of stereochemistry will be discussed. Oxetane formation has been studied by many research groups. Yang et al., studied the reaction of benzaldehyde and 2-methyl-2-butene to form, among other products, oxetanes 2 and 3 (2,3). The mechanism was shown to involve the triplet state of

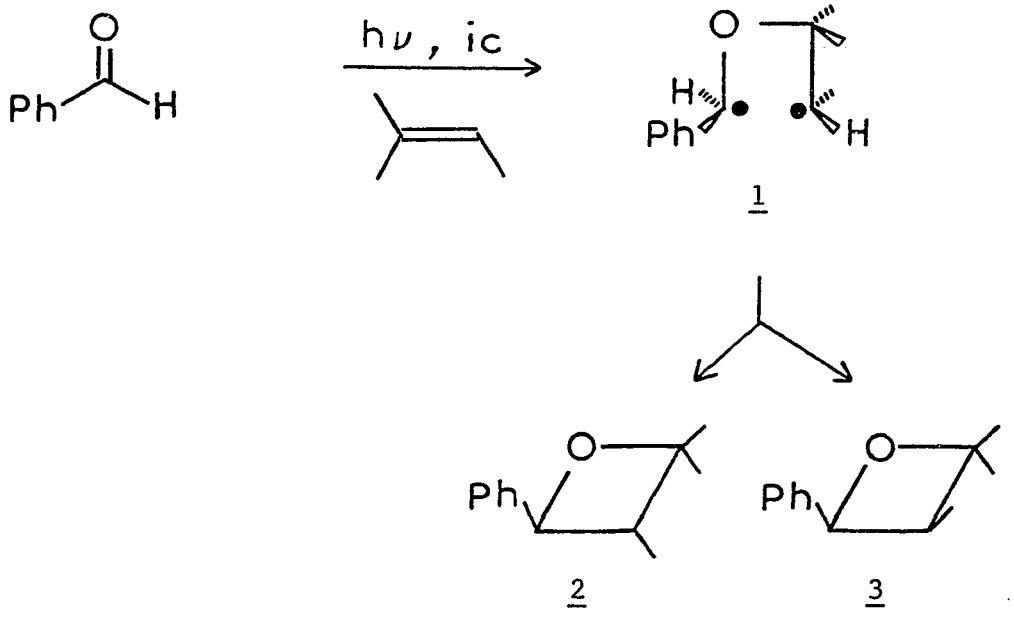

benzaldehyde. Formation of the two oxetanes arises from rotation of the 1,4-diradical intermediate 1. Turro et al., studied the reaction of acetone and dicyanoethylene to yield 4 from trans-dicyanoethylene and 5 from cis-dicyanoethylene. This mechanism was shown to involve complexation

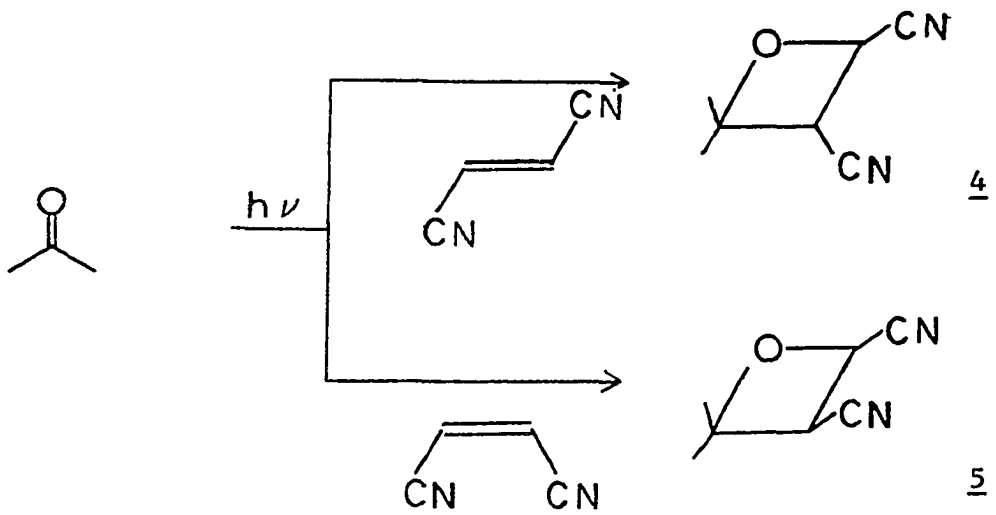

of singlet acetone to ground state dicyanoethylene to form an exciplex, which yields the stereospecific products (4,5,6).

Corey et al., have studied the addition of 2-cyclohexeneone to 1,1-dimethoxyethylene to form products 8 and 9 (7). A mechanism

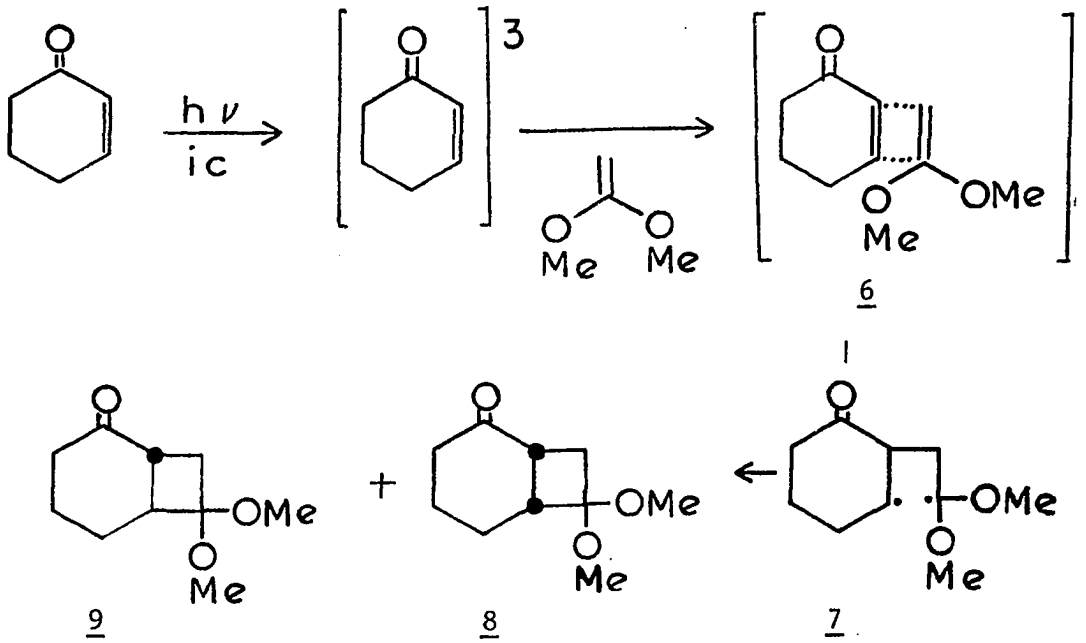

involving the triplet which forms an oriented π-complex 6 was proposed. The π-complex decays to diradical 7, which closes to form the products.

Addition of excited molecules to cyclohexene has been shown to depend on the nature of the adding species (8,9). The highly stereo-

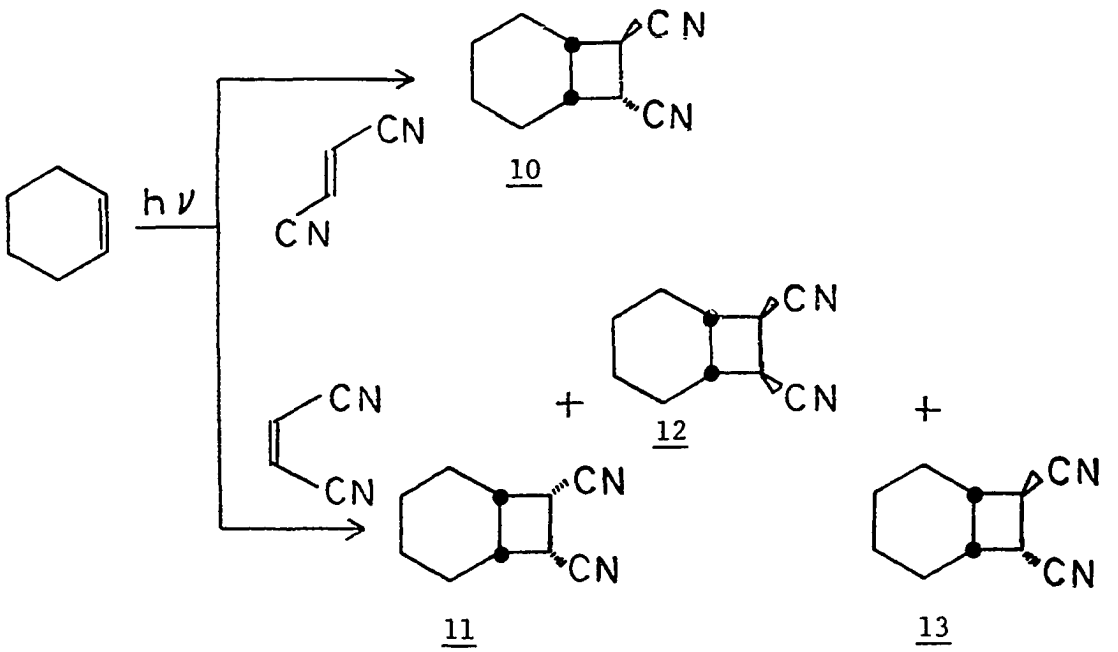

selective addition of fumaronitrile to cyclohexene to form 10 and maleonitrile to cyclohexene to form 11, 12 and 13 has been shown to

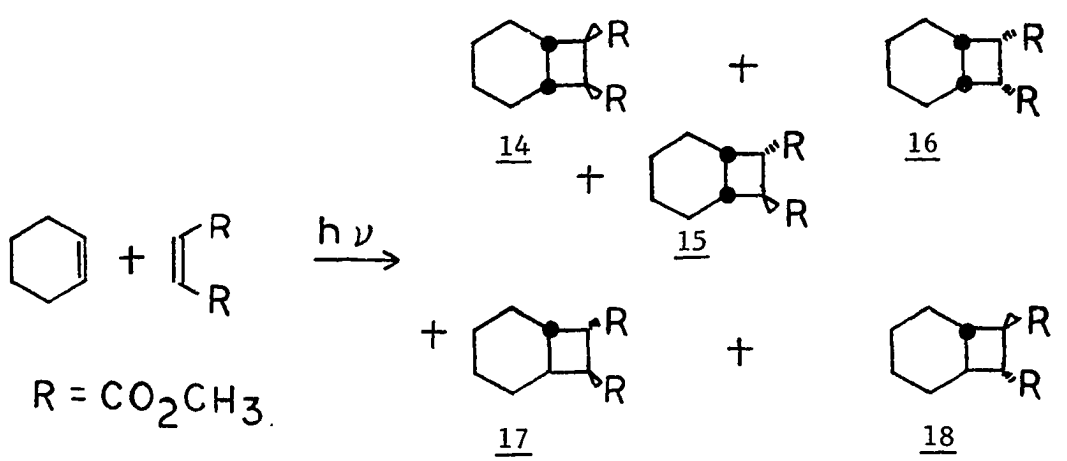

involve excitation of a ground state complex, which decays to product. The high degree of selectivity of this reaction can be contrasted to the addition of dimethy maleate to cyclohexene to form 14-18. This reaction has been shown not to involve a ground state complex. The mechanism proceeds via a 1,4-diradical which can give rise to the products by various rotations and closure.

The dimerization of cis and trans-2-butene has been studied (10).

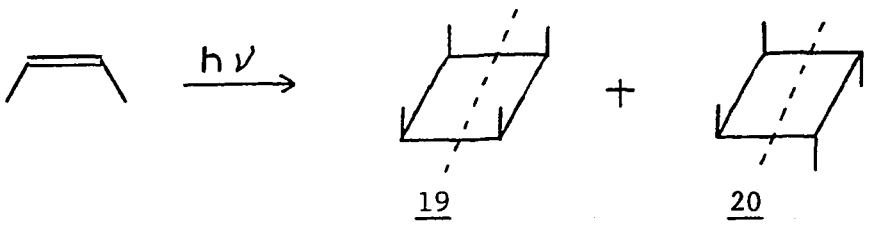

19 20

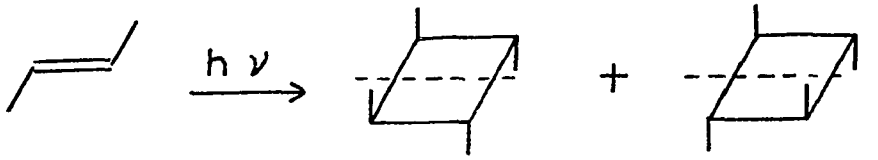

21 22

The two dimers obtained from cis-2-butene 19 and 20 are seen as arising from the possible orientations of two cis-2-butenes. Likewise the dimers from trans-2-butene 21 and 22 arise from the two orientations of two trans molecules. The mechanism is believed to involve the singlet excited state of the butenes.

The dimerization of 1,3-butadiene can be sensitized to form 23 and

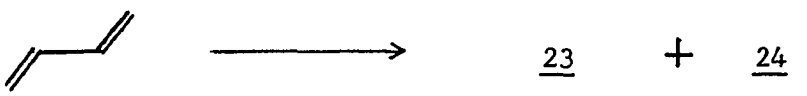

23 24

24 (11). The triplet mechanism involves addition of a triplet transoid

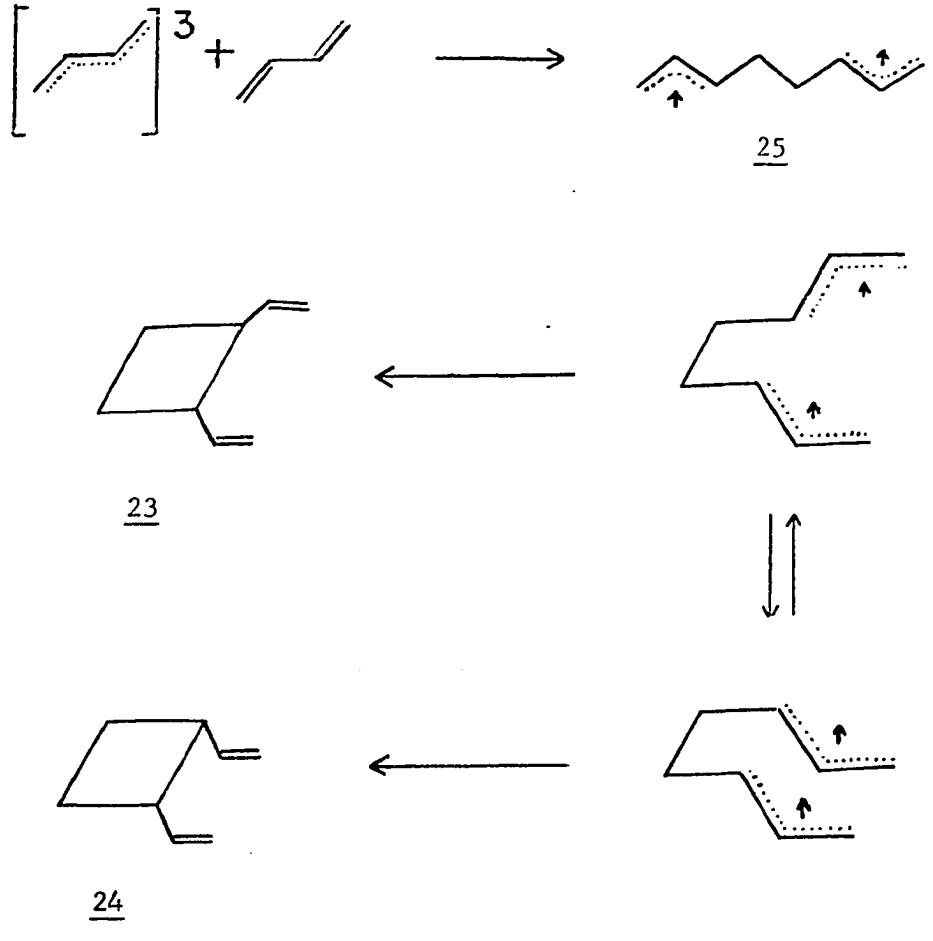

molecule to a ground state transoid molecule to form the diradical 25. Via various rotations of this diradical and resultant closure the two products are obtained.

From the few representative reactions presented, several trends in cycloadditions can be seen. Triplet reactions tend to be non-stereospecific, due to the long lifetime of the diradical with respect to rotation or the twisted character of the triplet, 90° where possible. Triplet reactions which are stereospecific can be expected to have a form of stabilization, such as formation of a ground state complex,

which holds the molecules somewhat rigid. Singlet reactions have a tendency to be stereospecific by virtue of the binding strength of the exciplex or short lifetime of a diradical.

Stilbene

Stilbene has been one of the most widely studied systems in organic photochemistry for the past 30 years. To aid in understanding the research which has been conducted and the accompanying diversification of opinion on the mechanistic aspects, a brief summary of the electronic nature, both observed and calculated, of cis and trans-stilbene will be presented.

The ground state of cis-stilbene is 6-10 kcal/mole higher in energy than the corresponding state of trans-stilbene (12,13). The first and second excited singlet states of trans-stilbene are at 94 and 120 kcal/mole respectively (14), as measured from emission studies. The corresponding states of cis-stilbene lie at 100 and 127 kcal/mole (14). Triplets states of trans-stilbene have been located at 50 kcal/mole, by oxygen perturbation methods (15), and 73 kcal/mole, observed as a transient intermediate at 77° K by flash photolysis (16). Other triplets have been inferred, from components of emission, at 87 and 92 kcal/mole (14). Low lying triplets of cis-stilbene exist at 63, 86 and 99 kcal/mole (17). An energy level diagram is represented in Figure 1.

Theoretical calculations using SCF-MO methods by Beveridge and Jaffe (18) lead to the construction of an energy level diagram for cis and

trans-stilbene shown in Figure 2. The calculated values are in good agreement with those directly observed. The values for cis-stilbene were calculated assuming that the aromatic rings are twisted 30° from the coplanar conformation. This is consistent with the known conformation of cis-stilbene (19).

Borrell and Greenwood (20), also using SCF-MO methods, have calculated the energy of the various levels as a function of rotation around the ethylenic central bond. The results are shown in Figure 3. This diagram reveals that both the lowest triplet and excited singlet states are expected to have an energy minimum in a twisted conformation. It can also be seen that the potential surface of the first excited singlet crosses that of an isoenergetic triplet. The considerations of this diagram will become important in understanding the controversy concerning trans to cis isomerization.

cis-trans Isomerization of stilbene has been the subject of active debate, with respect to the mechanism of the direct isomerization. The mechanism of the sensitized isomerization is a subject of general agreement (21,22,23,24,25 and 26 and references cited therein). The lowest triplet, reached by use of various triplet sensitizers, rotates around the central bond to reduce the interaction of the two unpaired electrons. At 90° rotation, the interaction is at a minimum. The 90° twisted triplet, phantom triplet, is a common state for both cis and trans-stilbene. The twisted triplet is supported by the calculations of Borrell and Greenwood (20). The phantom triplet then can decay to ground state cis and trans-stilbene as shown in Figure 4.

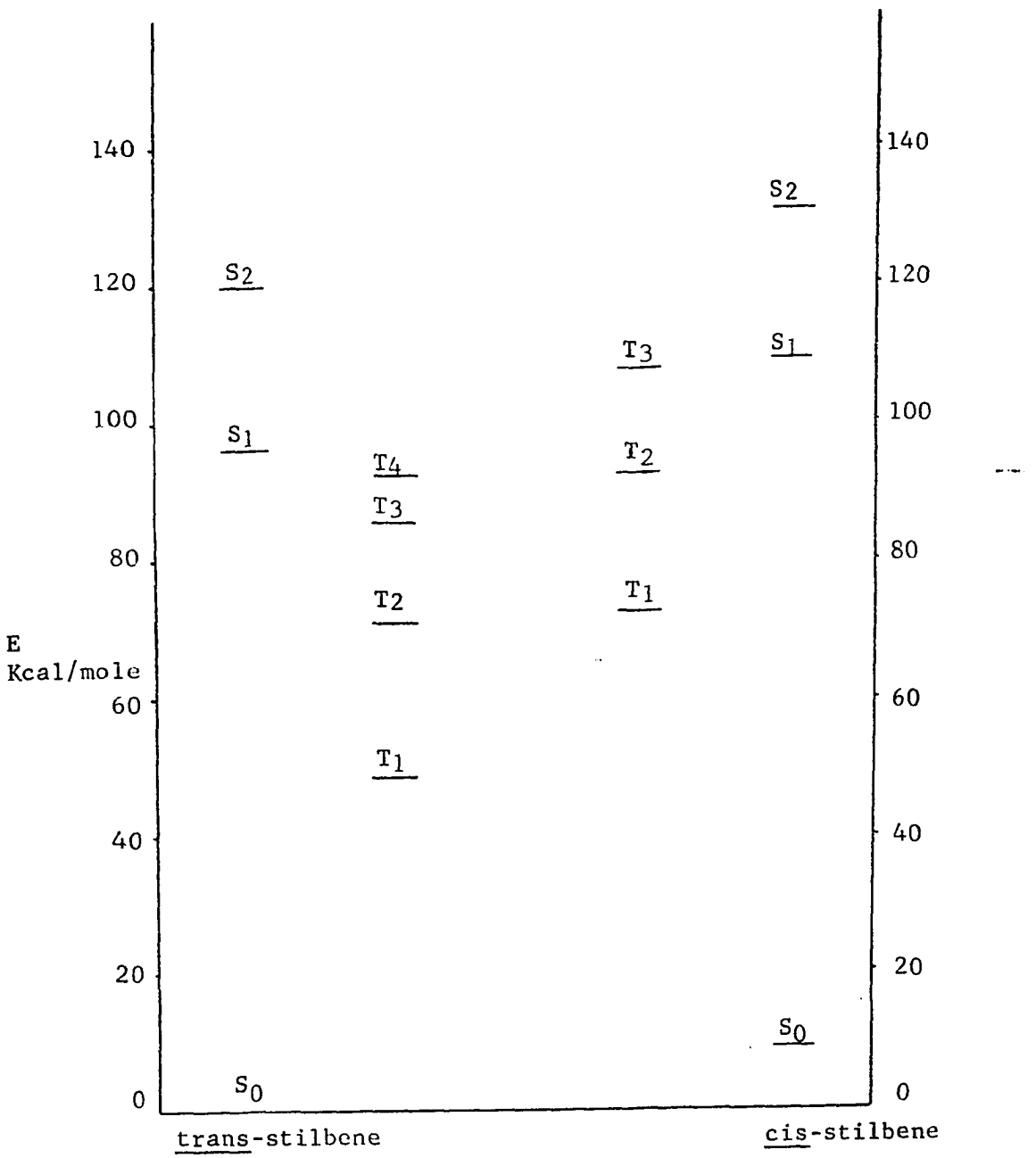

Figure 1. Energy level diagram of trans-stilbene and cis-stilbene

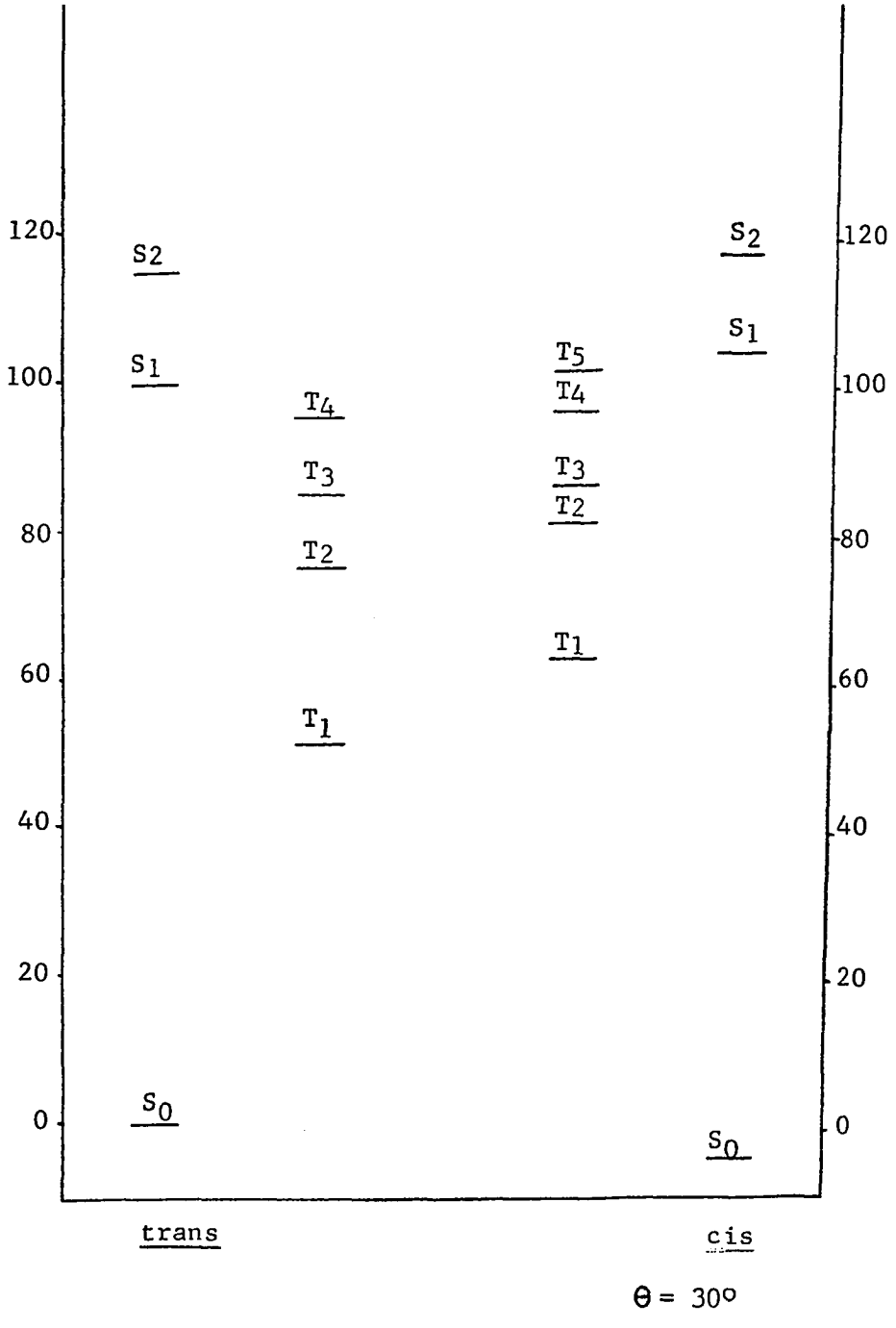

Figure 2. SCF-MO electronic energy diagram for cis-trans-stilbene

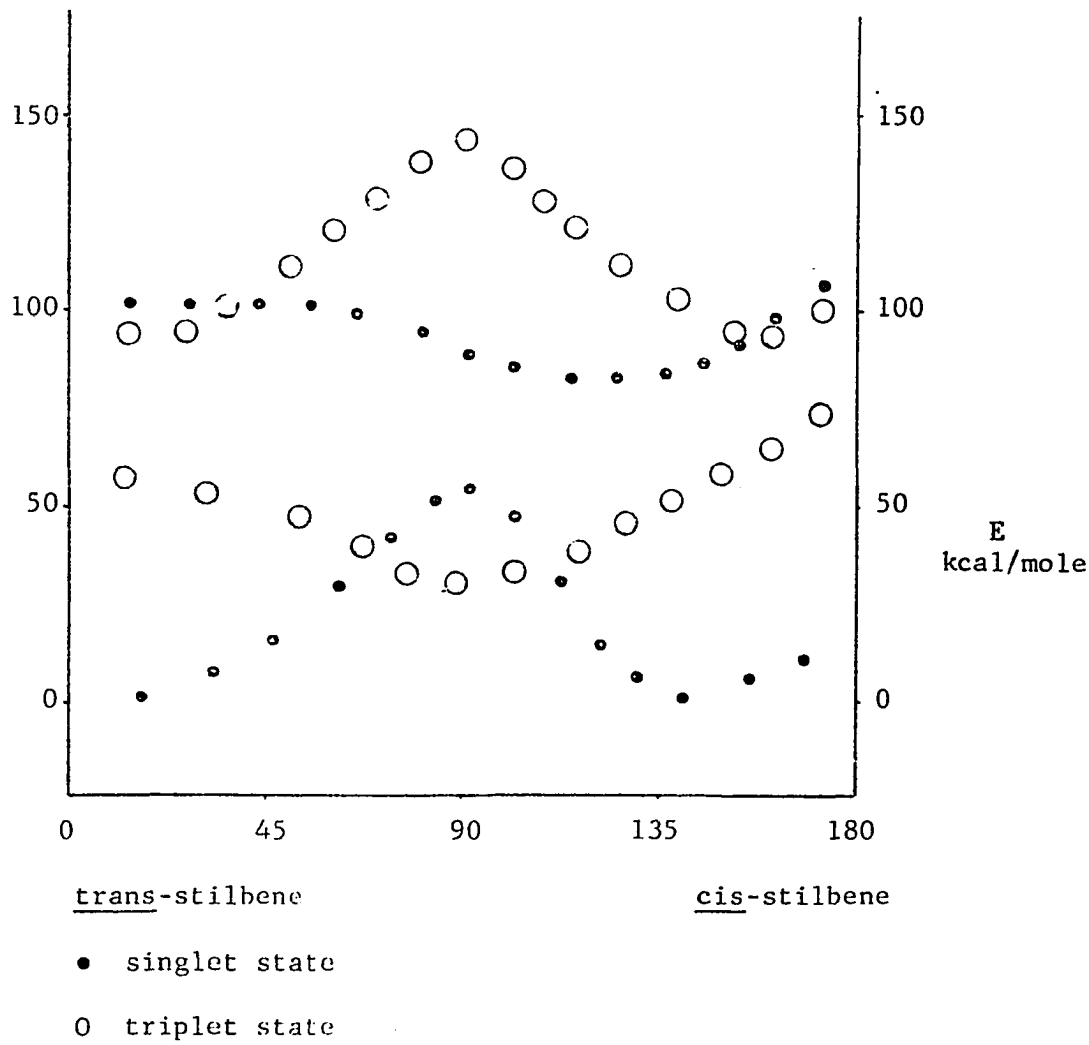

Figure 3. SCF-MO energy level diagram as a function of rotation around ethylenic central bond

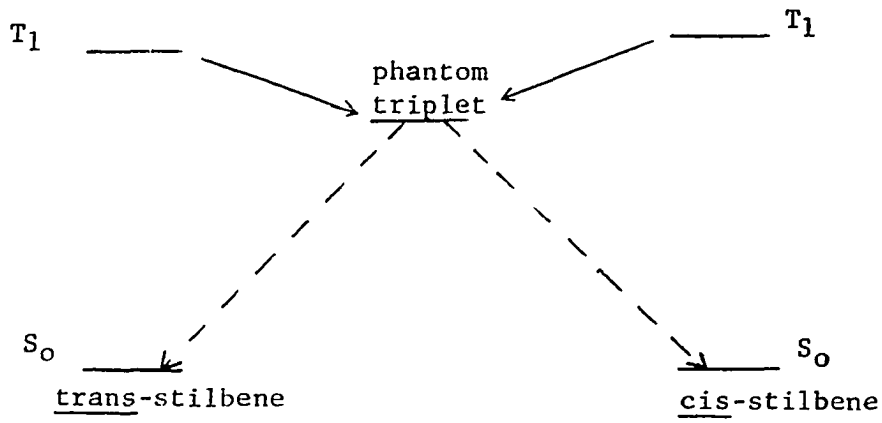

Figure 4. Mechanism of sensitized cis-trans isomerization of stilbene

The direct isomerization of stilbene is the subject of debate. Fischer and co-workers (22,27,28 and 29) argue that the direct isomerization obtains the same mechanism as the sensitized reaction. Their interpretation is based on several observations: the quantum yield of direct isomerization (trans-cis) decreases markedly as temperature decreases while the benzophenone sensitized isomerization is not temperature dependent to -140°, (this demonstrates that there is a potential barrier between the singlet and the state responsible for isomerization;) utilization of a heavy atom solvent, which is known to facilitate intersystem crossing, enhances the isomerization at low temperatures; and the decay ratio, from the proposed common intermediate, is the same for direct and sensitized isomerizations.

Fischer proposes the overall mechanistic scheme in Figure 5. Initial excitation to an upper vibrational level of the first excited singlet or higher singlet is followed by rapid decay to the lowest

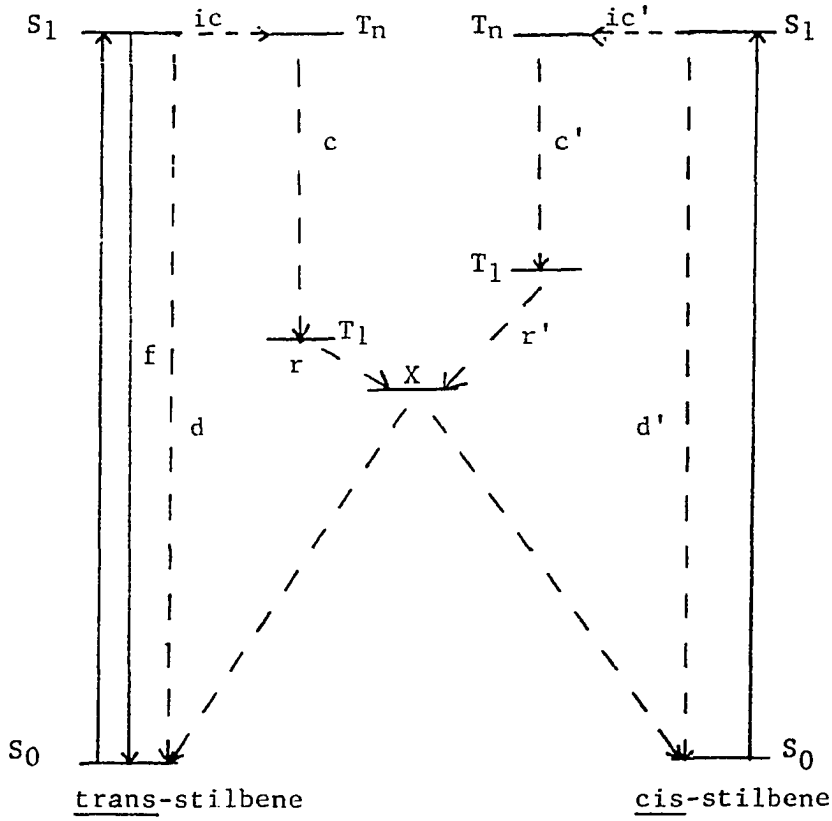

Solid lines represent radiative processes
Dashed lines represent nonradiative processes

Figure 5. Triplet mechanism for cis-trans isomerization

vibrational level of the first excited singlet. The singlet can then fluoresce to ground state (f), undergo radiationless decay to ground state (d) or undergo intersystem crossing to an isoenergetic triplet (ic). The presence of an isoenergetic triplet crossing the potential surface of the lowest singlet is verified by the calculations summarized in Figure 3. The upper triplet then cascades down the triplet manifold to the lowest vibrational level of the lowest triplet (c). The lowest triplet twists to the phantom triplet (r), which serves as a common intermediate for cis and trans-stilbene. Decay of the phantom triplet then produces ground state cis and trans-stilbene, as in the sensitized isomerization. The reaction pathway for cis-stilbene is similar to that of trans-stilbene with one exception, cis-stilbene is not known to fluoresce.

G. N. Lewis et al., (12) proposed a singlet mechanism based on absorption and fluorescence spectra of stilbene. The mechanism assumes the lowest singlet changes electronic to vibrational and rotational energy. The highly vibrationally excited ground state has sufficient energy to rotate around the central bond, resulting in isomerization.

Saltiel et al., (26, 30-32) believe in a singlet isomerization on the basis of an anomolous azulene quenching effect, no effect on the photostationary state of isomerization upon changing to perdeuterostilbene, which should increase the triplet lifetime and subsequentially be expected to alter the decay ratio, and a frequency factor of 10^{12}, which is too high for a spin forbidden process. Saltiel's mechanism differs from that of Lewis in that Saltiel favors participation of a phantom singlet state. Calculations (20) predict a minimum

in the singlet potential surface at a twist of 120° from trans around the central bond. The phantom singlet then decays to ground state cis and trans-stilbene as for Figure 6.

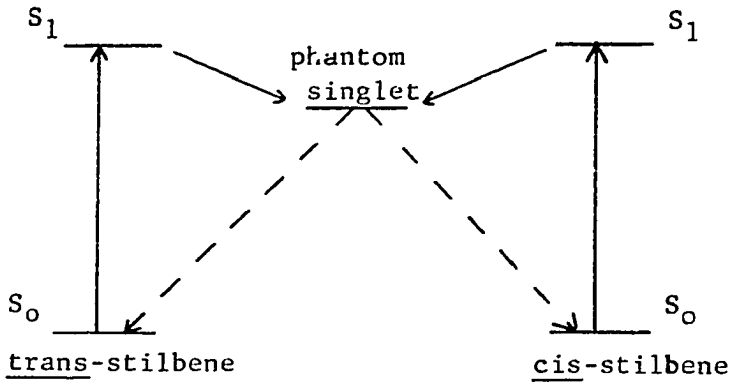

Figure 6. Phantom singlet isomerization of stilbene

Both the triplet and singlet mechanism are criticized by Dyck and McClure (14). From spectroscopic measurements they point out that in both the singlet and triplets the central bond retains a substantial double bond character. They therefore feel there is a large barrier to rotation around the central bond, casting serious doubt on the concept of twisted singlets or triplets being responsible for isomerization.

In addition to cis-trans isomerization, stilbene is known to undergo intramolecular cyclization to form a dihydrophenanthrene 26 (33).

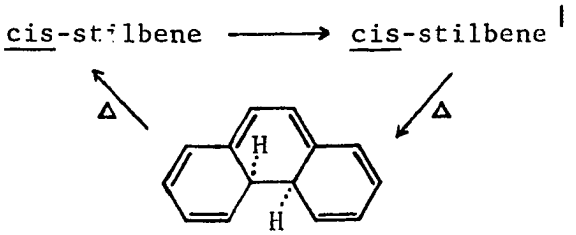

26

The reaction has been shown to involve closure of cis-stilbene from the first excited singlet state (34,35). Dihydrophenanthrene accounts for 13 per cent of the stilbene at the photostationary state and can thermally as well as photochemically revert to cis-stilbene.

Stilbene dimerizes very slowly in solution to produce 27 and 28 of of four possible dimers 27-30 (36). Dimers are also produced, in good

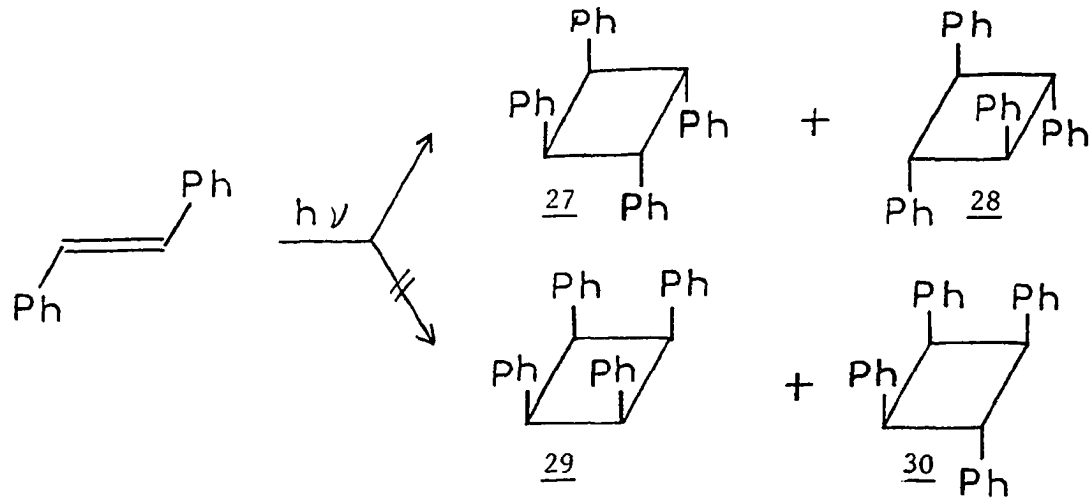

yield, by irradiating crystals of trans-stilbene (37).

Photocycloadditions involving stilbene as either the excited or ground state partner have been studied. Rosenberg et al., (38) studied the addition of excited cis and trans-stilbene to 2,3-dihydropyran to yield two stilbene dimers and two photoadducts, 7,8-cis-exo-diphenyl-2-oxa-bicyclo [4.2.0] octane 31 and 7-exo-8-endo-diphenyl-2-oxa-bicyclo [4.2.0] octane 32. Based on failure of sensitization attempts, a triplet mechanism was rejected. The mechanism was thought not to involve the lowest singlet as the photoadduct ratio was insensitive to starting material, cis or trans-stilbene. A singlet reaction would be

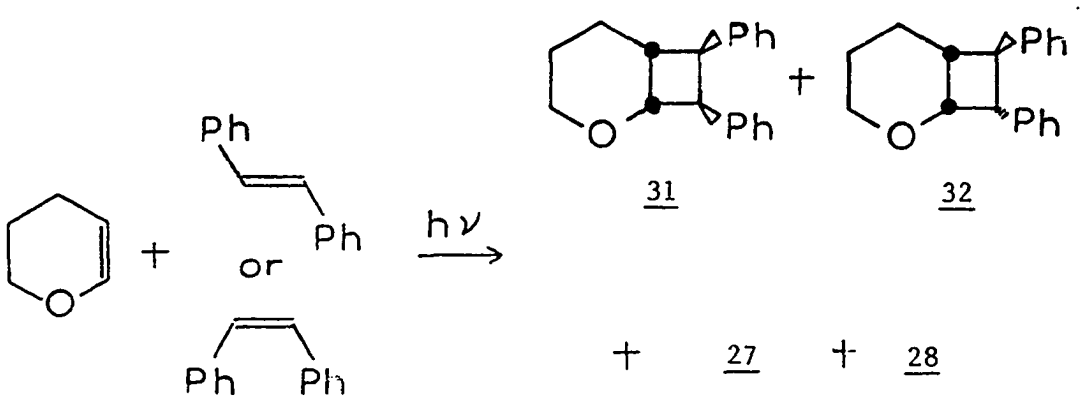

31 32

27 28

expected to show preference to the stereochemistry of the starting material, cis or trans-stilbene. As a result the authors favor a vibrationally excited ground state molecule reached from conversion of the lowest singlet. A more probable explanation would involve an upper triplet or twisted singlet interacting to produce a diradical or dipolar intermediate.

Two research groups have studied cycloadditions of excited tetrachloro-o-quinone and 9,10-phenanthroquinone to ground state stilbene. (39,40 and 41). The mechanism for the formation of 33 and 34 is envisioned as proceeding through a singlet 1,6-diradical 38 which contains considerable contribution from a dipolar species 39. The diradical is postulated to account for the loss of stereochemistry in 34. Product 35 is formed via initial formation of 40 by a concerted suprafacial photodehydrogenation of cis-stilbene and/or adduct 34 by quinone. Intermediate 40 is then attacked by a second molecule of quinone to yield 35. Products 36 and 37 are formed from a 1,6-diradical.

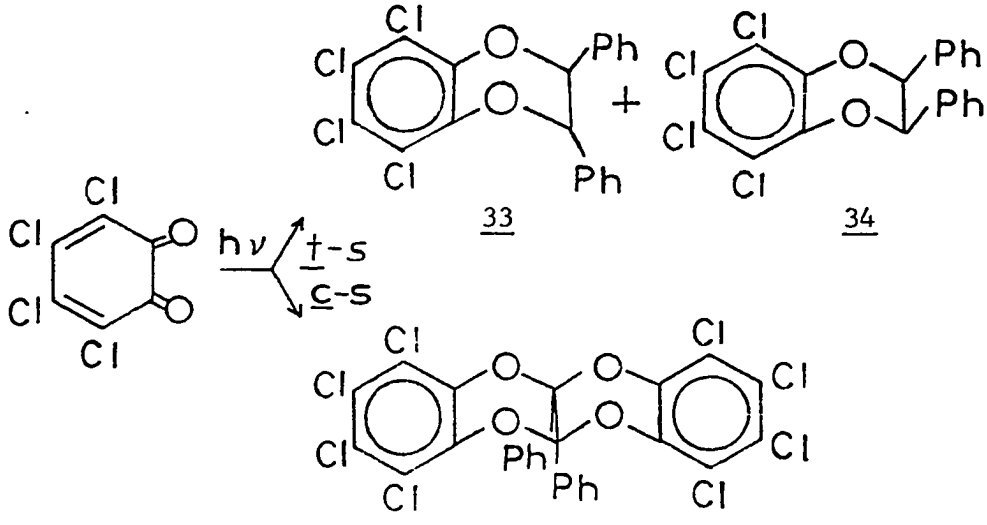

33 34

35

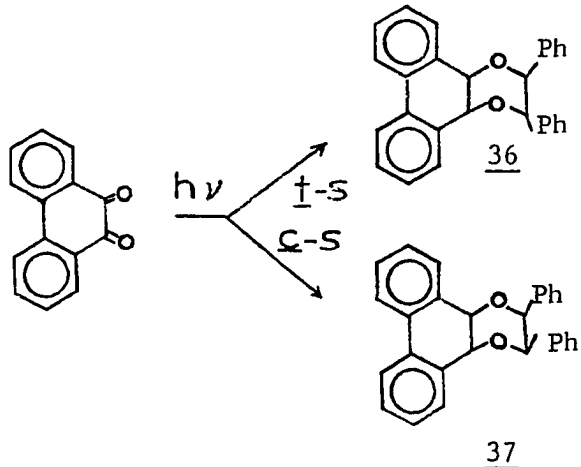

36

37

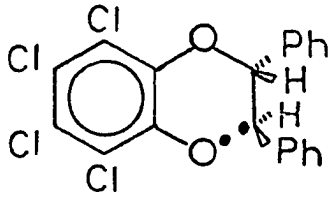

38

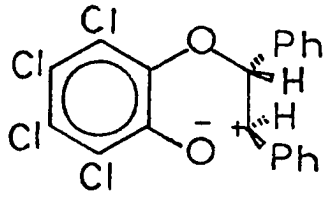

39

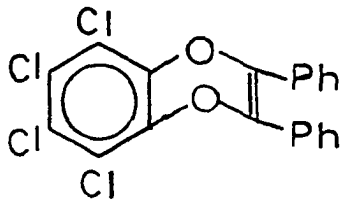

40

The possible photochemical reactions of the stilbene system are summarized in Figure 7. trans-Stilbene in the ground state can either react with an excited state molecule to form an adduct (i) or it can be promoted to an excited state (a). The excited state can decay to ground state, either by fluorescence or radiationless decay (k), react with a ground state molecule to form an adduct (h), react with a ground state stilbene molecule to form a dimer (m) or decay to ground state cis-stilbene (e). Ground state cis-stilbene can react with an excited molecule to form an adduct (j), or be promoted to an excited state (b). Excited cis-stilbene can undergo internal cyclization to form the dihydrophenanthrene (c), decay to ground state (l), react with a ground state stilbene to form a dimer (n), react with a ground state molecule to form an adduct (g) or decay to produce ground state trans-stilbene (f).

Excimers and Exciplexes

The concentration dependence of fluorescence of many organic compounds has been known for many years (42). Fluorescence intensities decrease as the concentration of the fluorescing compound is raised.

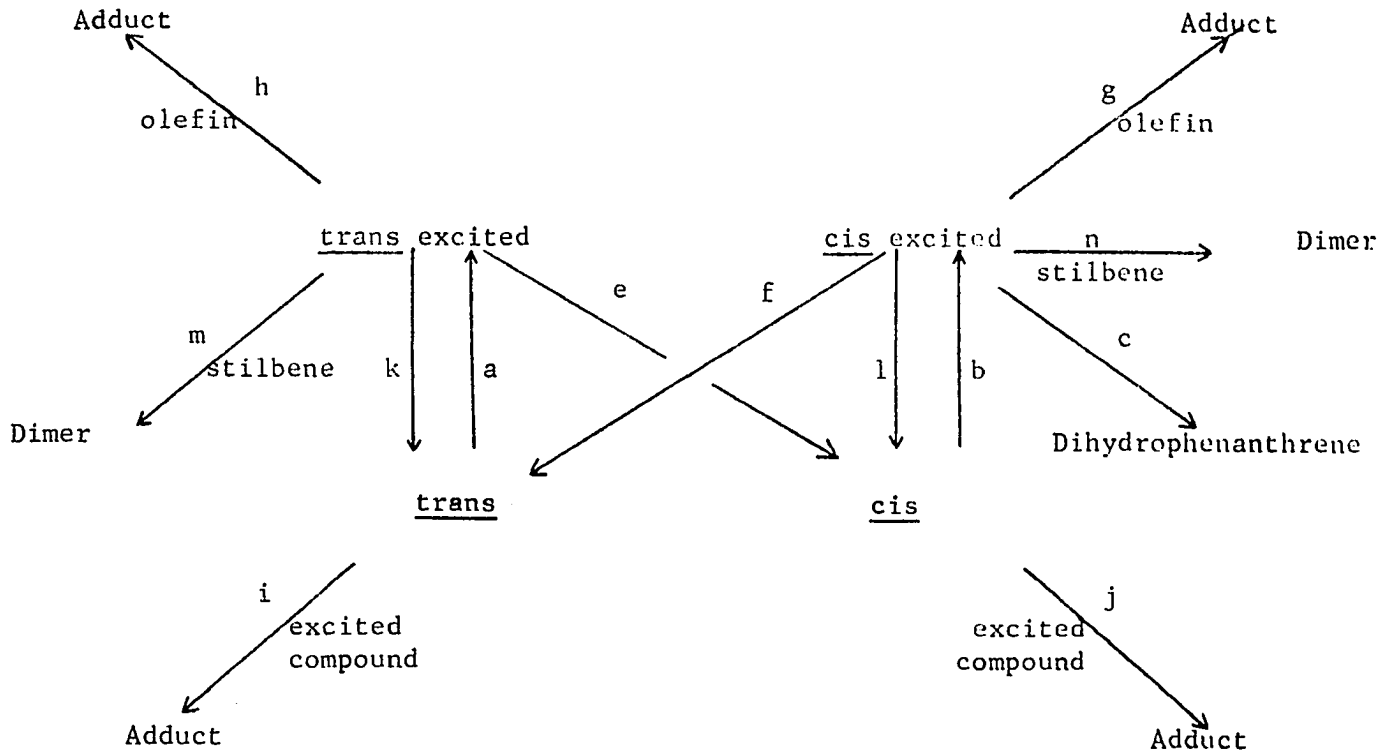

Figure 7. Possible photochemical reactions of cis and trans-stilbene

This decrease in intensity is often associated with the appearance of a new structureless emission peak, usually at lower energy than the monomer fluorescence, as is seen by the example of pyrene in Figure 8. No change is observed in the absorption spectrum on raising the concentration, therefore the new emitting species is formed only after initial excitation. The term excimer was originally intended to denote a species formed from the combination of an excited state molecule with a ground state molecule of the same species (43). It has since been frequently used to denote a species formed from any excited state molecule combining with a ground state molecule.

Excimers have been eloquently reviewed by Forster (44) and only a brief survey of the subject will be presented. Excimers have been observed for pyrene (45), perylene (46), anthracene (46), naphthalene (47), benzene (48) and many others. Excimers are not restricted to two identical molecules, as mixed excimers, which is actually a misnomer as they are exciplexes, have been observed for pyrene and 1-methylpyrene (49) and anthrancene with 9-alkyl or 9,10-dialkylanthracene (50) to name only two.

Excimers are known to exist in four different types as is seen in Table 1. Type I, such as perylene exhibit excimer emission which is accompanied by a new absorption at longer wavelengths attributed to formation of fluorescent dimers which are stable upon emission to the ground state. Type II, such as pyrene, exhibit excimer emission with no change in the absorption spectrum from the monomer. Type III, such as anthrancene, do not exhibit excimer emission but show a change in the absorption spectrum, due to formation of nonfluorescent dimers which

Figure 8. Pyrene fluorescence

Top: Fluorescence spectra of pyrene as a function of concentration

a 5×10^{-5} moles/liter
b 1.8×10^{-4}
c 3.1×10^{-4}
d 7.0×10^{-4}

Bottom: Pyrene monomer and excimer emission versus temperature

• Excimer emission
ᶜ Monomer emission

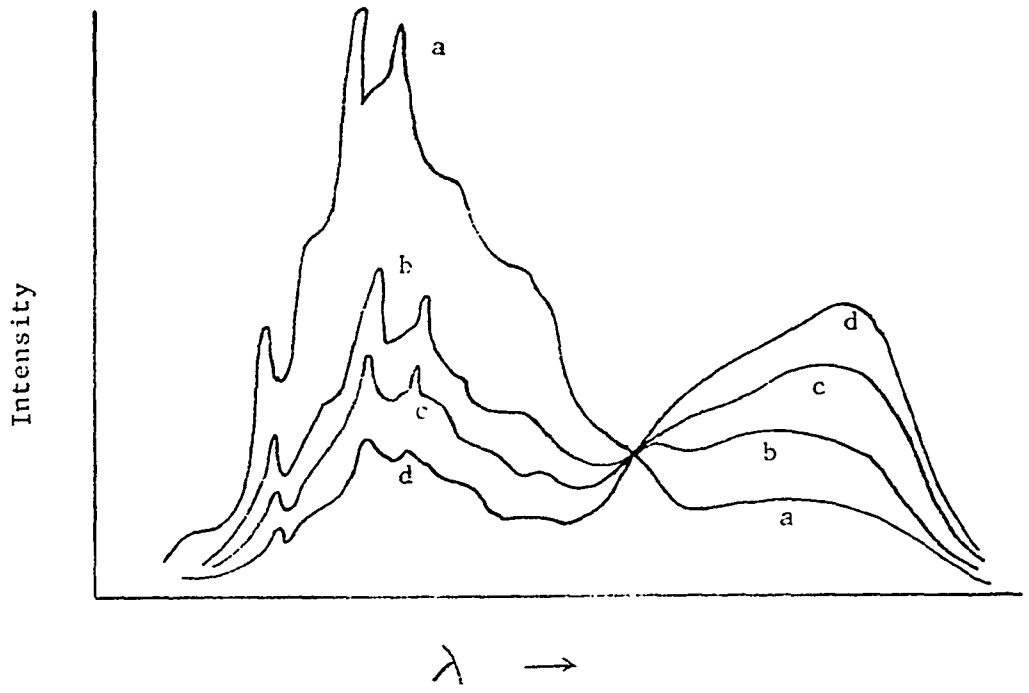
Intensity
a
b
c
d
d
c
b
a
λ →

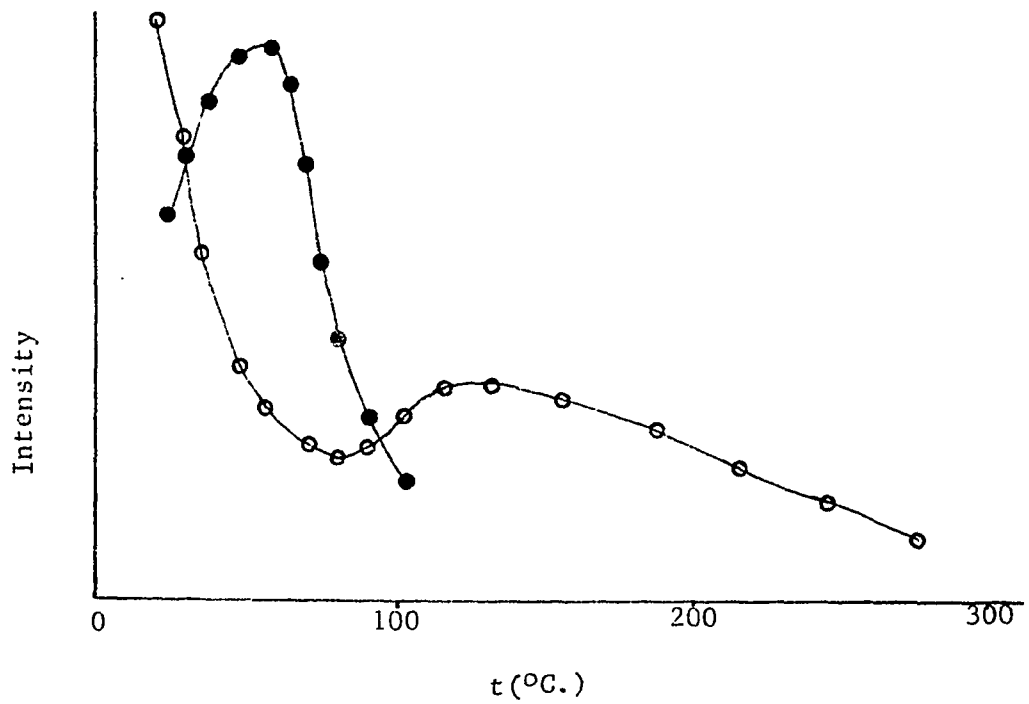
Intensity
0
100
200
300
t (°C.)

Table 1. Types of excimers

Type	Concentration quenching	Dimer emission	Dimer absorption
I	Yes	Yes	Yes
II	Yes	Yes	No
III	Yes	No	Yes
IV	Yes	No	No

are stable in the ground state. Type IV shows no new emission or change in the absorption spectrum.

In emitting excimers, the two emission peaks are known to be temperature dependent as shown for pyrene in Figure 8 (45). It is seen that at temperatures below 80° excimer formation predominates while at higher temperatures the excimer dissociates with reformation of the excited monomer, as is seen in the rise of monomer emission with fall of excimer.

These facts and the time dependence (51) of excitation lead to the mechanism of excimer formation shown in Figure 9. The excited

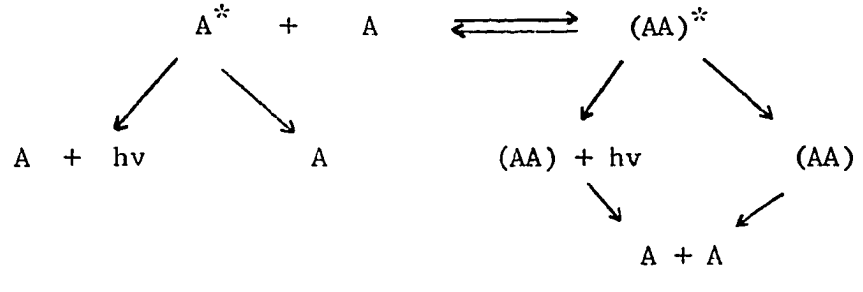

Figure 9. Mechanism of excimer formation

monomer can either fluoresce, undergo radiationless decay or combine with a ground state molecule to form the excimer. The excimer can then fluoresce, undergo radiationless decay or dissociate to excited monomer and ground state molecule.

The exact nature of the excimer is not fully understood. It is a closely associated complex, as the intermolecular distance is smaller in an excimer than for the two same molecules in the ground state (52). Excimers can be visualized as sandwich pairs with extensive π interactions. The unusual long lifetime of some excimers (43) is interpreted as being due to the complexation affecting the radiative properties, i.e. causing the radiative transitions from excited to non-excited states to become orbitally forbidden processes. The nature of the binding energy of an excimer is seen as a combination of two effects, a charge transfer contribution (52,53), which can be stabilized by resonance of the type in equation 1, and contribution from the uniform distribution of the

$$A^+ A^- \longleftrightarrow A^- A^+ \qquad (1)$$

excited state energy over both components, as in equation 2 (54).

$$A^*A \longleftrightarrow AA^* \qquad (2)$$

Semiempirical MO theory treating excimers as "supermolecules", considering all π electron of the interacting molecules, satisfactorily explains the observed properties of excimers (49).

The excimers mentioned thus far are singlet excimers. Triplet excimers have received less attention. Several reports of triplet excimers based on phosphorescence of halogenated benzenes have been

made (55,56 and 57). They all report the excimer type emission in the low temperature phosphorescence. The emission follows known patterns of excimer behavior, appearance at high concentrations and low temperature absorption spectrum is that for monomeric material. The triplet nature is verified from the facts that the emission is partially quenched by dissolved oxygen, and the emission can be detected when the halogenated benzene is excited directly to the lowest triplet state. It has been shown that triplet energy transfer efficiency of (π - π^*) sensitizers is concentration dependent (58), decreasing with increasing concentration. To account for these results the formation of a triplet excimer at high concentrations is proposed as one possibility. Inefficiencies in several known triplet reactions have been attributed to triplet excimers (59,60 and 61). In these studies plots of $1/\Phi$ vs. $1/[Q]$ intercept not at 1, which is expected if the reaction involves only excited monomer, but from 3 to 10. This is explained by excimer formation with partitioning of the excimer between products (equation 3)

$$A^* + A \longrightarrow AA^*$$
$$AA^* \longrightarrow \text{product} \qquad (3)$$

and decay to two ground state molecules (equation 4).

$$AA^* \longrightarrow A + A \qquad (4)$$

The less frequent observation of the triplet excimer than the singlet is expected on the basis of theoretical predictions (62). Using the same "supermolecule" technique for triplets as for singlets, the triplet excimer is expected to have a much weaker binding energy and would be expected to readily decay to monomer triplet and monomer

ground state.

The last three cases mentioned are a special type of excimer called an exciplex. The exciplex can be described as an excimer type complex which is often an intermediate in a chemical, bond forming, reaction (63). These are for most cases, between two electronically different molecules.

The exciplex binding energy is believed to be very similar to that of an excimer with a large contribution from a charge-transfer state. The possibility of bonding as proposed by Schenk (64), formation of localized bonds which can subsequently be broken, cannot be rigorously excluded.

Exciplexes have been proposed for numerous reactions, but only a few representative examples will be discussed. Singer and coworkers (65,66 and 67) have studied the cycloaddition of ketenimines to ketones to yield the two photoadducts 41 and 42. Both a singlet and triplet

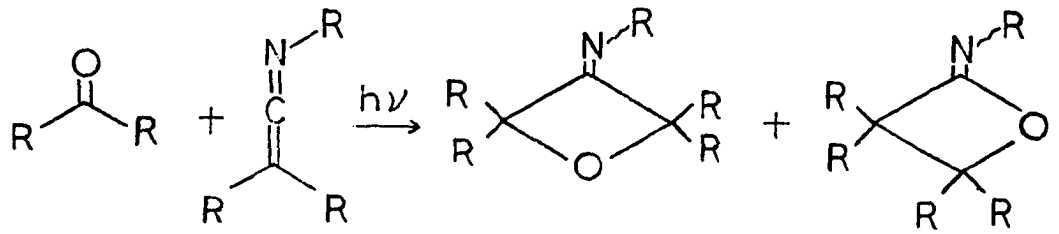

41 42

exciplex have been proposed for the reaction when different components are used. Fluorenone fluorescence is efficiently quenched by dimethyl-N-cyclohexyl-ketenimine; there is no accompanying change in shape or appearance of a new emission peak. The plot of $1/\Phi$ vs. $1/[Q]$ curves

sharply upward at high olefin concentration. On the basis of these observations a singlet exciplex at high concentrations is invoked. The same reaction using benzophenone and diphenyl-N-phenyl-ketenimine proceeds via a solely triplet mechanism. The ketenimine quenches benzophenone photoreduction and naphthalene quenches photoaddition. A plot of $1/\Phi$ vs. $1/[0]$ is linear, but the intercept is above 1. A triplet excilpex is invoked to explain the overall triplet nature and inefficiency of addition.

Stereospecific oxetane formation, 43 and 44, from ketones and cis and trans-dicyanoethylene has been studied (4, 5 and 6). A

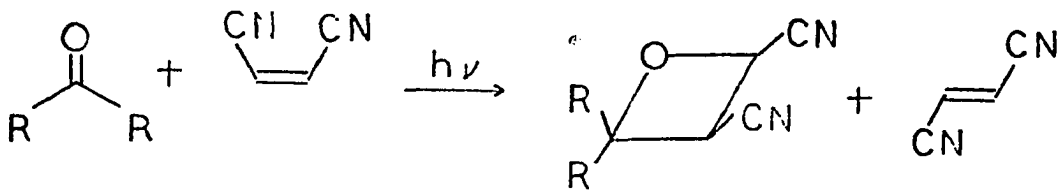

43

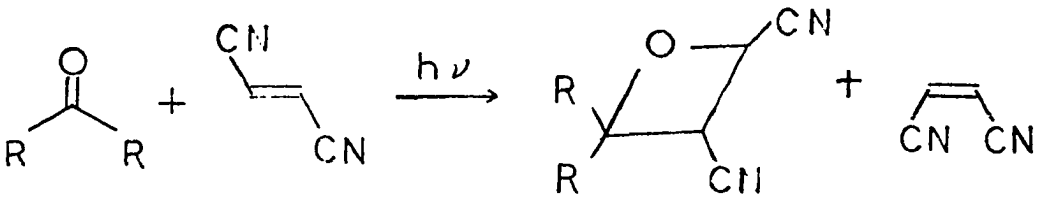

44

singlet exciplex accounts for the experimental observations (efficient fluorescence quenching coupled to overall reaction inefficiency, intercept of $1/\Phi$ vs. $1/[O]$ plot being 13). Oxetane formation is only slightly affected by the concentration of 1,3-pentadiene which quenches 80 per cent of cis - trans isomerization. Attempts to sensitize the addition result only in cis-trans isomerization of the dicyanoethylene, further demonstrating the singlet nature of the reaction.

A triplet complex has been proposed in the cycloaddition of cyclopentenone to olefins (equation 5) (68). The reaction was shown to

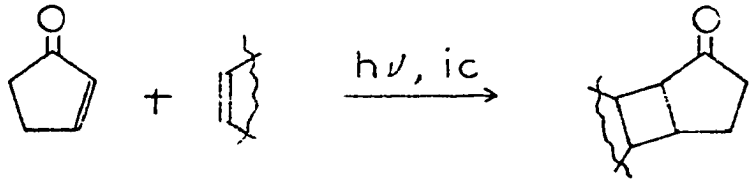

(5)

proceed via the triplet. Quantum yield of addition is temperature dependent, increasing with decreasing temperature. To account for the temperature dependence a partitioning of the complex between diradical and ground state and similiar partitioning of the diradical is proposed (Figure 10).

The reaction of tolan and naphthalene to produce 45 has been shown to involve reverse exiplex formation (equation 6) (69). A mechanism totally analogous to excimer formation was proposed. Reverse exciplex formation is, in kinetic studies, usually ignored due to complication of rate constant calculation.

A triplet complex has been proposed to explain certain

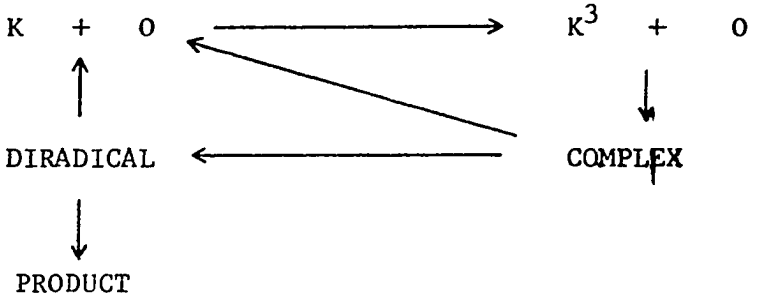

Figure 10. Mechanism of 2-cyclopentenone addition

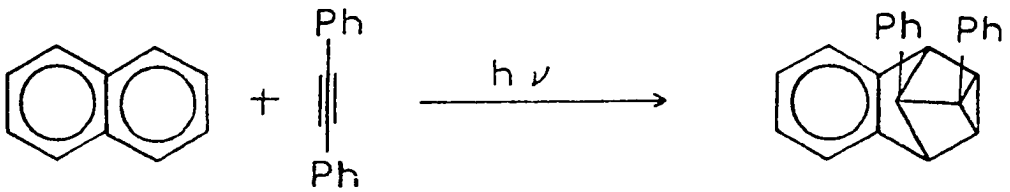

45

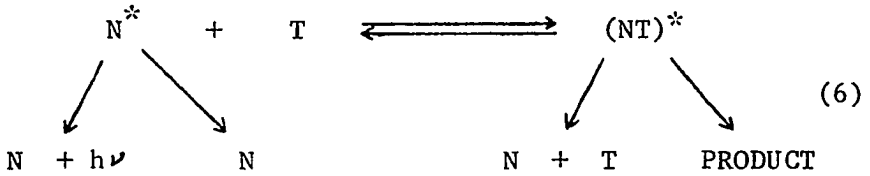

(6)

sensitization reaction (63,70 and 71). Fluorescence of naphthalene is quenched by 46. It is known that 46 does not have a singlet below that of naphthalene, therefore no simple singlet-singlet energy transfer is involved. The conversion of quadricyclene 46 to norbornadiene 47

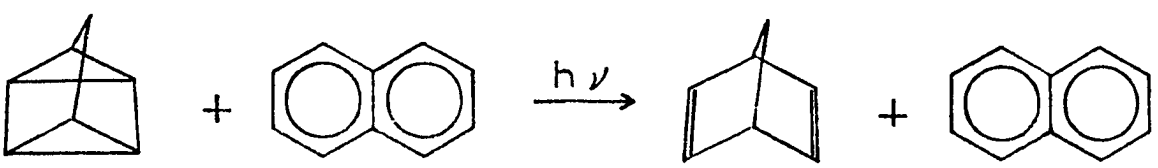

46 47

via sensitization is seen as proceeding via partition decay of the exciplex (Figure 11). It is also known that arylsulfoxides can be

$$S \longrightarrow S^1$$

$$S^1 \longrightarrow S^3$$

$$S^1 + \underline{46} \rightarrow \text{EXCIPLEX}$$

$$\text{EXCIPLEX} \longrightarrow \underline{46} + S$$

$$\text{EXCIPLEX} \longrightarrow \underline{47} + S$$

Figure 11. Exciplex mechanism for quadricyclene sensitized isomerization

racimized by naphthalene sensitization (equation 7). The proposed

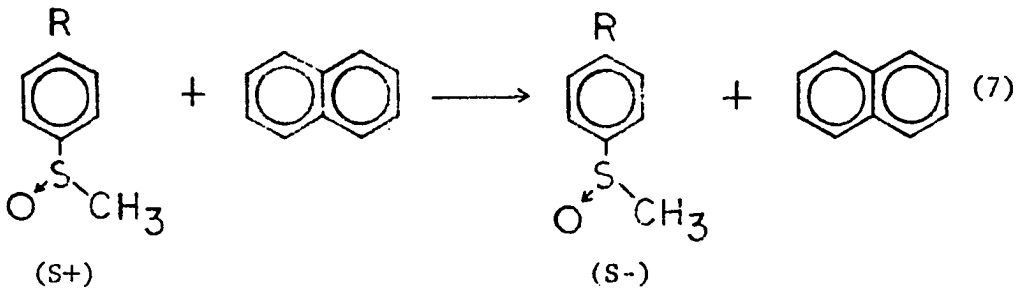

(S+) (S-) (7)

mechanism is the same as that for quadricyclene isomerization.

As has been shown, exciplexes can be proposed for a wide variety of photochemical reactions and undoubtably are involved in many more. Exciplexes have been postulated on the basis of; efficient fluorescence quenching coupled to low quantum yield of reaction at high concentration, showing that the mechanism involves more than just excited monomolecular species which can partition between product and ground state molecules; unusual temperature dependences of quantum yield, showing

affect of partitioning of an intermediate between the excited monomeric molecule and products; and strong fluorescence quenching by a molecule which is known not to have a singlet below that of the fluorescing compound.

Triplet exciplexes are proposed more frequently than the corresponding triplet excimer. This is probably due to the stronger binding energy in triplet exciplexes, possibly from a contribution of Schenk-type bonding, compared to the weaker bonding in triplet excimers, which do not give rise to bond forming reactions.

RESULTS AND DISCUSSION

Photocycloadditions of trans-Stilbene to Olefins

The majority of mechanistic studies of photocycloaddition reactions have been conducted involving carbonyl containing compounds. These studies are complicated by the participation of the two different excited states of the carbonyl, (n, π^*) and (π, π^*). To fully understand the mechanistic intricacies of a $\pi^2 + \pi^2$ cycloaddition it is desirable to have only one type of reactive state participating. Therefore the cycloaddition of cis or trans-stilbene to 2,3-dimethyl-2-butene (TME) yielding trans-1,2-diphenyl,3,3,4,4-tetramethylcyclobutane 48 described by Adams and Chapman (72) presents an opportunity for such

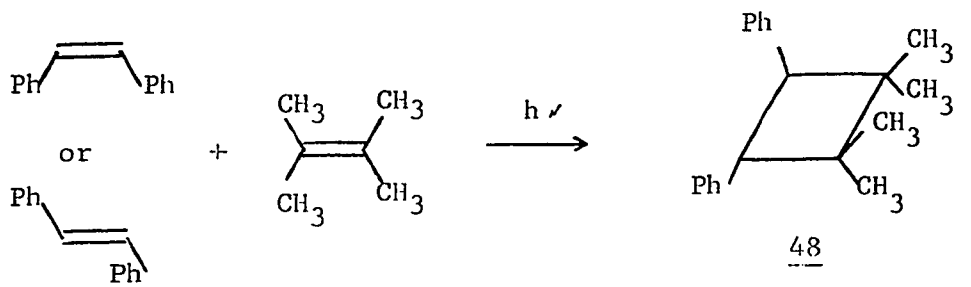

48

a study involving a reactive (π, π^*) state. Three aspects of the cycloaddition were chosen as major points of investigation. Stereospecificity with respect to both the excited and ground state partners was investigated. Multiplicity of the reactive state of stilbene responsible for the addition was determined and kinetic data for the addition of stilbene to a variety of alkyl substituted olefins was obtained.

To ascertain the stereospecificity trans-stilbene was irradiated in the presence of a variety of olefins, chosen on the basis of the alkyl substitution such that normal spectral methods would allow conclusive stereochemical assignment. The irradiation of trans-stilbene in the presence of cis-2-butene afforded one photoadduct, in low quantum efficiency. The structure of the adduct was determined to be trans-1,2-diphenyl-cis-3,4-dimethylcyclobutane 49 on the basis of spectral evidence. The infrared spectrum (Figure 12) shows absorptions

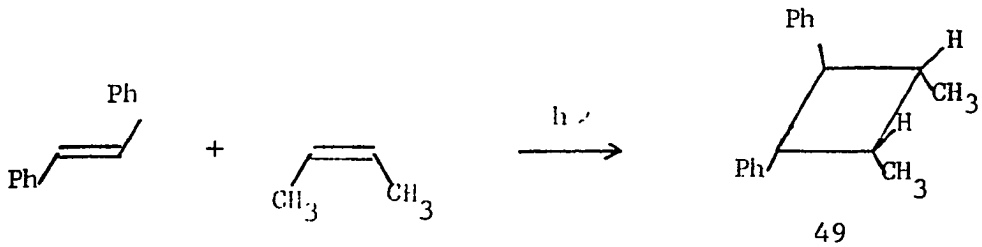

49

at 3.32, 3.34, 3.38, 3.38, 3.41, 3.46, 5.15, 5.35, 5.55, 5.80, 6.21, 6.70, 6.90, 7.25, 9.70, 10.4, 13.4 and 14.4μ. These bands are consistent for the structure of the adduct 49 by close resemblance to the infrared spectrum of the TME adduct reported by Adams (72), indicating that there is little structural difference between the two products. The mass spectrum (Table 2) indicates a 1:1 adduct, m/e 236, 5%. The base peak, m/e 118, results from the symmetrical cleavage of the cyclobutane

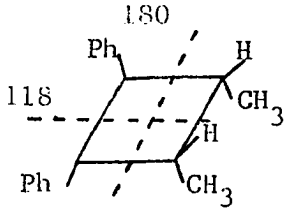

Table 2. Mass spectra of adducts 49, 50 or 51 and 52

49		50 or 51		52	
m/e	rel. int.	m/e	rel. int.	m/e	rel. int
237	trace	236	1.0	250	trace
236	5.0	181	7.8	181	16.1
181	10.0	180	79.5	180	100.0
180	65.0	179	65.0	179	32.2
179	48.0	178	45.5	178	30.0
178	35.0	177	10.4	177	5.6
177	8.0	176	9.0	176	5.6
176	5.0	119	10.0	133	4.6
119	10.0	118	100.0	132	26.4
118	100.0	117	18.0	118	5.7
91	7.0	91	8.0	117	12.2
77	5.0			91	9.0
				77	6.0

to form two β-methyl styrene moieties. The other major peaks are those arising from stilbene, m/e 180, as would be expected as the other favored fragmentation is the elimination of stilbene. The nmr spectrum (Figure 13) revealed two sharp singlets at 7.11 and 7.13δ , integrating for 10 aromatic protons. The position and shape of the aromatic signal is in accord with that expected for a trans-1,2-diphenyl system on a cyclobutane ring (73). The appearance of two aromatic singlets is reasonable due to the slight magnetic nonequivalence of the phenyl groups due to different environment with respect to the methyl groups. A

Figure 12. Infrared spectra

Top: trans-1,2-diphenyl-cis-3-methyl-4,4-dimethylcyclobutane

Middle: trans-1,2-diphenyl-syn-trans-3,4-dimethylcyclobutane or trans-1,2-diphenyl-anti-trans-3,4-dimethylcyclobutane

Bottom: trans-1,2-diphenyl-cis-3,4-dimethylcyclobutane

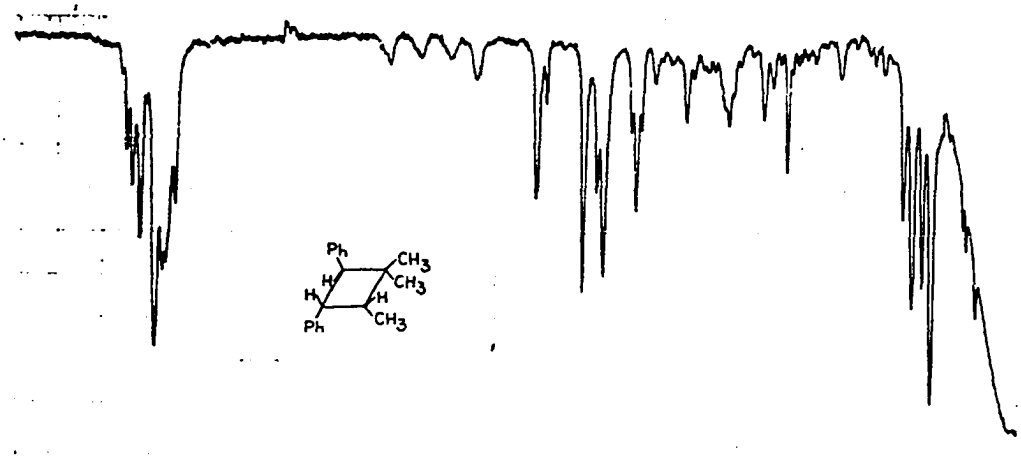
Ph
CH3
H
CH3
H
H
Ph
CH3

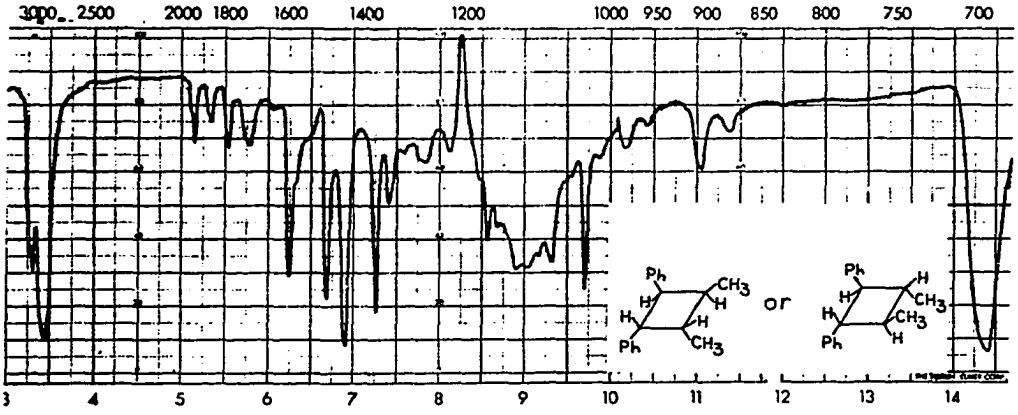
3000
2500
2000
1800
1600
1400
1200
1000
950
900
850
800
750
700
3
4
5
6
7
8
9
10
11
12
13
14
or

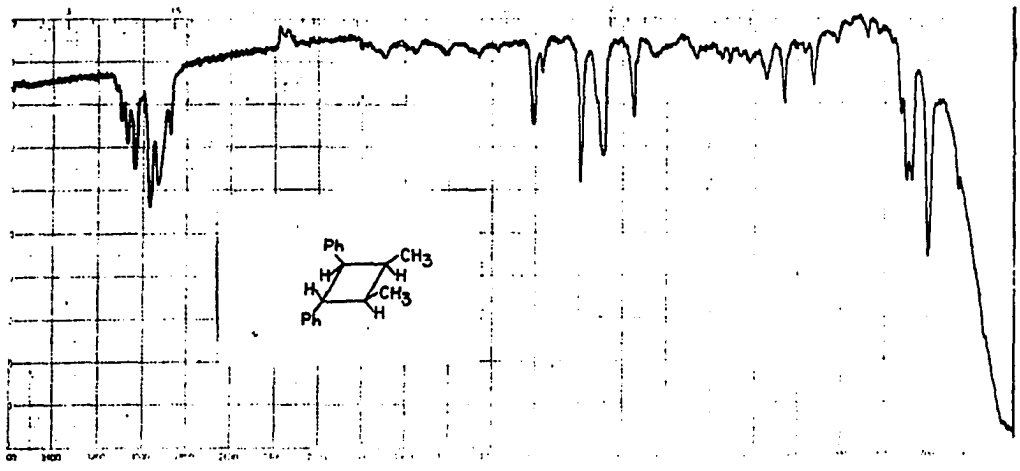
Ph
CH3
H
H
CH3
Ph
H

Figure 13: Nuclear magnetic resonance spectra

Top: trans-1,2-diphenyl-cis-3,4-dimethylcyclobutane

Middle: trans-1,2-diphenyl-syn-trans-3,4-dimethylcyclobutane or trans-1,2-diphenyl-anti-trans-3,4-dimethylcyclobutane

Bottom: trans-1,2-diphenyl-cis-3-methyl-4,4-dimethylcyclobutane

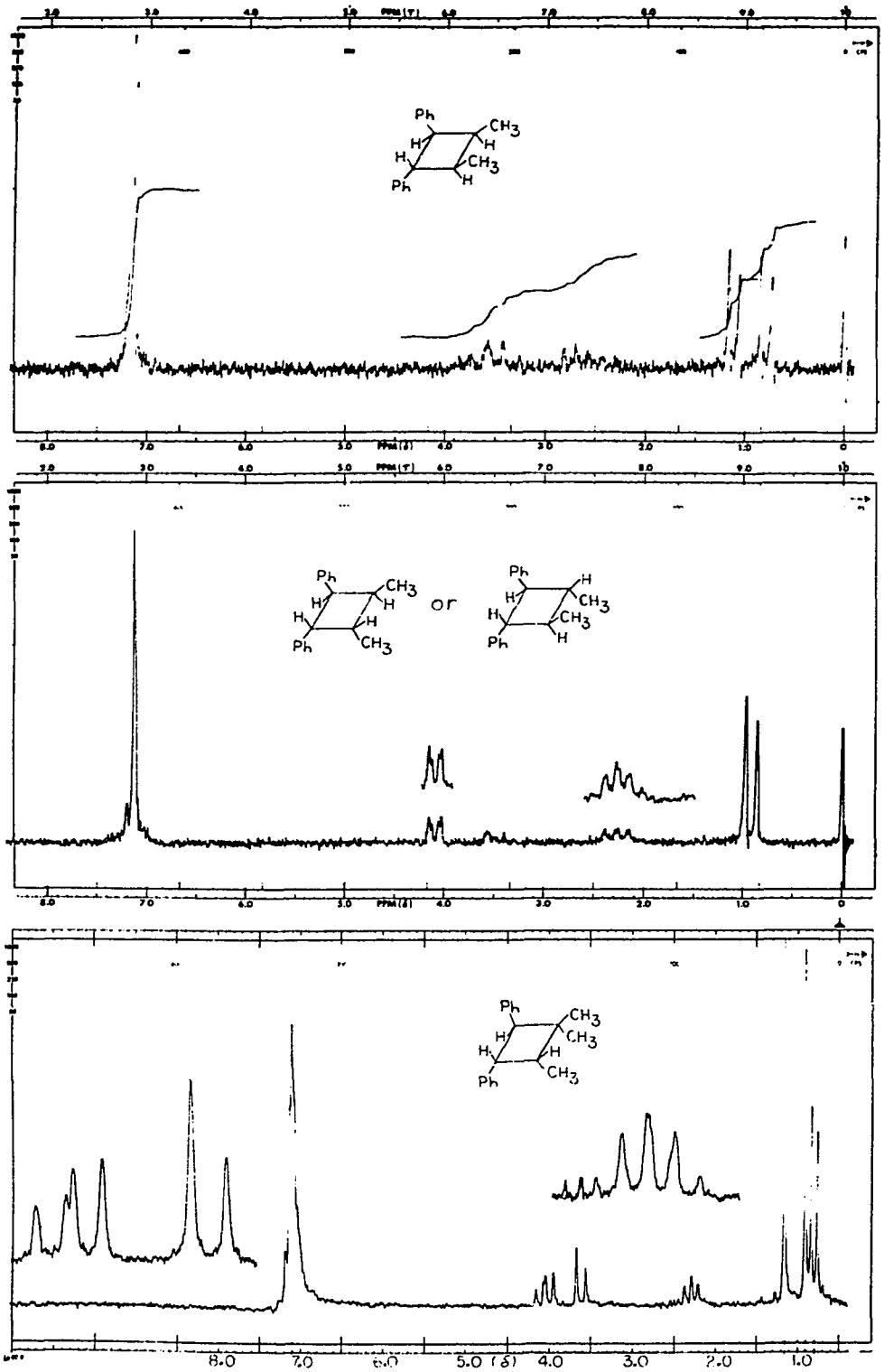
Ph
CH3
H
H
CH3
H
Ph
or
8.0
7.0
6.0
5.0 (δ)
4.0
3.0
2.0
1.0

multiplet centered at 3.50δ integrates for 2 benzylic protons. This positioning is consistent for the benzylic protons of trans-1,2-diphenylcyclobutane (73). A multiplet centered at 2.65δ integrates for 2 methine protons. Two methyl doublets (J 8 Hz) appear at 0.80 and 1.15δ, each integrating for three protons. The position of the methyl resonances is consistent with the two type of methyl groups from the TME adduct (72). The methyl group centered at 0.80δ is assigned cis to the phenyl group as it would be expected to be in the shielding cone of the phenyl ring (74).

trans-Stilbene irradiated in the presence of trans-2-butene afforded one photoadduct, in low quantum efficiency. The structure of the adduct was determined to be either trans-1,2-diphenyl-syn-trans-3,4-dimethylcyclobutane 50 or trans-1,2-diphenyl-anti-trans-3,4-dimethylcyclobutane 51 from spectral evidence. The infrared spectrum (Figure 12)

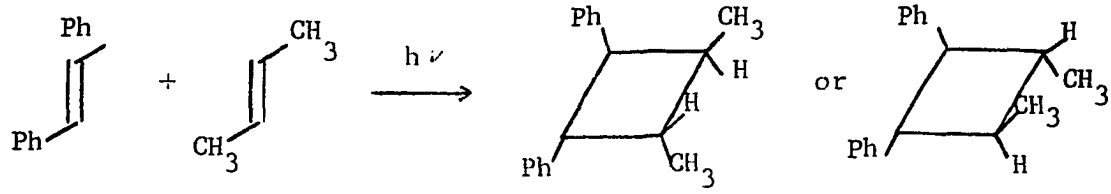

50 51

shows absorptions at 3.30, 3.45, 5.15, 5.35, 5.55, 5.80, 6.23, 6.68, 6.93, 7.28 and 9.74μ, again very similar to the TME adduct (72). The mass spectrum (Table 2) indicates a 1:1 adduct m/e 236, trace. The base peak, as in the cis-2-butene adduct, is m/e 118. The next largest peak

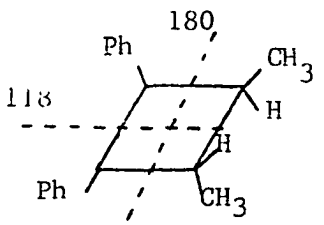

is the molecular ion of stilbene, m/e 180. The other fragmentations results from fragmentations similar to those obtained for stilbene itself. The nmr spectrum (Figure 13) reveals a sharp singlet at 7.13δ, integrating for 10 aromatic protons. The benzylic protons appear as two doublets (J=1.5Hz) at 4.03 and 4.15δ , integrating for a total of two protons. The 1.5 Hz coupling is assigned between benzylic and methine proton, with no coupling between the benzylic protons. A multiplet centered at 2.20δ , integrating for two methine protons, shows coupling constants of 1.5 Hz, to the benzylic proton, and 8Hz, methyl and possibly methine coupling. The multiplet is insufficiently resolved for complete analysis. The methyl signal appears as one doublet (J=8Hz) centered at 0.95δ , integrating for 6 protons. The positioning of the methyl doublet almost exactly between that of the two from the cis-2-butene adduct precludes a decision between structures 50 or 51. Assignment of the structure on the basis of coupling constants in four membered rings is at best highly tenuous (75).

From the nmr spectrum of the cis-2-butene adduct 49, it is obvious that there are two magnetically different methyl groups and from the nmr spectrum of the trans-2-butene adduct 50 or 51 it can be seen that

both methyl groups are magnetically equivalent. Therefore, the assignment of the exact structure to the trans-2-butene adduct is not essential to the stereochemical argument of the addition mechanism.

Two stereochemical addition mechanisms are possible based solely on the nmr methyl signals of the 2-butene adducts as shown in Figure 14.

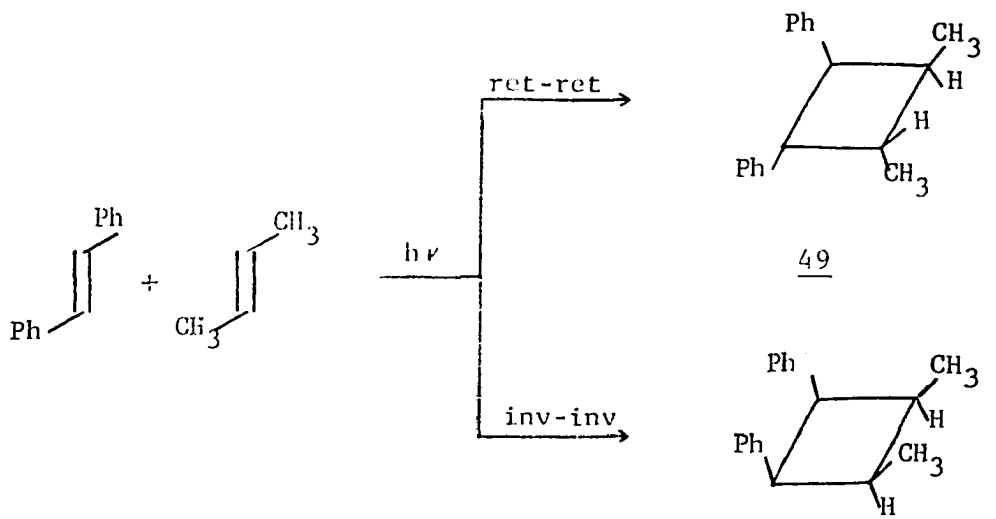

Figure 14. Possible stereochemical mechanisms of cycloaddition

The reaction may proceed with retention of stereochemistry with respect to both the stilbene and olefin, ret-ret, which produced two magnetically different methyls in the case of cis-2-butene adduct 49. The other possibility involves inversion of stereochemistry with respect to both stilbene and 2-butene, inv-inv, again two magnetically different methyl groups are formed. The possibility of the inv-inv mechanism operating is not in agreement with the findings of Adams (72). However, it can be categorically eliminated by the findings of the additions of

1,2-dimethylcyclohexene, 1,2-dimethylcyclopentene and 2-methyl-2-butene to trans-stilbene.

Irradiating trans-stilbene in the presence of 2-methyl-2-butene produced two adducts in a 3:1 ratio. The major adduct 52 was identified

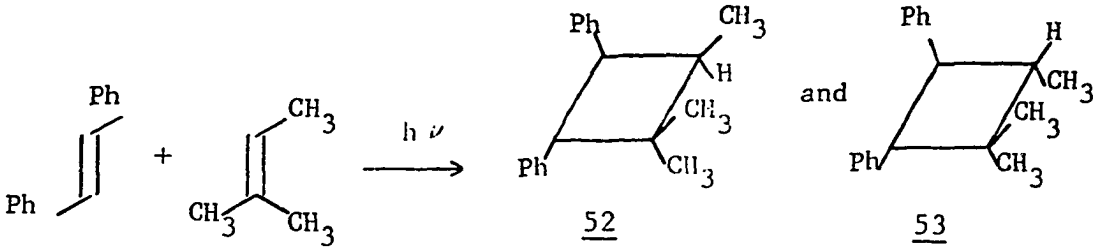

as trans-1,2-diphenyl-cis-3-methyl-4,4-dimethylcyclobutane on the basis of spectral evidence. The infrared spectrum (Figure 12) shows absorptions at 3.32, 3.34, 3.36, 3.42, 3.47, 5.15, 5.35, 5.55, 5.75, 6.23, 6.62, 6.90, 7.23, 9.60, 13.0, 13.3, 13.8 and 14.3μ, consistent with the absorptions observed by Adams for the TME adduct (72). The mass spectrum (Table 2) reveals a 1:1 adduct m/e 250, trace. The base peak is the molecular ion of stilbene, m/e 180. Peaks at m/e 118 and 132

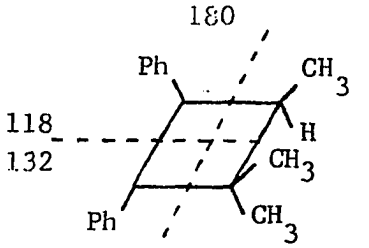

arise from the cleavage of the cylobutane to the β-substituted styrenes. The nmr spectrum (Figure 13) shows a singlet at 7.11δ, integrating for 10 aromatic protons. The benzylic protons appear as an ABX pattern at 3.5-4.15δ (J_{AB}=5.5 Hz, J_{BX}=6 HZ), integrating for

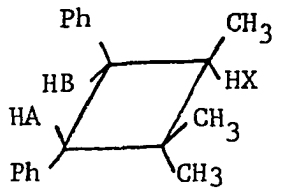

2 protons. The methine proton appears as a multiplet at 2.10-2.50δ, integrating for one proton. The methyl region exists as two sharp singlets at 0.91 and 1.16δ and a doublet (J=6 Hz) at 0.80δ, integrating for a total of 9 protons. The methyl doublet at 0.80δ is attributed to the methyl cis to the phenyl group.

The minor adduct 53 was identified as trans-1,2-diphenyl-trans-3-methyl-4,4-dimethylcyclobutane on the basis of spectral data. It was not possible to isolate the minor adduct in pure form. A 1:1 mixture of major and minor adduct was used for the spectral identification of the minor adduct. The infrared spectrum of the mixture (Figure 15) reveals absorptions at 3.32, 3.34, 3.36, 3,42, 3.47, 5.15, 5.35, 5.55, 5.75, 6.22, 6.68, 6.90, 7.23, 9.60, 12.4, 13.8 and 14.3μ. The absence of any new absorptions indicates that the structure of the two adducts must be very similar. The mass spectrum (Table 3) of the mixture exhibits the same fragmentation patterns as that of the pure major adduct. This would be expected if the structures of the adducts are as similar as

Figure 15. Infrared spectra

Top: trans-1,2-diphenyl-cis-3-methyl-4,4-dimethylcyclobutane and trans-1,2-diphenyl-trans-3-methyl-4,4-dimethylcyclobutane

Bottom: 1,2-diphenyl-3,4,4-trimethyl-cyclobutene

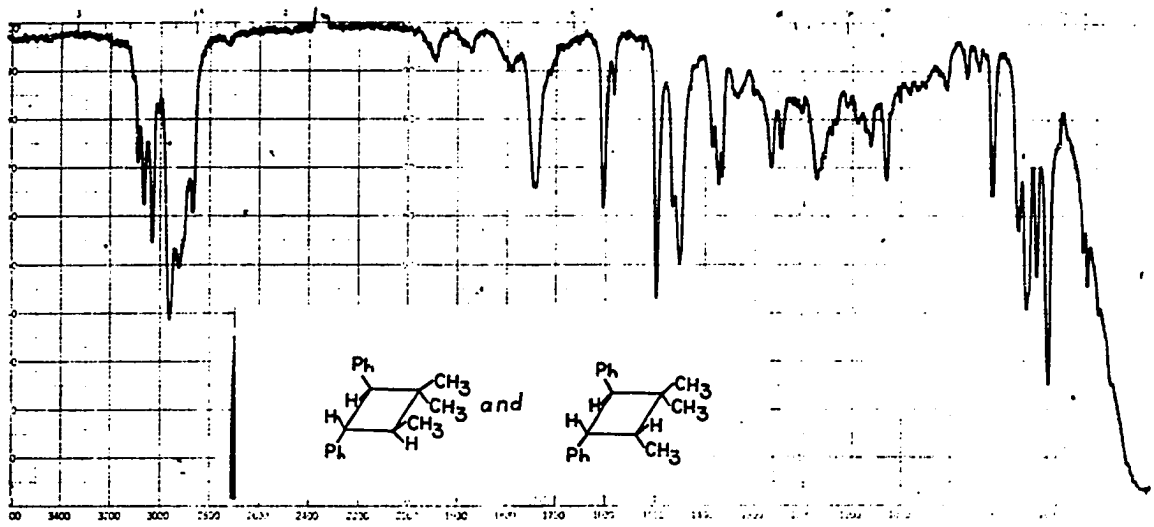
Ph
H
H
Ph
CH3
CH3
CH3
H
and
Ph
H
H
Ph
CH3
CH3
H
CH3

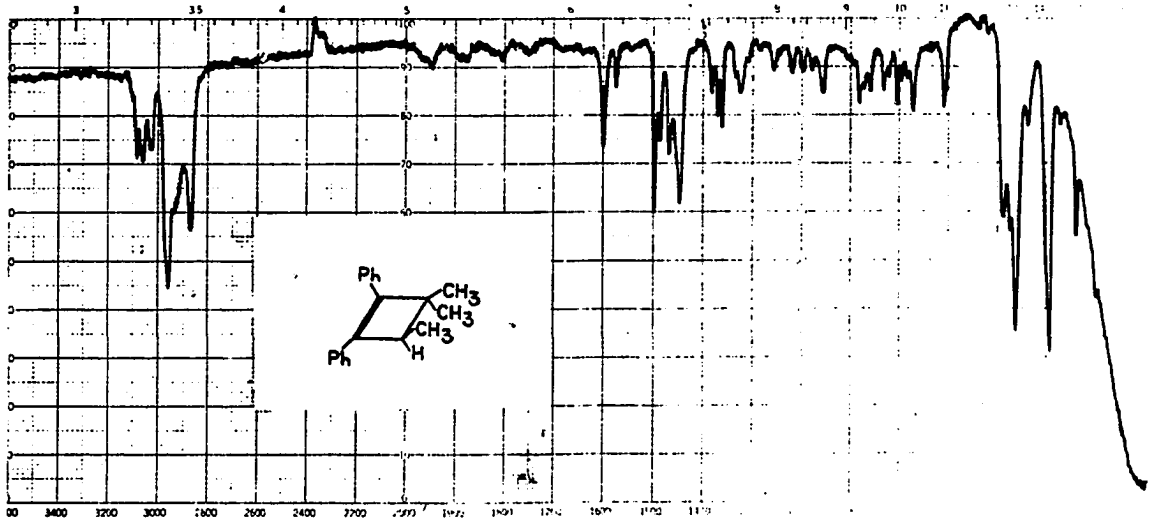
Ph
Ph
CH3
CH3
CH3
H

Figure 16. Nuclear magnetic resonance spectra

Top: trans-1,2-diphenyl-cis-3-methyl-4,4-dimethylcyclobutane and trans-1,2-diphenyl-trans-3-methyl-4,4-dimethylcyclobutane

Middle: trans-1,2-diphenyl-trans-3-methyl-4,4-dimethylcyclobutane (by difference)

Bottom: 1,2-diphenyl-3,4,4-trimethylcyclobutene

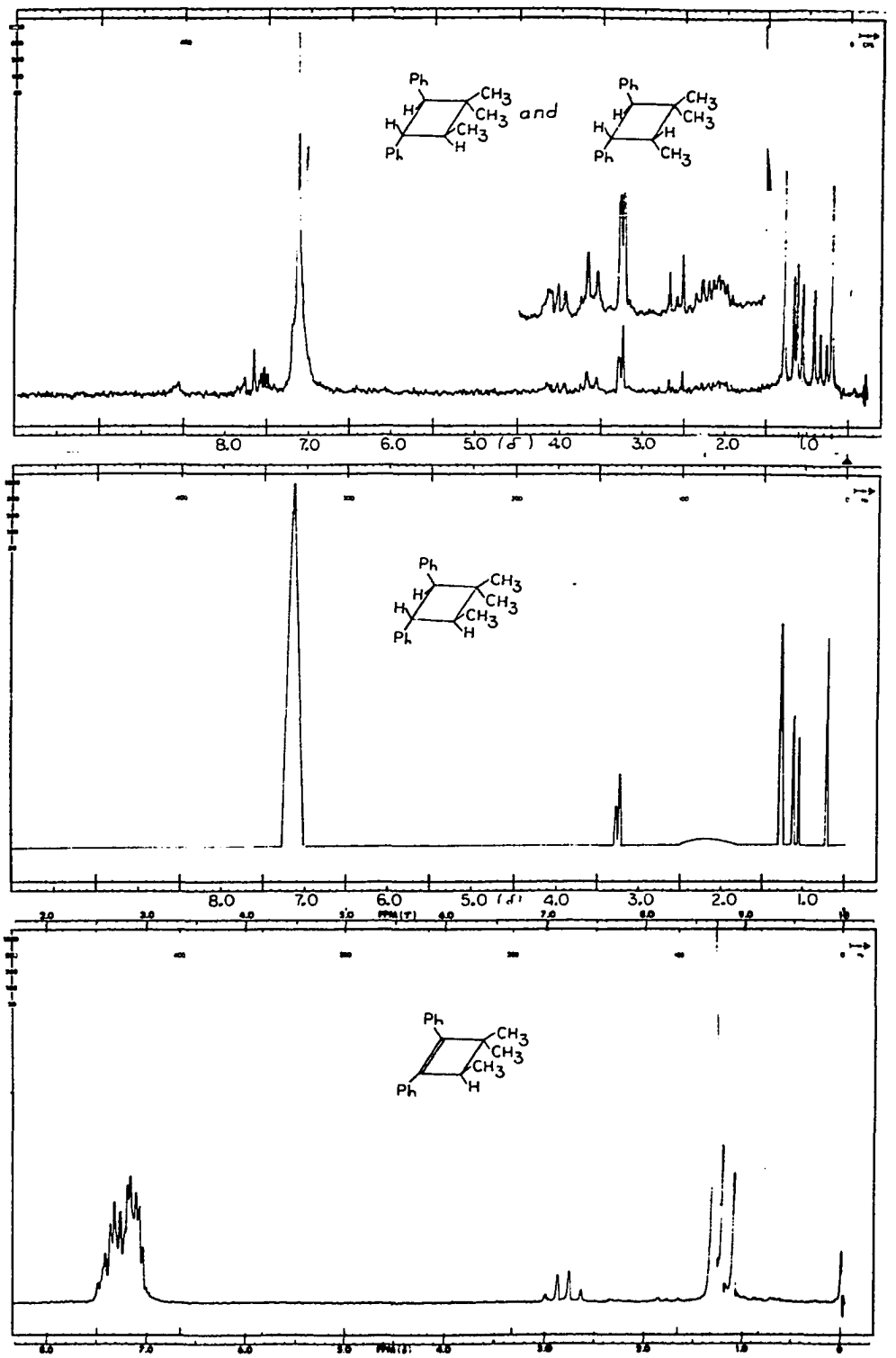
Ph
CH3
H
CH3
CH3
H
Ph
and
8.0
7.0
6.0
5.0 (δ)
4.0
3.0
2.0
1.0

Table 3. Mass spectra of adducts 52 and 53, 54 and 56

52 and 53		54		56	
m/e	rel. int.	m/e	rel. int.	m/e	rel. int.
250	trace	249	20.0	290	trace
181	28.0	248	100.0	275	trace
180	100.0	234	13.4	260	trace
179	50.0	233	76.7	181	16.6
178	29.0	219	12.0	180	100.0
177	5.0	218	50.0	179	20.0
176	5.0	203	20.0	178	12.2
133	3.0	178	33.3	177	2.2
132	17.5	91	6.0	110	3.2
118	3.5			91	4.4
117	10.0			77	3.3
91	10.0				
77	9.0				

those proposed for 52 and 53. The nmr spectrum of the mixture (Figure 16) integrates for the proper number of the respective types of protons present in the expected 1:1 photoadduct. The separated spectrum of the minor product (Figure 16) obtained by subtracting the peaks known to belong to the major adduct from the signals in the mixture spectrum. The aromatic hydrogens appear as a sharp singlet at 7.12 δ. The benzylic protons appear as a sharp singlet at 3.20δ and a doublet (J=1.5 Hz) at 3.28 δ. The methine proton exists in the region 2.10-2.60δ. Methyl

resonances appear as a singlet at 0.70δ, a doublet (J=7 Hz) centered at 1.16δ and a singlet at 1.28δ. The methyl doublet at 1.16δ is assigned to the methyl group trans to the phenyl ring.

The two adducts were shown to be stable under the irradiation conditions (Table 21). The mixture of adducts was irradiated in the presence and absence of trans-stilbene and shown not to change the product ratio after irradiation. The stability of the adducts eliminates the type of conversion of 1,2-diphenyl cyclobutanes discovered by Brown and Markezick (76), as in equation 8.

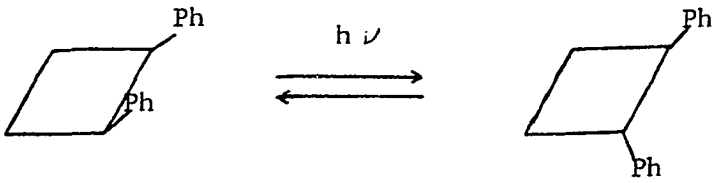

(8)

Verification of the trans nature of the phenyl groups in the two adducts was obtained from the reduction of 1,2-diphenyl-3,4,4-trimethylcyclobutene by the procedure of Johnson et al. (77) Diphenylacetylene was irradiated in the presence of 2-methyl-2-butene to produce an adduct, identified as 1,2-diphenyl-3,4,4-trimethylcyclobutene 54 on the basis of spectral data. The infrared spectrum (Figure 15) reveals absorptions at 3.32, 3.34, 3.36, 3.45, 3.48, 6.25, 6.90, 7.30, 13.4 and 14.2μ. This spectrum is similar to that obtained for 1, 2-diphenyl-3-3,4,4-tetramethylcyclobutene (72). The mass spectrum (Table 3) shows a 1:1 adduct, m/e 248, 100%. Peaks at m/e 233, 218 and

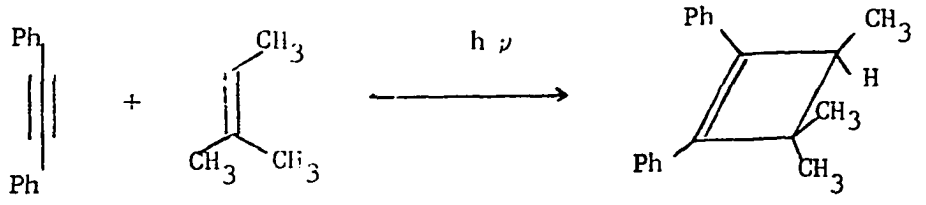

54

203 result from loss of the methyl groups from the parent ion. The peak at m/e 178 is the molecular ion of diphenylacetylene. The nmr spectrum (Figure 16) shows a complex aromatic multiplet at 7.0-7.5δ, integrating for 10 protons. A methine quartet (J=6 Hz) centered at 2.30δ integrates for 1 proton. The methyl resonances consist of a sharp singlet at 1.30δ and a doublet (J=6 Hz) centered at 1.17δ, integrating for 9 protons. The position of 1.30δ for the gem-dimethyl group is consistent with that for the gem-dimethyl in 1,2-diphenyl-3,3,4,4-tetramethylcyclobutene (72).

The cyclobutene was treated with potassium in liquid ammonia to yield three products. Two of the products had partially overlapping peaks in the gas chromatographic spectrum and were collected together. The gas chromatographic retention times on several columns and the nmr spectrum (Figure 18) of this mixture was identical to that of the mixture of authentic photoadducts 52 and 53. The reduction of the double bond by potassium and liquid ammonia is known to proceed via trans reduction Therefore obtaining the same two adducts from the reduction of the cyclobutene as from the photoaddition verifies the trans nature of the phenyl groups in both adducts.

The third product obtained from the reduction was assigned to a ring opened product 55 on the basis of the mass spectrum, which has a molecular ion m/e 252 compared to 250 for the cyclic compounds. The nmr spectrum has several features which also eliminate a cyclic compound.

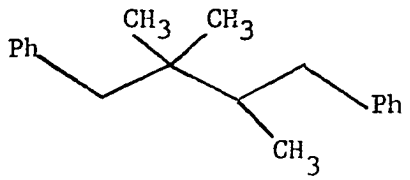

55

The total integration for the methine and benzylic protons is five protons, not the three required by a cyclic system. The methyl region exists as a singlet at 0.70δ and a doublet centered at 0.60δ, integrating for 9 protons. A ring system is not consistent with one singlet and a doublet in the methyl region.

The irradiation of trans-stilbene in the presence of 1,2-dimethyl-cyclohexene produced one adduct, in high quantum efficiency. The adduct was assigned the structure cis-1,6-dimethyl-7-endo-8-exo-diphenyl-bicyclo [4.2.0] octane 56 on the basis of spectral data. The

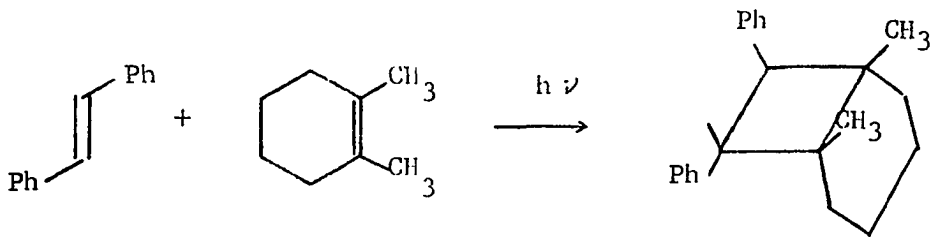

56

infrared spectrum (Figure 17) shows absorptions at 3.32, 3.34, 3.36, 3.40, 3.45, 6.21, 6.63, 6.92, 7.25, 7.99, 9.70 and 11.53μ. The mass spectrum (Table 3) reveals a 1:1 adduct m/e 290, trace. Peaks at m/e 290 and 275 result from loss of the methyl groups of the photoadduct. As expected for such an adduct the base peak is that from the splitting out of stilbene m/e 180. The nmr spectrum (Figure 18) shows a singlet at 7.12δ, integrating for 10 aromatic protons. The benzylic protons appear as two singlets at 3.70 and 3.76δ, integrating for 2 protons. A broad structureless peak from 1.1-1.9δ, with a sharp singlet at 1.21δ, integrates for 14 protons. The second methyl singlet appears at 0.75δ, integrating for 3 protons. The high field methyl is assigned cis to the phenyl ring.

Irradiation of trans-stilbene in the presence of 1,2-dimethyl-cyclopentene produced one photoadduct, in high quantum efficiency. The structure of the adduct was determined to be cis-1,5-dimethyl-6-endo-7-exo-diphenyl-bicyclo [3.2.0] heptane 57 on the basis of spectral data.

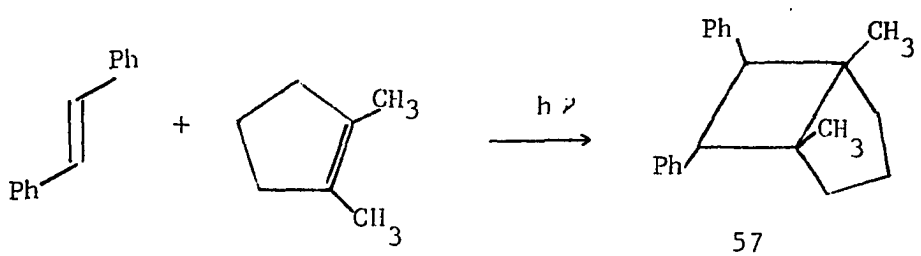

57

The infrared spectrum (Figure 17) showed absorptions at 3.32, 3.34, 3.36, 3.40, 3.45, 6.21, 6.63, 6.95, 7.30, 9.80, 13.7, 13.8 and 14.6μ. The mass spectrum (Table 4) revealed a 1:1 adduct m/e 276, 1%. Peaks

Figure 17. Infrared spectra

Top: cis-1,6-dimethyl-7-endo-8-exo-diphenyl-bicyclo [4.2.0] octane

Bottom: cis-1,5-dimethyl-6-endo-7-exo-diphenyl-bicyclo [3.2.0] heptane

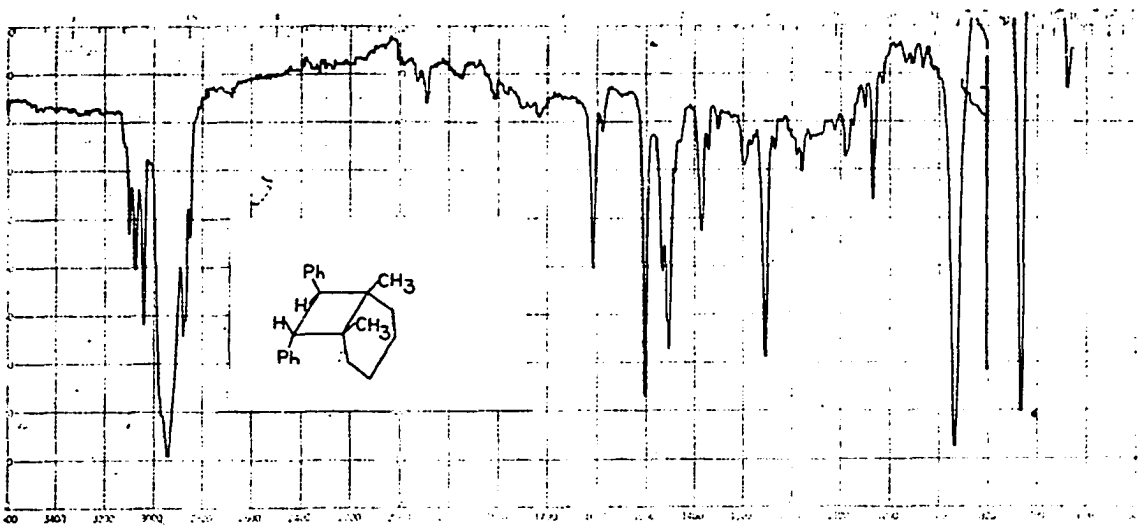
Ph
CH3
H
H
CH3
Ph

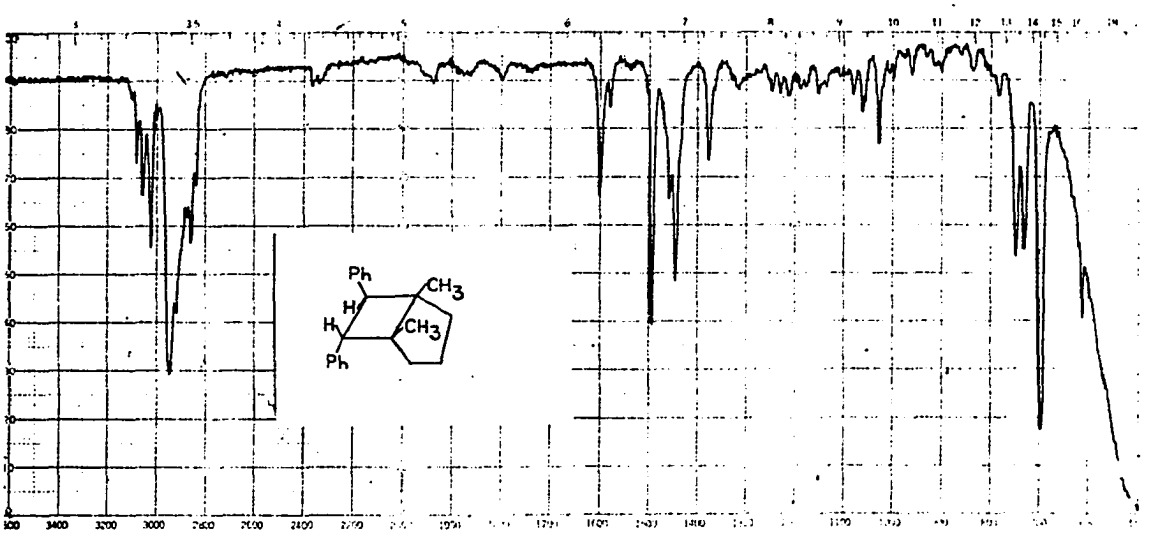
Ph
CH3
H
H
CH3
Ph

Figure 18. Nuclear magnetic resonance spectra

Top: trans-1,2-diphenyl-cis-3-methyl-4,4-dimethylcyclobutane and trans-1,2-diphenyl-trans-3-methyl-4,4-dimethylcyclobutane

Middle: cis-1,6-dimethyl-7-endo-8-exo-diphenyl-bicyclo [4.2.0]octane

Bottom: cis-1,5-dimethyl-6-endo-7-exo-diphenyl-bicyclo [3.2.0] heptane

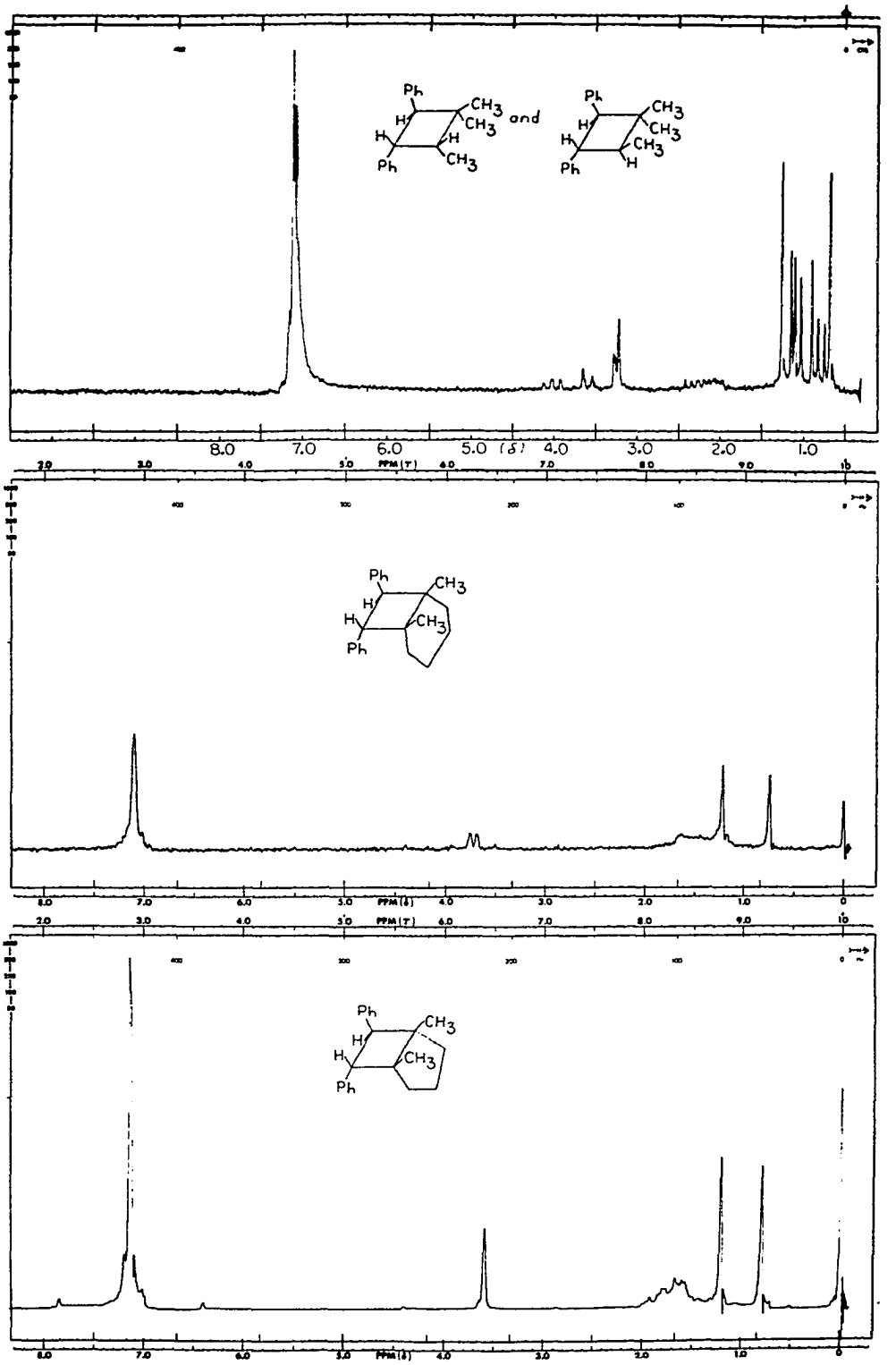
Ph
CH3
H
CH3
H
H
CH3
Ph
and
Ph
CH3
H
CH3
H
CH3
Ph
8.0
7.0
6.0
5.0 (δ)
4.0
3.0
2.0
1.0
PPM(τ)
Ph
CH3
H
H
CH3
Ph
PPM(δ)
Ph
CH3
H
H
CH3
Ph
PPM(δ)

Table 4. Mass spectra of adducts 57, 58 and 59

m/e	57 rel. int.	m/e	58 rel. int.	m/e	59 rel. int.
276	trace	276	trace	262	25.0
261	trace	261	trace	206	3.0
246	trace	181	20.0	205	10.0
181	12.0	180	100.0	181	14.0
180	100.0	179	26.4	180	100.0
179	15.0	178	12.0	179	60.7
178	12.0	177	2.5	178	50.0
177	2.0	176	2.3	177	5.6
91	3.5	91	5.0	176	6.7
77	2.5	77	3.8	91	4.0

at m/e 261 and 246 are those resulting from loss of the methyl groups from the molecular ion. The base peak m/e 180 is that from the elimination of stilbene. As with the dimethylcyclohexene adduct the favored fragmentation would be the elimination of stilbene. The nmr spectrum (Figure 18) shows a sharp singlet at 7.13δ, integrating for 10 aromatic protons. The benzylic protons appear as a sharp singlet at 3.53δ, integrating for 2 protons. A broad structureless band from 1.30-2.10δ integrates for 6 methylene protons. Two sharp methyl singlets at 1.21 and 0.80δ integrate for three protons each.

Again analyzing from the point of view of the methyl groups the presence of two methyl resonances in the spectra of 56 and 57 reinforces the ret-ret or inv-inv mechanism. Inv-inv can be eliminated on

the basis of the rapid formation of the bicyclic adducts. For the inv-inv mechanism to operate, trans-bicyclo [4.2.0] octane and trans-bicyclo [3.2.0] heptane systems must be formed. The formation of the trans [3.2.0] system is totally unacceptable on steric grounds. Therefore the cycloaddition can be shown to proceed with retention of stereochemistry of both the excited and ground state partners.

The total stereospecificity of the reaction limits the overall mechanism to the three possibilities shown in Figure 19. Two

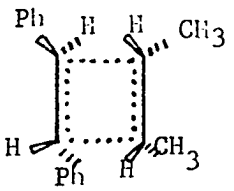

Concerted

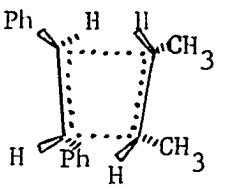

quasi-Concerted

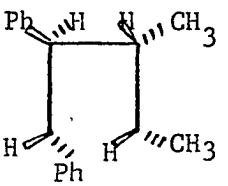

Diradical

Figure 19. Possible mechanisms for ret-ret reaction

possibilities involve degrees of a concerted reaction, which are in agreement with stereochemical preditions based on orbital symmetry considerations (78). A fully concerted reaction involves the simultaneous, equal formation of the two new sigma bonds, that is equal overlap of the p orbitals in both forming bonds. The quasi-concerted mechanism involves simultaneous formation of the two sigma bonds, but with one

having a higher degree of obital overlap than the other. The third mechanism can be visualized as an extreme of the quasi-concerted mechanism, one sigma bond is fully formed before the second has any appreciable p orbital overlap. This results in the formation of a 1,4-diradical which must now close before rotation around the sigma bonds can destroy the stereochemistry.

Calculation on cycloadditions indicate the quasi-concerted mechanism is preferred over the fully concerted mechanism (79). This can be rationalized on the basis of a quasi-concerted reaction allowing a higher number of orientations of the two approaching molecules. The mechanism has all the fully concerted modes plus the varying angles of approach which do not allow equal overlap, yet do allow partial overlap of both sets of interacting p orbitals.

A diradical mechanism would require a very high rate constant of closure, such that $k_{closure} >> k_{rotation}$. In light of the known information on rates of diradical closure, the diradical mechanism is not considered probable (see REVIEW OF LITERATURE section). Therefore a quasi-concerted mechanism is favored for adduct formation.

The multiplicity of the reactive state of trans-stilbene involved in the cycloaddition can be ellucidated from sensitization data and fluorescence quenching data. Attempts were made to sensitize adduct formation of trans-2-butene, cis-2-butene, tetramethylethylene, 2-methyl-2-butene, 1-methylcyclohexene and cyclohexene to trans-stilbene.

The adduct formed from the addition of trans-stilbene to 1-methylcyclohexene was identified as 1-methyl-7-endo-8-exo-diphenyl-cis-bicyclo [4.2.0] octane 58 on the basis of spectral evidence.

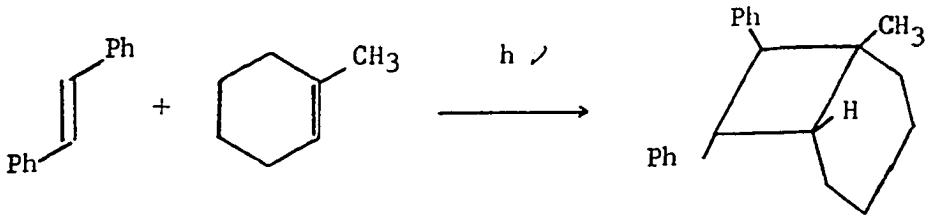

58

The infrared spectrum (Figure 20) reveals absorptions at 3.32, 3.34, 3.36, 3.42, 3.48, 6.21, 6.65, 6.90, 7.30, 9.70, 13.6 and 14.4 μ. The mass spectrum (Table 4) reveals a 1:1 adduct m/e 276, trace. The base peak m/e 180 is derived from the elimination of stilbene. The other major fragmentations are those from the stilbene portion of the molecule. The nmr spectrum (Figure 21) shows a signal at 7.11 δ, integrating for 10 aromatic protons. The benzlic region consists of a complex multiplet at 3.20-4.20 δ, integrating for 12 protons. The methyl singlet appears at 0.88 δ and is therefore assigned cis to the phenyl.

Irradiating trans-stilbene in the presence of cyclohexene produces one adduct, in low quantum efficiency. The adduct, 7-endo-8-exo-diphenyl-cis-bicyclo [4.2.0] octane 59, was identified from spectral

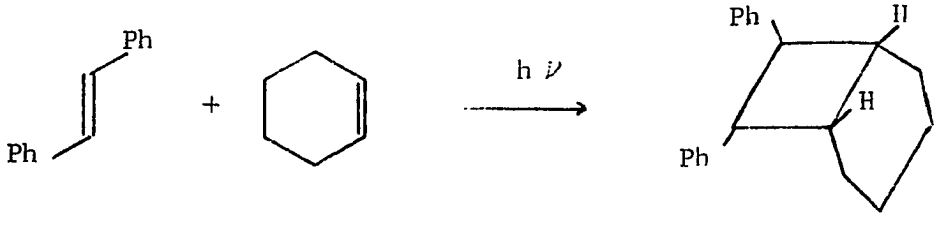

59

data. The infrared spectrum (Figure 20) 3.32, 3.34, 3.36, 3.48, 5.15, 5.30, 5.55, 5.75, 6.21, 6.70, 6.90, 9.70, 13.4 and 14.4μ. The mass spectrum (Table 4) reveals a 1:1 adduct m/e 262, 25%. The peaks at 206 and 205 result from the loss of the four methylenes. The base peak m/e 180 is derived from stilbene. The nmr spectrum (Figure 21) reveals two phenyl singlets at 7.08 and 7.16δ, integrating for a total of 10 aromatic protons. The two signals are due to the different environment of the exo and endo phenyl rings. A multiplet centered at 3.70δ integrates for 2 benzylic protons. A broad region, 1.00-2.80δ, integrates for 10 protons, methylene and methine.

The results of the sensitization experiments are shown in Tables 13, 14, 21, 26 and 32. The experiments were designed such that the sensitizers used were high enough in triplet energy to efficiently transfer to both cis and trans-stilbene, $E_t > 61$ Kcal/mole (80). The sensitizers were also chosen on the basis of having a large extinction coefficient where stilbene possesses a very low extinction, this is to insure that there is no competition for light between the sensitizer and stilbene. The concentration of the sensitizers were such that they absorbed > 99% of the light at the wavelength and bandwidth used. In each case a blank, which contained no sensitizer, was run to demonstrate that adduct formation would occur under the reaction conditions were it not for the absorption of the light by the sensitizer.

All the tables show a small adduct formation in the absence of sensitizer accompanied by the production of cis-stilbene. The presence of sensitizer with TME (Table 14), cis and trans-2-butene (Table 13) and 2-methyl-2-butene (Table 21) results in the formation of cis-stilbene,

Figure 20. Infrared spectra

Top: 7-endo-8-exo-diphenyl-cis-bicyclo [4.2.0] octane

Bottom: 1-methyl-7-endo-8-exo-diphenyl- cis-bicyclo-[4.2.0]octane

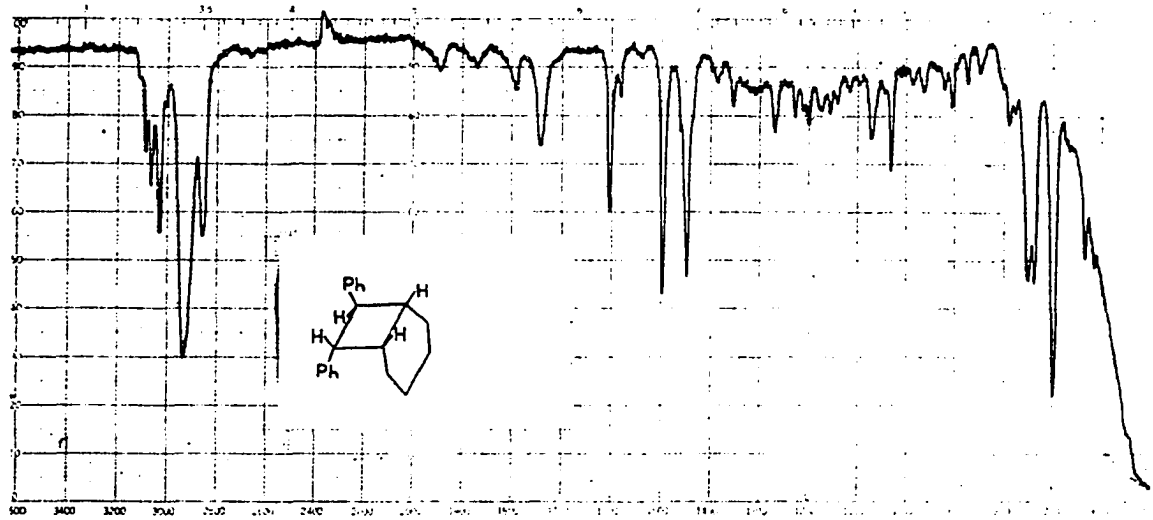
Ph
H
H
H
Ph

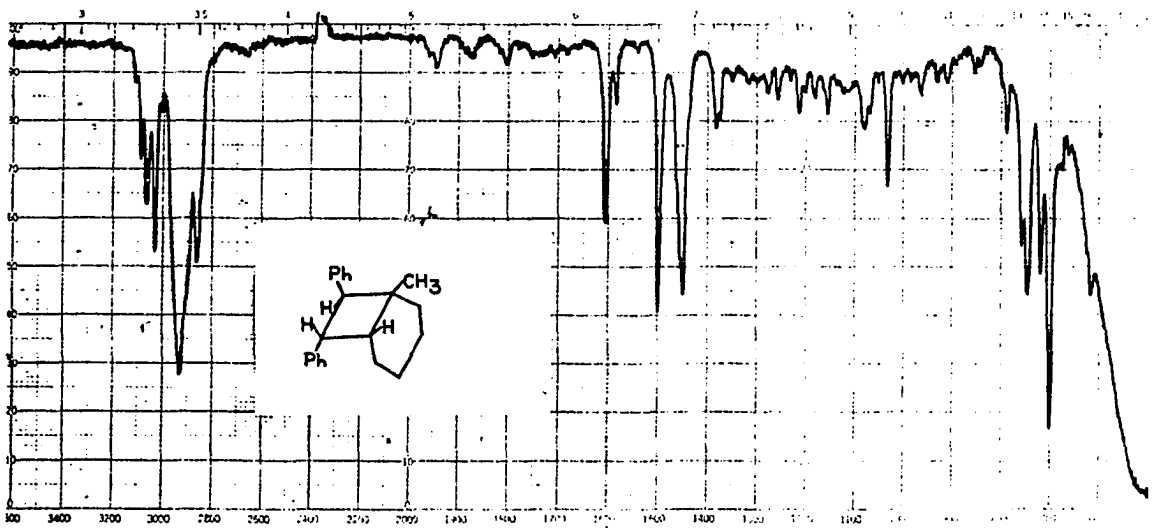
Ph
CH3
H
H
Ph

Figure 21. Nuclear magnetic resonance spectra

Top: 1-methyl-7-endo-8-exo-diphenyl-cis-bicyclo [4.2.0] octane

Bottom: 7-endo-8-exo-diphenyl-cis-bicyclo-[4.2.0] octane

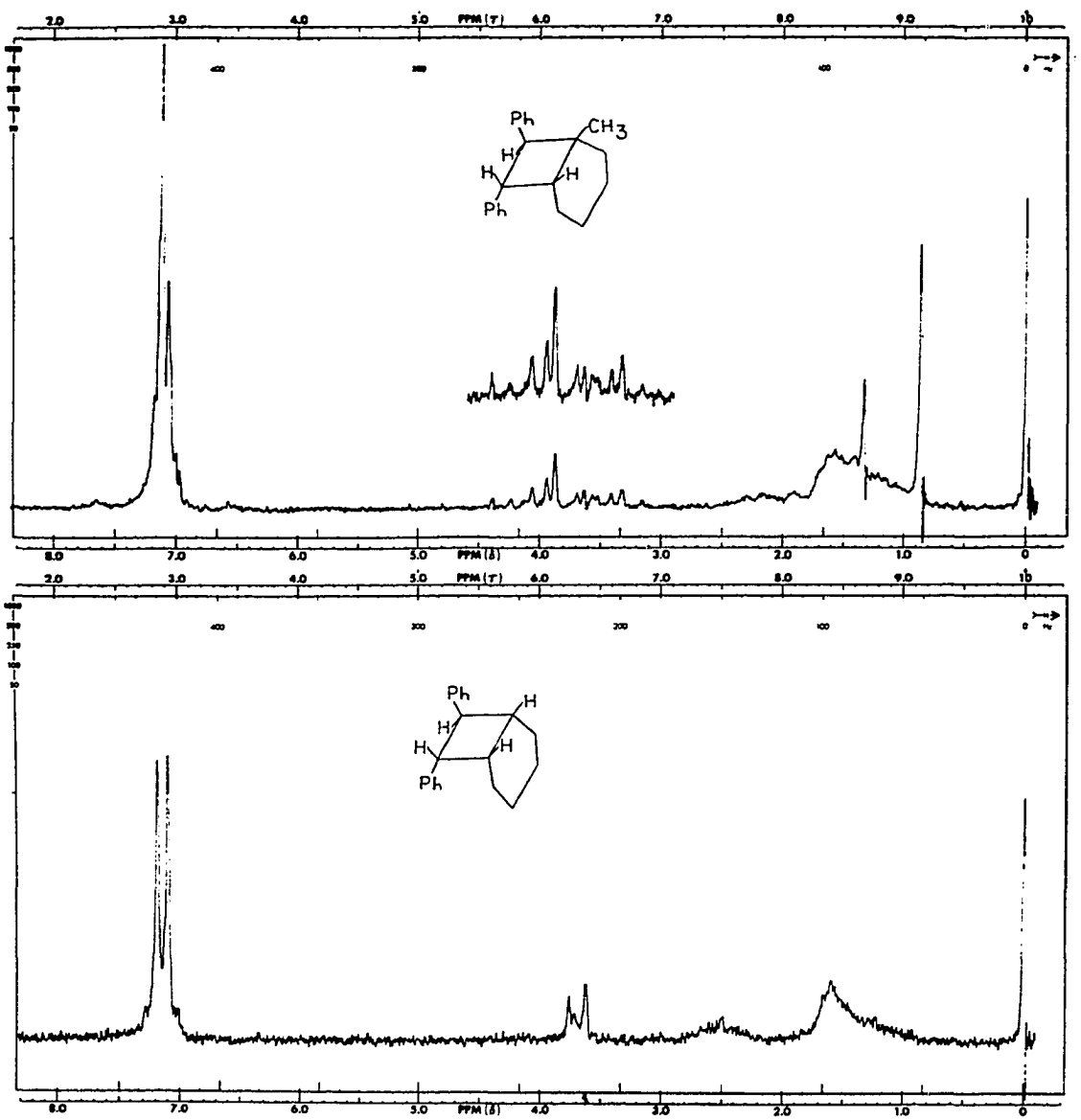
Ph
CH3
H
H
H
Ph
PPM (τ)
PPM (δ)
Ph
H
H
H
H
Ph
PPM (τ)
PPM (δ)

cis:trans 1:1, with total exclusion of adduct formation. The slight adduct formation in the cyclohexene results (Table 32) is probably due to the unusually long irradiation times. The sensitizers, Michler's ketone and thioxanthone, are known to undergo intramolecular photochemical reactions (81). The decomposition of the sensitizers on prolonged irradiation may reduce the absorption of light by sensitizer sufficiently for stilbene to compete for light in the later stages of the irradiation. The stilbene to adduct ratio in the absence of sensitizer is 22:1 compared to 104:1 for thioxanthone and 90:1 for Michler's ketone. These ratios are consistent with the decomposition of sensitizer as a large stilbene to adduct ratio would be expected as adduct is produced only in the later stages of the reaction and would therefore be in low concentration. The thioxanthone sensitization results for 1-methylcyclohexene (Table 20) are anomolous and at this time cannot be explained. However, Michler's ketone exhibits the same sensitizing properties it does in the presence of the other olefins.

The sensitization results would indicate either a singlet reaction of one proceeding from an upper triplet, $E_t > 70$ Kcal/mole. Reactions proceeding from upper triplets have been reported recently . (82, 83 and 84). An upper triplet is also involved in Fischer's mechanism for isomerization of stilbene (28).

A higher energy triplet participating in the reaction can be eliminated on the basis of the quenching of trans-stilbene fluorescence by several olefins. Stern-Volmer plots of fluorescence quenching are shown in Figure 22 for TME, Figure 23 for 2-methyl-2-butene, and Figure 24 for 1-methylcyclohexene. At 4 molar olefin concentration TME is

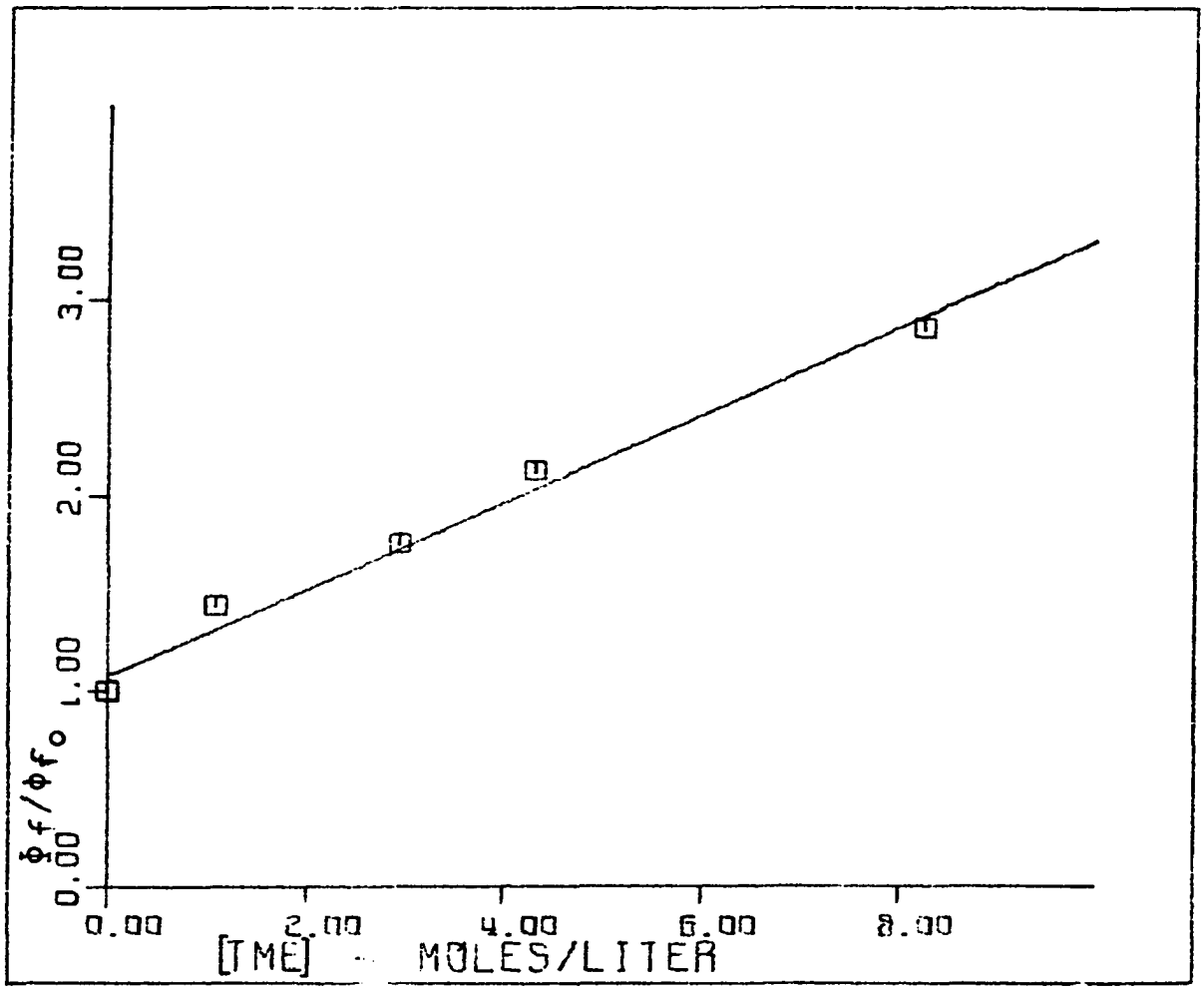

Figure 22. Stern-Volmer plot for fluorescence quenching by TME

Slope = 0.22 ± 0.01 M^{-1}

Intercept = $1.08 \pm .05$

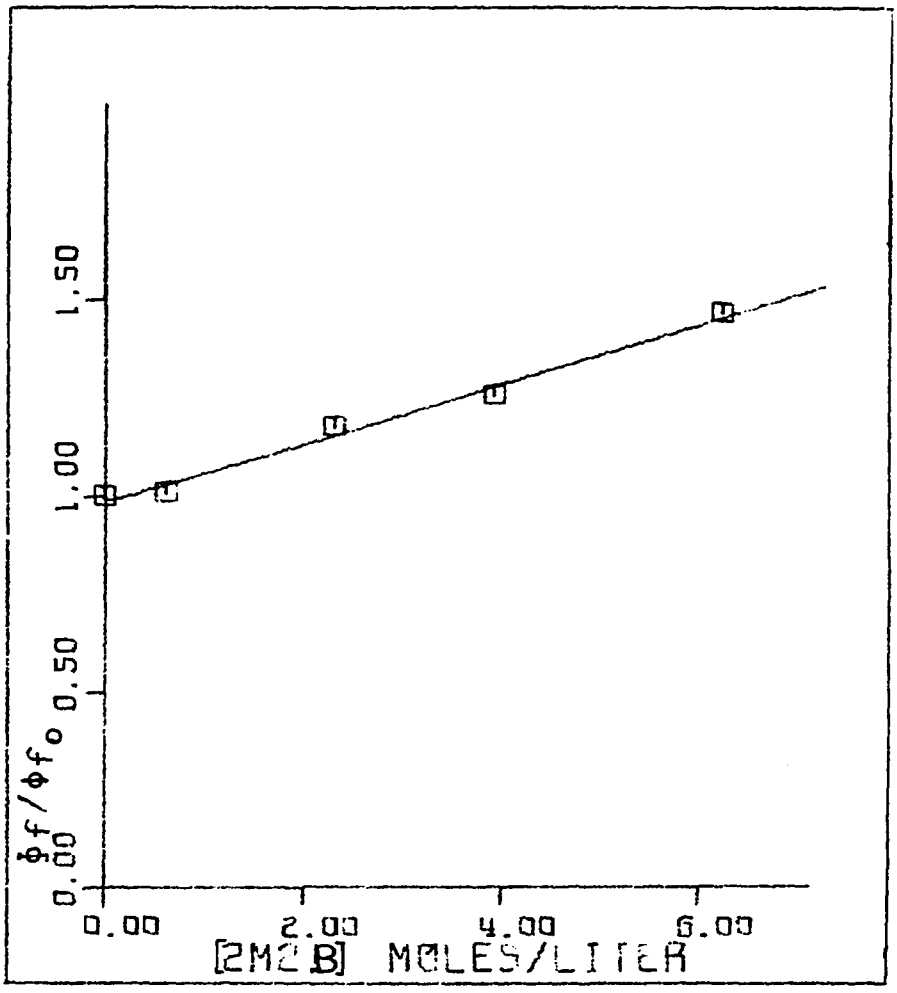

Figure 23. Stern-Volmer plot of fluorescence quenching by 2-methyl-2-butene

Slope = 0.076 ± 0.004 M^{-1}

Intercept = 0.98 ± 0.02

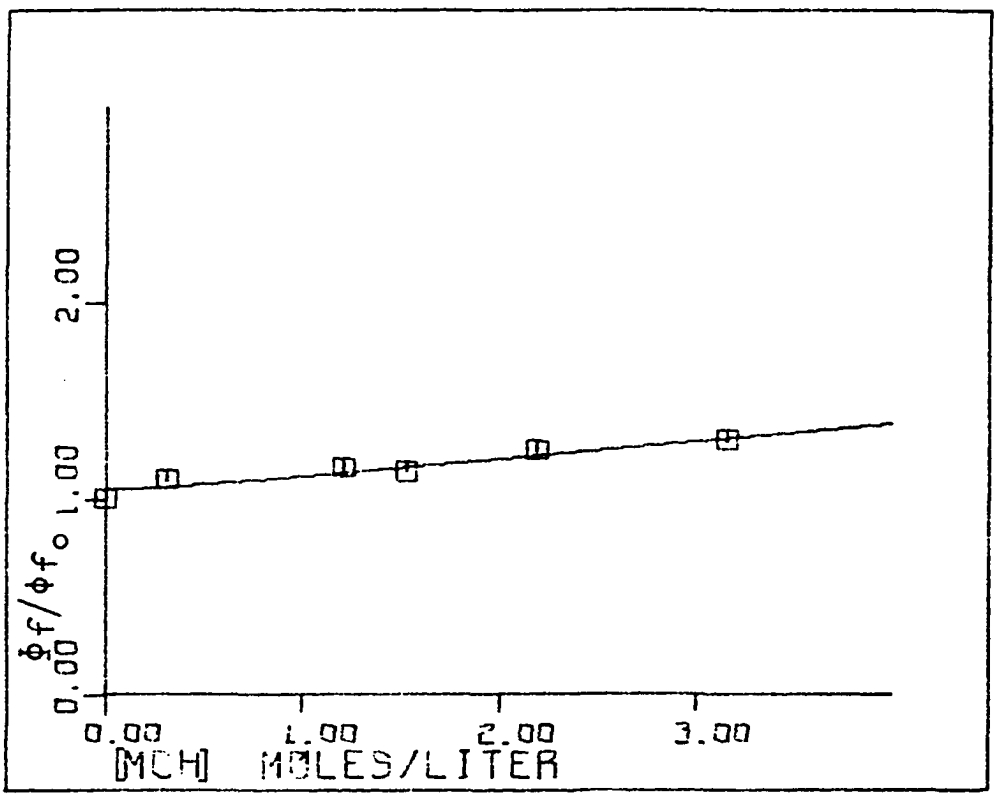

Figure 24. Stern-Volmer plot of fluorescence quenching by 1-methylcyclohexene

Slope = 0.087 ± 0.013 M^{-1}

Intercept = 1.03 ± 0.02

seen to quench 50% of trans-stilbene fluorescence, while the quantum yield of adduct formation, Φ_{add}, is 0.54, or 54% efficient, in good agreement for adduct formation resulting from the process quenching trans-stilbene fluorescence. In 4 molar concentration 2-methyl-2-butene quenches 20% of the fluorescence, while the value of Φ_{add} is 0.10, 10% efficient. Under the same conditions, 1-methylcyclohexene quenches 20% of the fluorescence while the value of Φ_{add} is 0.043, 4%. In all cases fluorescence quenching is accompanied with adduct formation, verifying a singlet mechanism.

The mechanism of fluorescence quenching is similar to that proposed by Hammond and coworkers (63) to account for endothermic quenching of aromatic hydrocarbon fluorescence, quenching by molecules which do not possess a singlet below that of the fluorescing compound. The singlet energy of TME, 2-methyl-2-butene and cyclohexene are 145, 148, and 152 kcal/mole respectively (85). An exciplex is formed upon interaction of the excited trans-stilbene molecule with the ground state molecule (equation 9), as singlet-singlet energy transfer, to account for the fluores-

$$^1S_t + 0 \rightarrow {}^{k_e}- \text{Exciplex} \qquad (9)$$

cence quenching, is energetically impossible. A ground state complex has been shown not to be involved as the UV absorption spectrum of trans-stilbene is not altered by adding TME.

The exciplex once formed can have several decay modes as are shown in Figure 25. The exciplex may undergo radiationless decay producing cis and trans-stilbene (equation 10 and 11) in analogy to the naphthalene sensitized isomerization of quadricyclene to norbornadiene (63). The exciplex may dissociate to singlet trans-stilbene and ground state olefin

$$\text{Exciplex} \xrightarrow{k_{cd_t}} S_t + 0 \qquad (10)$$

$$\text{Exciplex} \xrightarrow{k_{cd_c}} S_c + 0 \qquad (11)$$

$$\text{Exciplex} \xrightarrow{k_{-e}} {}^1S_t + 0 \qquad (12)$$

$$\text{Exciplex} \xrightarrow{k_{-e_p}} {}^1S_p + 0 \qquad (13)$$

$$\text{Exciplex} \xrightarrow{k_a} \text{Adduct} \qquad (14)$$

Figure 25. Decay modes of the exciplex

(equation 12) in agreement with the mechanism of McDonald and Selinger (69). Dissociation of the exciplex to singlet cis-stilbene and ground state olefin is not considered important due to the higher singlet energy of cis-stilbene compared to trans-stilbene, 12 kcal/mole. The exciplex can decay to produce twisted "phantom" singlet and ground state olefin (equation 13). This decay mode is consistent with the proposed isomerization mechanism for stilbene of Saltiel and Megarity (32). Finally the exciplex may deactivate to form adduct (equation 14).

The modes of reaction of the exciplex can be determined by analyzing the expected rate equations for one possible mechanism presented in Figure 26 and comparing these to experimentally available quantities. The mechanism involves initial excitation of trans-stilbene to the singlet (equation 15). The singlet can undergo first order deactivation processes radiationless decay (equation 16), fluorescence (equation 17), intersystem crossing (equation 18), and isomerization from the singlet (equation 19), in accord with the Saltiel mechanism (32). Phantom singlet can react with ground state olefin to form the exciplex (equation 20). It is proposed, in this case, that the same exciplex is formed from

$$S_t \longrightarrow {}^1S_t \qquad (15)$$

$${}^1S_t \xrightarrow{k_d} S_t \qquad (16)$$

$${}^1S_t \xrightarrow{k_f} S_t + h\nu_f \qquad (17)$$

$${}^1S_t \xrightarrow{k_{ic}} {}^3S_t \qquad (18)$$

$${}^1S_t \xrightarrow{k_i} S_c \qquad (19)$$

$${}^1S_t + 0 \xrightarrow{k_e} Ex$$

$$Ex \xrightarrow{k_{cd_t}} S_t + 0$$

$$Ex \xrightarrow{k_{cd_c}} S_c + 0$$

$$Ex \xrightarrow{k_{-e}} {}^1S_t + 0$$

$$Ex \xrightarrow{k_{-e_p}} {}^1S_p + 0$$

$$Ex \xrightarrow{k_a} Adduct$$

$${}^1S_p + 0 \xrightarrow{k_{e_p}} Exciplex \qquad (20)$$

$${}^1S_p \xrightarrow{k_i} S_t + S_c$$

Figure 26. Possible mechanism of adduct formation

phantom as from trans-stilbene. The decay modes of the exciplex have been discussed previously. The equation for $1/\Phi_{add}$ is given by equation 21.

Quantum yield measurements were conducted on several olefins to ellucidate the mechanism. For the quantum yield measurements to be

$$1/\Phi_{add} = \frac{(k_d + k_f + k_{ic} + k_i)(k_{cd_t} + k_{cd_c} + k_a + k_{-e} + k_{-ep})}{k_a k_e [0]}$$

$$- \left[\frac{k_{ep}k_{-ep}}{k_a(k_i + k_{ep}[0])}\right]\left[\frac{(k_d + k_f + k_{ic} + k_i)}{k_e} + [0]\right]$$

$$+ \frac{k_{cd_t} + k_{cd_c} + k_a + k_{-e_p}}{k_a} \qquad (21)$$

mechanistically meaningful, the cycloadditions involved must be independent of percent conversion. This is necessary in order to be primary processes free of secondary quenchers, molecules formed from the primary molecule which quench the primary reaction. Any dependence of the quantum yield on percent completion would render useless any quantum yield values as the only meaningful numbers for the process would be at time zero. A percent completion dependence could also render useless time zero measurements if a trace impurity which is destroyed on irradiation can quench the reaction at time zero. Studies of percent completion dependence for TME (Table 17), 1-methylcyclohexene (Table 29), and 2-methyl-2-butene (Table 24) are displayed in Figures 27, 28, and 29 respectively. Therefore, these reactions can be considered primary processes and render useful quantatitive data.

Values for $1/\Phi_{add}$ as a function of $1/[0]$ for TME (Table 16) are plotted in Figure 30. The slope of the plot is 4.27, while the intercept, the reciprocal of the quantum yield at infinite olefin

Figure 27. Plot of quantum yield of addition of 4 molar TME versus percent reaction completion

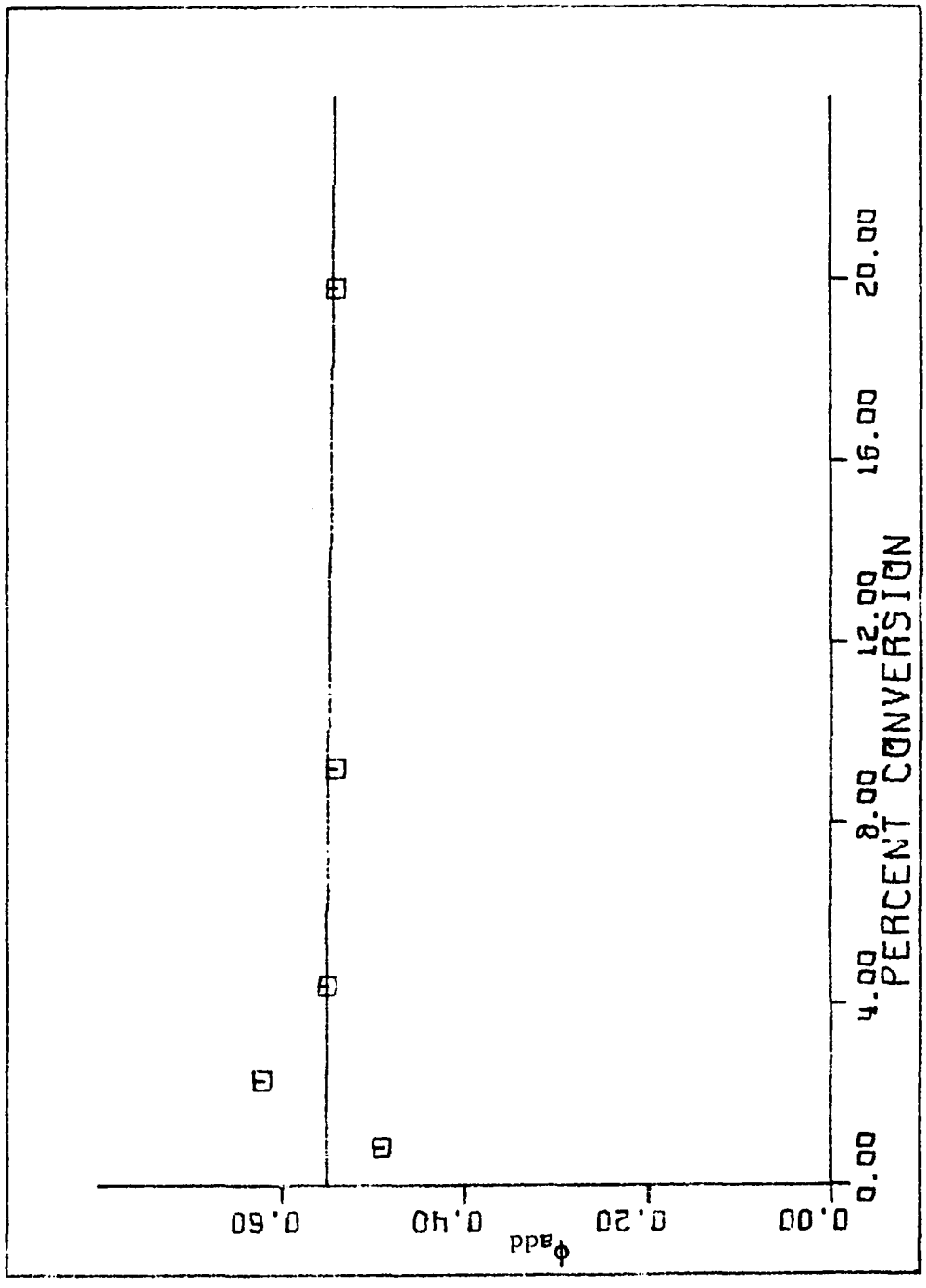
0.00
0.20
0.40
0.60
ϕ_{add}
0.00
4.00
8.00
12.00
16.00
20.00
PERCENT CONVERSION

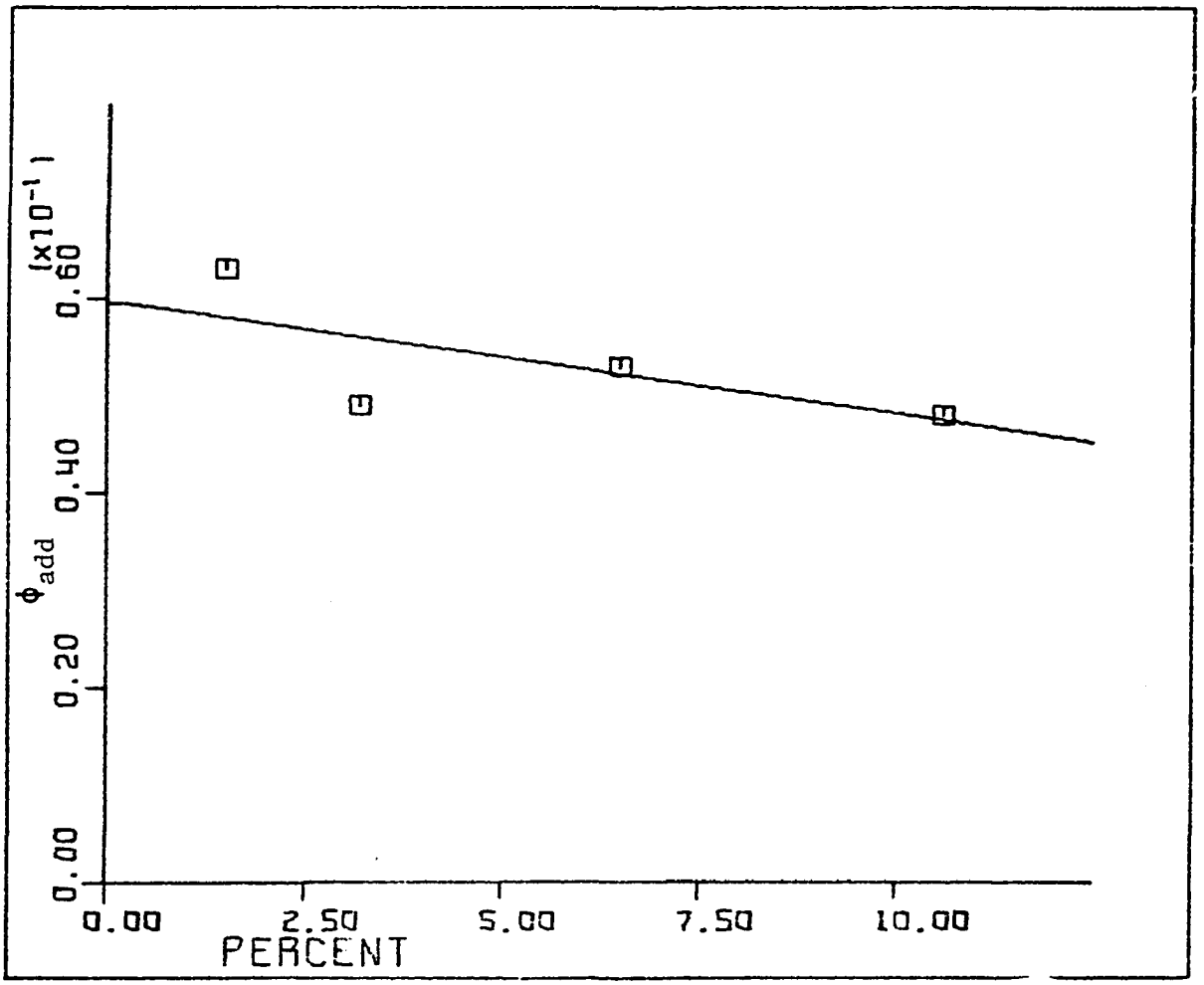

Figure 28. Plot of quantum yield of addition of 4 molar 1-methyl-cyclohexene versus percent reaction completion

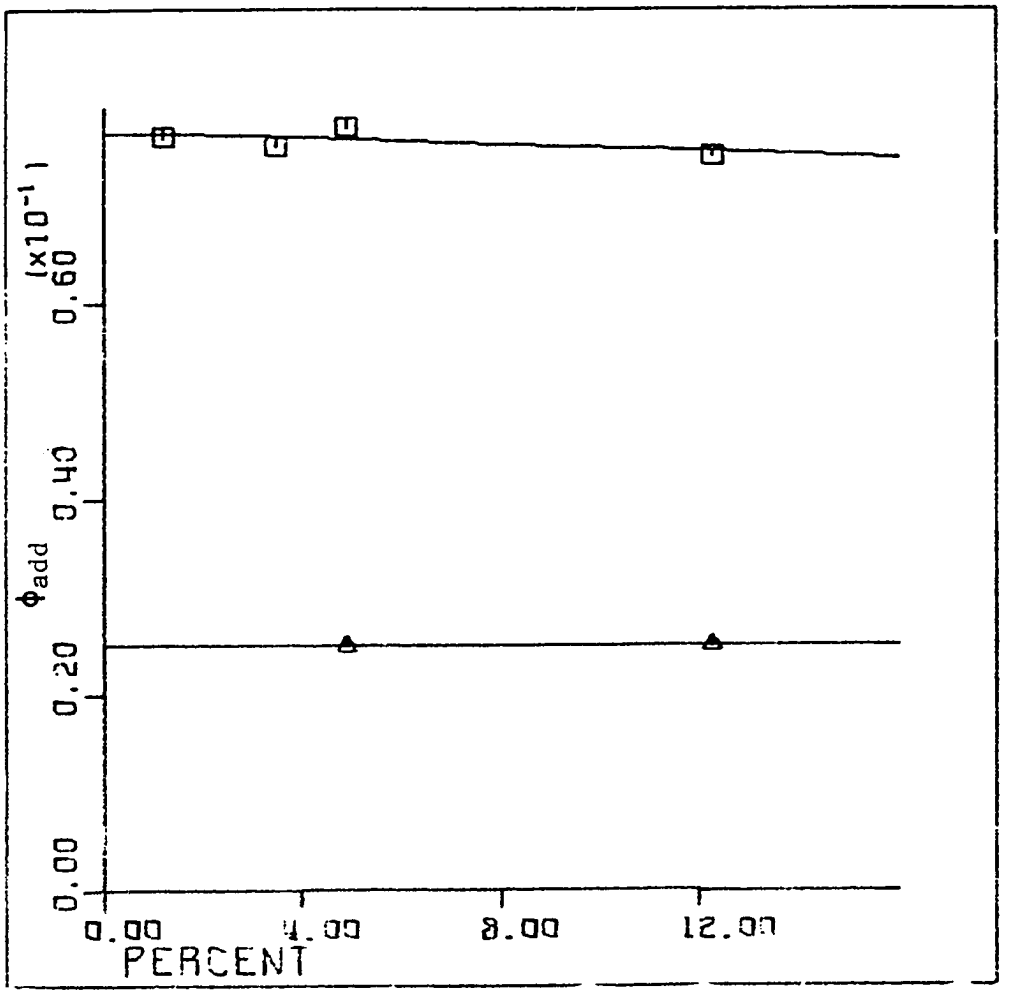

□- major adduct

Δ- minor adduct

Figure 29. Plot of quantum yield of addition of 4 molar 2-methyl-2-butene versus percent reaction completion

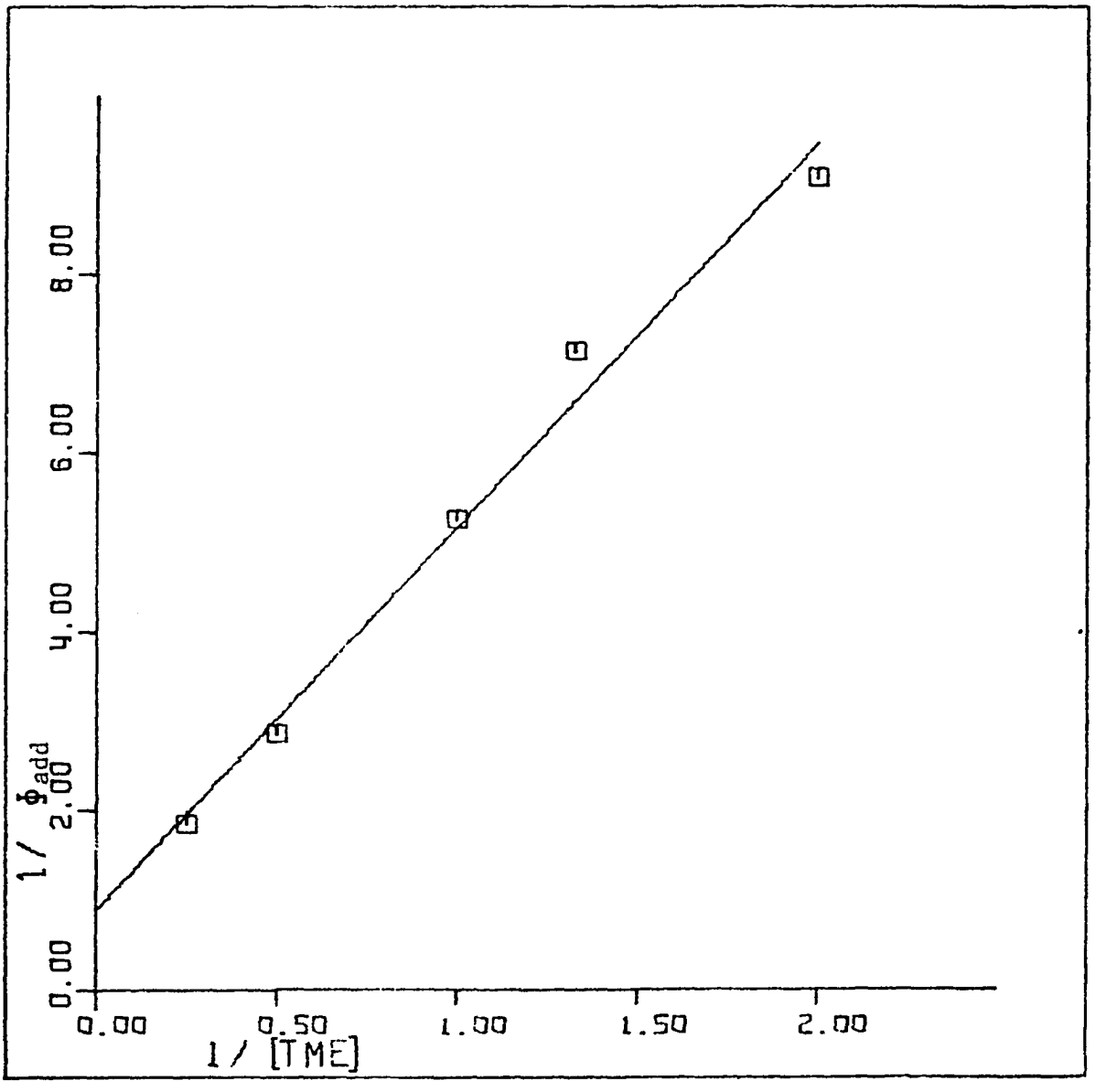

Figure 30. Plot of reciprocal of quantum yield of addition versus reciprocal of TME concentration at 25°

Slope = 4.27 ± 0.29 M

Intercept = 0.89 ± 0.35

concentration, is 0.89 $\pm$ 0.35. This value for the intercept is well within experimental limits of unity, indicating the value of Φ_{add} at infinite olefin concentration is 1.0. The value for Φ_{add} of 1.0 at infinite concentration is supported by similar results for 1-methylcyclohexene (Table 28) in Figure 31, intercept -4.2$\pm$2.1, and total adduct formation from 2-methyl-2-butene (Table 23) in Figure 32, intercept -0.95$\pm$1.01. These values for the intercept, though not as near the value of unity as that from TME, are subject to greater errors due to the method of analysis and are viewed as consistent with the assignment of intercept values of 1.0, as negative intercept values are meaningless, however the deviation range if taken from zero places the intercept within the range of unity.

The experimental value for the intercept can be set equal to the intercept term from equation 22. It can be seen that the only way in

$$\frac{k_{cd_t} + k_{cd_c} + k_a + k_{-e_p}}{k_a} = 1.0 \qquad (22)$$

which this equation can be satisfied is by the condition $k_a = k_a + k_{cd_t} + k_{cd_c} + k_{-e_p}$. On this basis decay modes of the exciplex leading to <u>cis</u> and <u>trans</u>-stilbene (equation 10 and 11), and production of the phantom singlet (equation 13) can be eliminated as negligible reactions. This conclusion also pertains to a mechanism in which a different exciplex is formed from the phantom singlet than from the spectroscopic singlet. The elimination of decay of the exciplex to phantom singlet and ground state by necessity eliminates any process involving the phantom singlet. The phantom singlet is therefore shown not to be involved in adduct

Figure 31. Plot of reciprocal of quantum yield of addition versus reciprocal of 1-methylcyclohexene concentration

Slope = 91.6 ± 0.2 M

Intercept = -4.2 ± 2.1

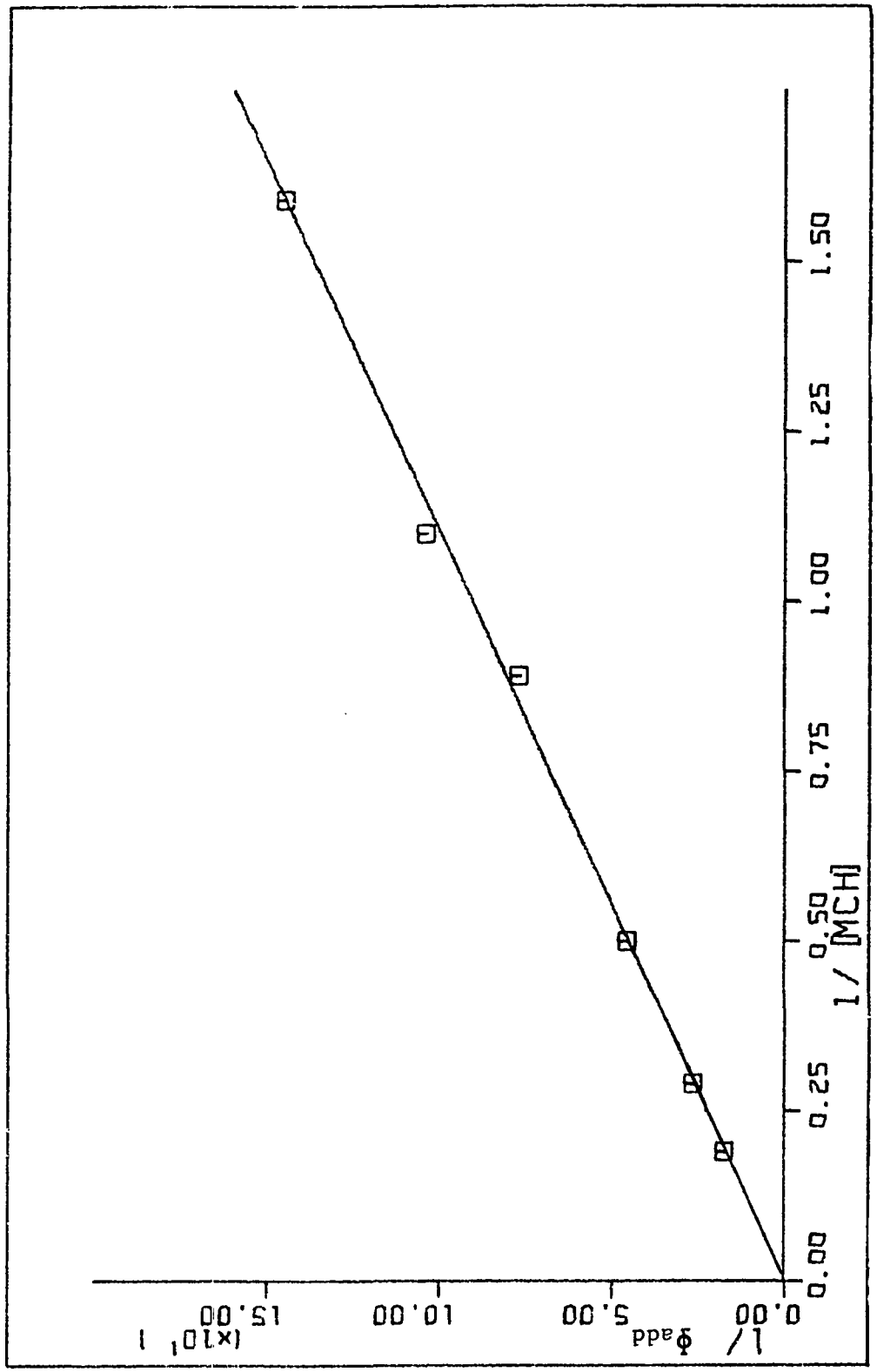
0.00
0.25
0.50
0.75
1.00
1.25
1.50
1/ [MCH]
0.00
5.00
10.00
15.00
1/ Φadd
(x10¹)

Figure 32. Plot of reciprocal of quantum yield of addition versus reciprocal of 2-methyl-2-butene

◇ Total adduct
Slope = 47.0 ± 1.1 M
Intercept = -0.99 ± 1.01

□ Major
Slope = 66.4 ± 1.8 M
Intercept = -2.3 ± 1.6

△ Minor
Slope = 149 ± 4 M
Intercept = 5.85 ± 3.34

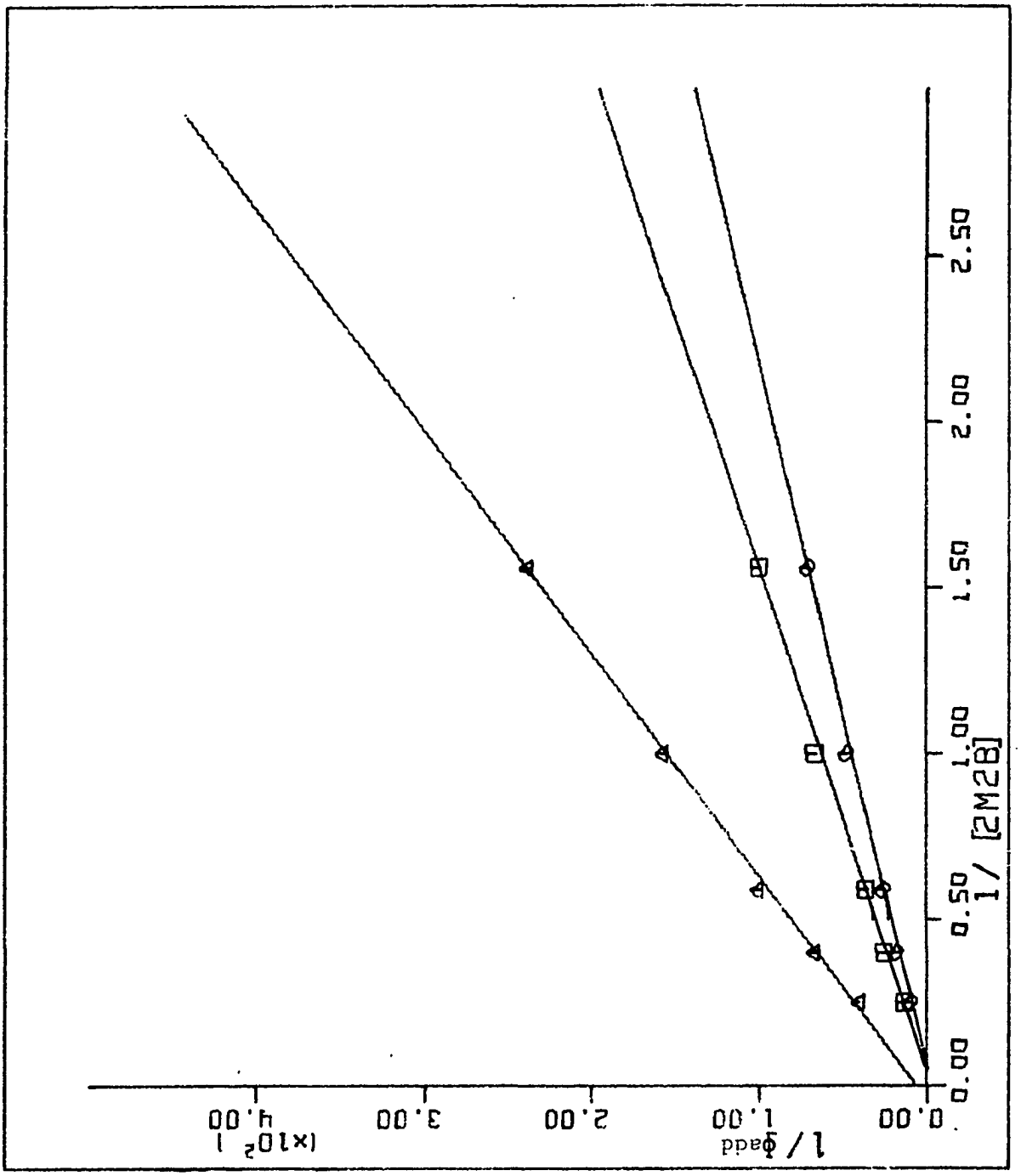
0.00
0.50
1.00
1.50
2.00
2.50
1/ [2M2B]
0.00
1.00
2.00
3.00
4.00
(x10² l
1/ φadd

formation in terms of parallel exciplexes. A mechanism involving exciplex formation purely from phantom singlet, Figure 33, is not in accord with the efficient quenching of trans-stilbene fluorescence by olefins.

$$S_t \longrightarrow {}^1S_t$$

$${}^1S_t \xrightarrow{k_d} S_t$$

$${}^1S_t \xrightarrow{k_f} S_t + h\nu_f$$

$${}^1S_t \xrightarrow{k_{ic}} {}^3S_t$$

$${}^1S_t \xrightarrow{k_p} {}^1S_p$$

$${}^1S_p \xrightarrow{k_c} S_c$$

$${}^1S_p + 0 \xrightarrow{k_e} \text{Exciplex}$$

$$\text{Exciplex} \xrightarrow{k_{-e}} {}^1S_p + 0$$

$$\text{Exciplex} \xrightarrow{k_a} \text{Adduct}$$

$$\text{Exciplex} \xrightarrow{k_{cd_t}} S_t + 0$$

$$\text{Exciplex} \xrightarrow{k_{cd_c}} S_c + 0$$

Figure 33. Mechanism for adduct formation from phantom singlet

On the basis of this information the possible mechanism can be reduced to that in Figure 34. The equation for $1/\Phi_{add}$ is now given by equation 23. This expression can be further simplified by the

$$S_t \longrightarrow {}^1S_t$$

$${}^1S_t \xrightarrow{k_d} S_t$$

$${}^1S_t \xrightarrow{k_i} S_c$$

$${}^1S_t \xrightarrow{k_f} S_t + h\nu_f$$

$${}^1S_t \xrightarrow{k_{ic}} {}^3S_t$$

$${}^1S_t + 0 \xrightarrow{k_e} \text{Exciplex}$$

$$\text{Exciplex} \xrightarrow{k_{-e}} {}^1S_t + 0$$

$$\text{Exciplex} \xrightarrow{k_a} \text{Adduct}$$

Figure 34. Mechanism of adduct formation

$$1/\Phi_{add} = \frac{(k_a + k_{-e})(k_d + k_f + k_{ic} + k_i)}{k_e k_a [0]} + 1 \qquad (23)$$

fact that $(k_d + k_f + k_{ic} + k_i)$, the sum of the first order singlet decay rate constants, is equal to the reciprocal of the singlet lifetime, $1/\tau$. The lifetime of trans-stilbene is known from several sources (86-91) and a value of 1.7×10^{-9} sec. (92) will be used consistently in in all calculations. This reduces equation 23 to equation 24.

$$1/\Phi_{add} = \frac{(k_a + k_{-e})}{\tau k_e k_a 0} + 1 \qquad (24)$$

This mechanism (Figure 34) leaves only two decay modes for the exciplex, decay to product and dissociation to singlet trans-stilbene and olefin. The concept of exciplex reversibility has been proposed

by McDonald and Selinger on the basis of experimentally obtained negative enthalpy of activation, $\Delta H^{\ddagger}$ (69).

Therefore a study was undertaken to determine the effect of temperature on the rate constant of addition of TME to trans-stilbene. From equation 30, the slope of the $1/\Phi_{add}$ vs. $1/[0]$ plot (Figure 30) is equal to $(k_a + k_{-e})/\tau k_e k_a$, if exciplex reversibility is operating and $1/\tau k_e$, if k_{-e} is zero or negligible compared to k_a. For the purposes of this study the slope is taken as $1/\tau k_{app}$, k_{app} being the apparent rate constant regardless which mechanism is operating.

Values for k_{app} were determined for TME at temperatures from 5° to 54° (Tables 16 and 19) from the slopes of Figures 30 and 35. For all the temperatures, the intercept values are within experimental error of unity. Thus it can be shown that raising or lowering the temperature does not activate any decay modes of the exciplex, decay of the exciplex to ground state stilbene and ground state olefin, which would raise the intercept to a value greater than unity. The values of k_{app} are summarized in Table 5. The rate constant is seen to increase by almost a factor of three in lowering the temperature from 54°, 7.3×10^7, to 5°, 2.0×10^8 l mole $^{-1}$sec^{-1}.

The values for k_{app} were plotted in Figure 36. as an Arrhenius Plot (93), the natural logarithm of the rate constant versus the reciprocal of the absolute temperature. The slope of such a plot is equal to $-E_a/R$, the negative of the activation energy divided by the universal gas constant. From the value of the activation energy the value for the enthalpy of activation, $\Delta H^{\ddagger}$, can be determined from

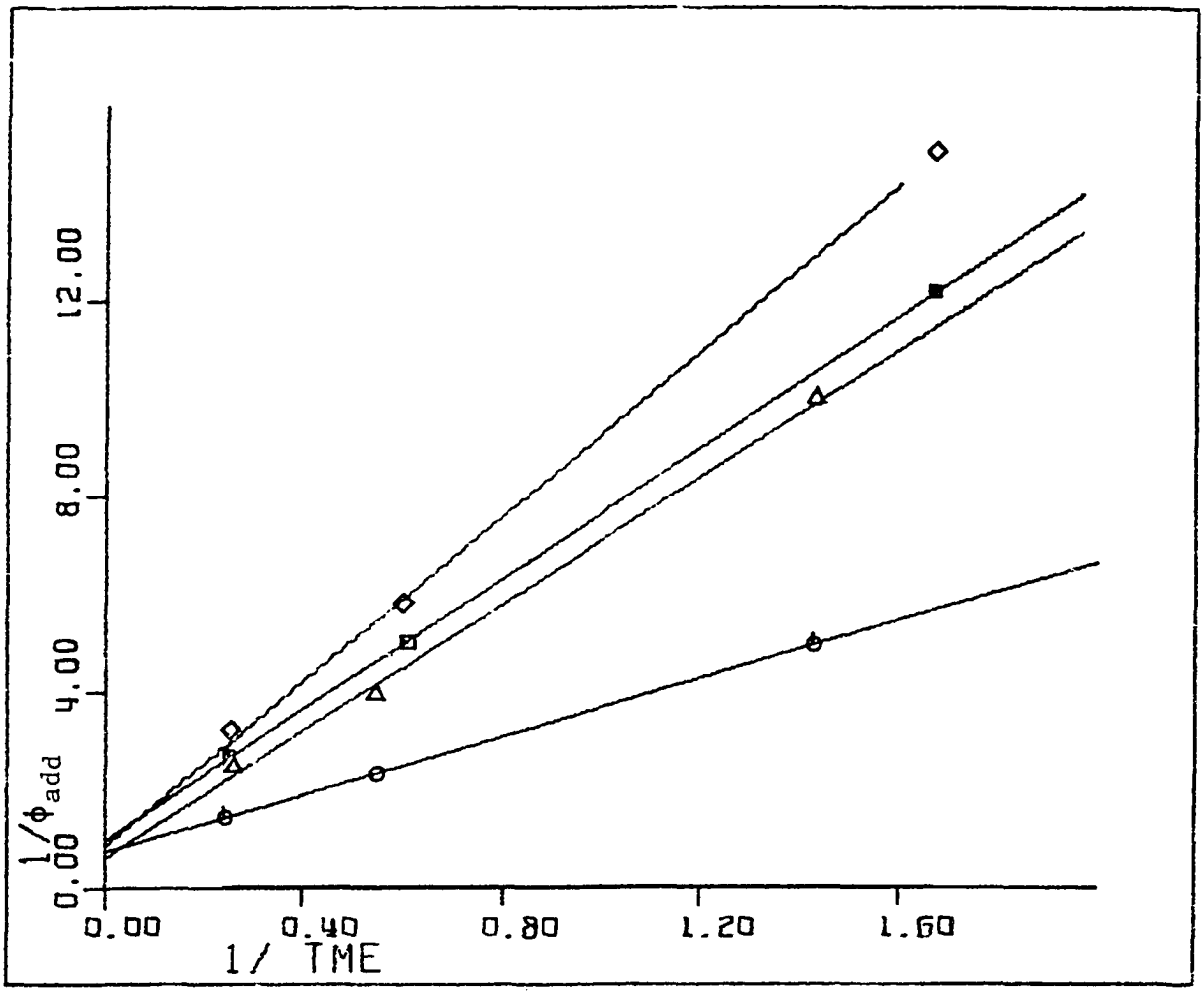

Figure 35. Plot of reciprocal of quantum yield of addition versus reciprocal of TME concentration at various temperatures

o- 5° Slope = 2.98 ± 0.01 M Intercept = 0.74 ± 0.01

Δ- 34° Slope = 6.51 ± 0.46 M Intercept = 0.63 ± 0.41

□- 44° Slope = 6.71 ± 0.05 M Intercept = 0.99 ± 0.05

◇- 54° Slope = 8.44 ± 0.21 M Intercept = 0.87 ± 0.21

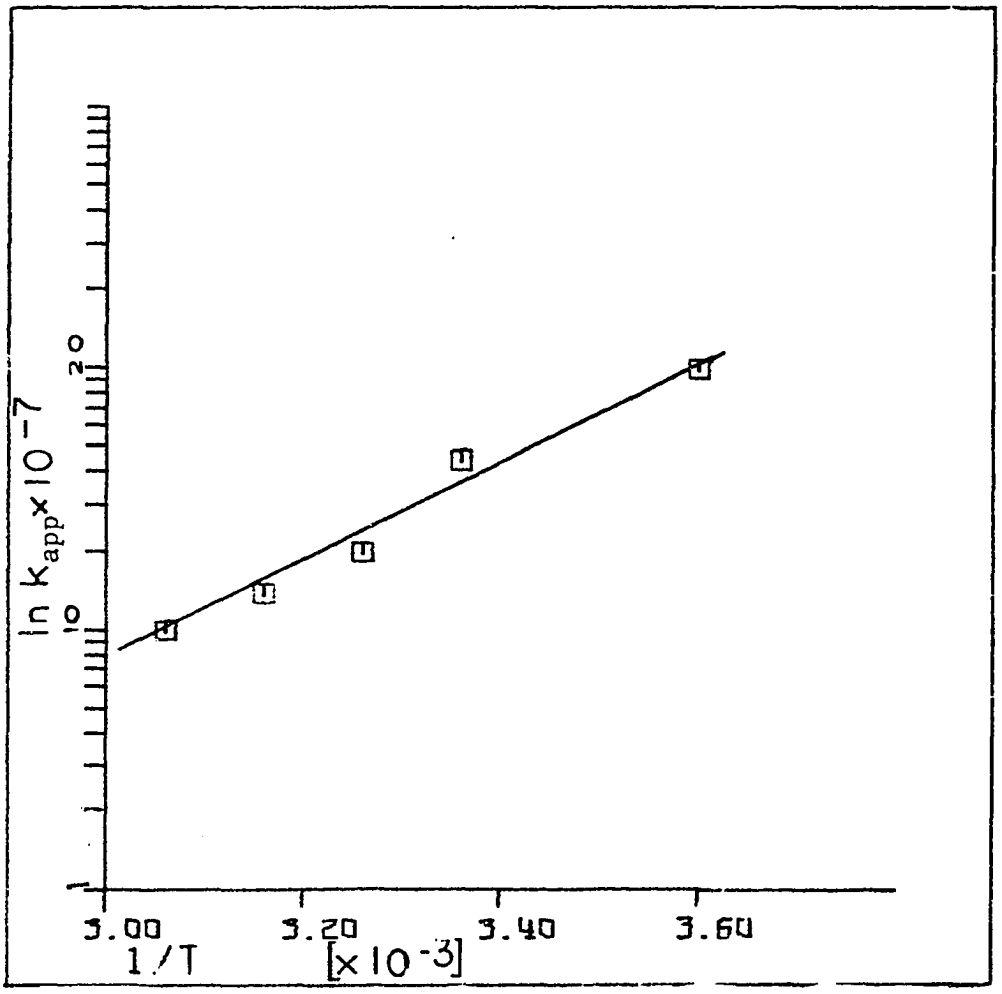

Figure 36. Plot of ln k_{app} versus reciprocal of absolute temperature
Slope 2.5 x 10^3 K

Table 5. Values of k_{app} for addition of TME at various temperatures

Temperature	k_{app} 1 mole^{-1} sec^{-1}
5°	2.0×10^8
25°	1.4×10^8
34°	1.0×10^8
44°	8.4×10^7
54°	7.3×10^7

equation 25.

$$E_a = \Delta H + RT \qquad (25)$$

A normal Arrhenius plot has a negative slope, decrease of the rate constant with decrease in temperature, leading to the calculation of a positive E_a and positive value for ΔH^*. The plot in Figure 36 is seen to have a positive curvature. If a straight line is extrapolated through the points, a slope of 2.5×10^3 K is obtained, leading to a value of E_a of -5.0 kcal/mole. The value of ΔH^* calculated from equation 31 is -5.6 kcal/mole. The value obtained by McDonald and Selinger was -6.8 kcal/mole (69).

From the calculated negative value for ΔH two possibilites arise. Exciplex reversibility may be operating, in which case the mechanism in Figure 33 is the correct mechanism, or the enhancement of quantum yield at low temperatures may be due to an increase in the lifetime of trans-singlet, due to a decrease in the thermal quenching portion of singlet deactivation (14, 94). At this time exciplex reversibility will be

assumed to be the operating step and data handled and explanations developed to handle such a mechanism, such that after all olefins have been treated the effect of lifetime dependence can be examined in light of all the data.

The negative value for ΔH obtained for a mechanism involving a reversible exciplex would be expected on the basis of reaction modes of the exciplex. The negative value indicates that of two competing rate constants, exciplex reversibility (equation 12) is increasing with temperature much more rapidly than the rate constant leading to product (equation 14). This is not surprising in view of the weak

Exciplex $\xrightarrow{k\text{-e}}$ excited stilbene + ground state olefin (12)

Exciplex $\xrightarrow{k_a}$ product (14)

binding energy of the exciplex. Any increase in temperature would increase the vibrational and rotational strain of the exciplex facilitating the reverse reaction, while the value of k_a, rate constant for the formation of the sigma bonds, would not be expected to vary significantly with respect to the change in $k\text{-e}$ over the narrow temperature range studied (95). The net affect of these two competing reactions is the effective decrease of the measured rate constant for reaction, while in fact both processes do increase with temperature.

Anomalous temperature affects have been observed by several workers. As mentioned in the REVIEW OF LITERATURE section, deMayo has studied the enhanced reaction at lower temperatures and attributed the effect to partitioning of the complex between diradical and ground state and partitioning of the diradical (68). The addition of dimethyl-fumarate and

maleate to cyclohexene is also temperature dependent, becoming much more stereospecific at lower temperatures (9). Byrce-Smith and Gilbert observed the addition of maleic anhydride to methyl benzenes to give two products is highly temperature dependent. He explains the effect on the basis of changes of equilibrium involving product precusor complexes, exciplexes (96). The change in the equilibrium, k_e/k_{-e}, would be due mainly to the change in k_{-e} as k_e being a bimolecular rate constant subsequently would be expected to be governed by changes in the diffusion controlled rate constant as calculated by the Debye equation (97).

The true expression for k_{app} is now seen to be the complex term $k_e k_a/(k_{-e} + k_a)$. This can be viewed as the value of the rate constant for exciplex formation, k_e, multiplied by the fraction of the exciplex which gives adduct $k_a/(k_a + k_{-e})$. The true value for k_e at 25° is therefore between the measured value of 1.4×10^8 1 $mole^{-1}sec^{-1}$ and the diffusion controlled rate constant, calculated from the Debye Equation (97) to be 2.3×10^{10} 1 $mole^{-1}sec^{-1}$ in n-hexane.

Total analysis of the complex rate term, $k_e k_a/(k_a + k_{-e})$, is not possible as the terms k_a, k_e and k_{-e} cannot be obtained independent of each other. The fact that the measured rate constant increases with with decreasing temperature (Table 5) indicates that by measuring rate constants at ever lower temperatures until there is a decrease or no change in the rate constant will give a more accurate measure of the minimum value for k_e.

The value for k_e may be limited in two ways. The quantum yield may reach unity at any concentration, indicating that k_{-e} has been eliminated as a competitive reaction, which would give a zero slope for

a $1/\Phi_{add}$ vs $1/[O]$ plot. This would lead to a calualtion of an infinite value for k_e, which would limit the value of k_e to the diffusion controlled rate constant for a bimolecular reaction at the particular temperature. The other possibility involves the temperature being reached, below which, though the quantum yield has not reached unity does not increase. This indicates that the $k_a/(k_a + k_{-e})$ value has reached its maximum, below unity.

On this basis the values of k_{app} were plotted as a function of temperature and on the same set of axis the calculated diffusion controlled rate constant was plotted as a function of temperature (Figure 37). The extrapolated curve of the measured rate constant is seen to intersect the diffusion controlled rate constant curve at a value near 5×10^9 1 $mole^{-1}sec^{-1}$, approximately 40 times the value at room temperature. Whether or not this graph has any significance depends on the quantum yield of addition at temperatures well below 0^oC. Figure 38 shows the plot of Φ_{add} at 4 molar TME as a function of temperature (Table 18). It is seen from this graph that the value for Φ_{add} is unity near -29^oC. indicating that the value of k_{-e} is negligible compared to k_a. Therefore, it can be seen that the two graphs are in qualitative agreement for the maxiumum rate constant of k_e. The calculated value for the diffusion controlled rate constant at -29^o is 9×10^9 1 $mole^{-1}sec^{-1}$. Also it can be seen that at -29^o the diffusion controlled rate constant is the value for k_e as the slope of the $1/\Phi_{add}$ vs. $1/[O]$ plot would be zero. As has been mentioned, k_e is a bimolecular rate constant and therefore would be expected to have the same temperature dependence as the diffusion controlled rate constant. This has been

Figure 37. Plot of rate constant versus temperature

Δk_{diff} diffusion controlled rate constant

$\square k_{app}$

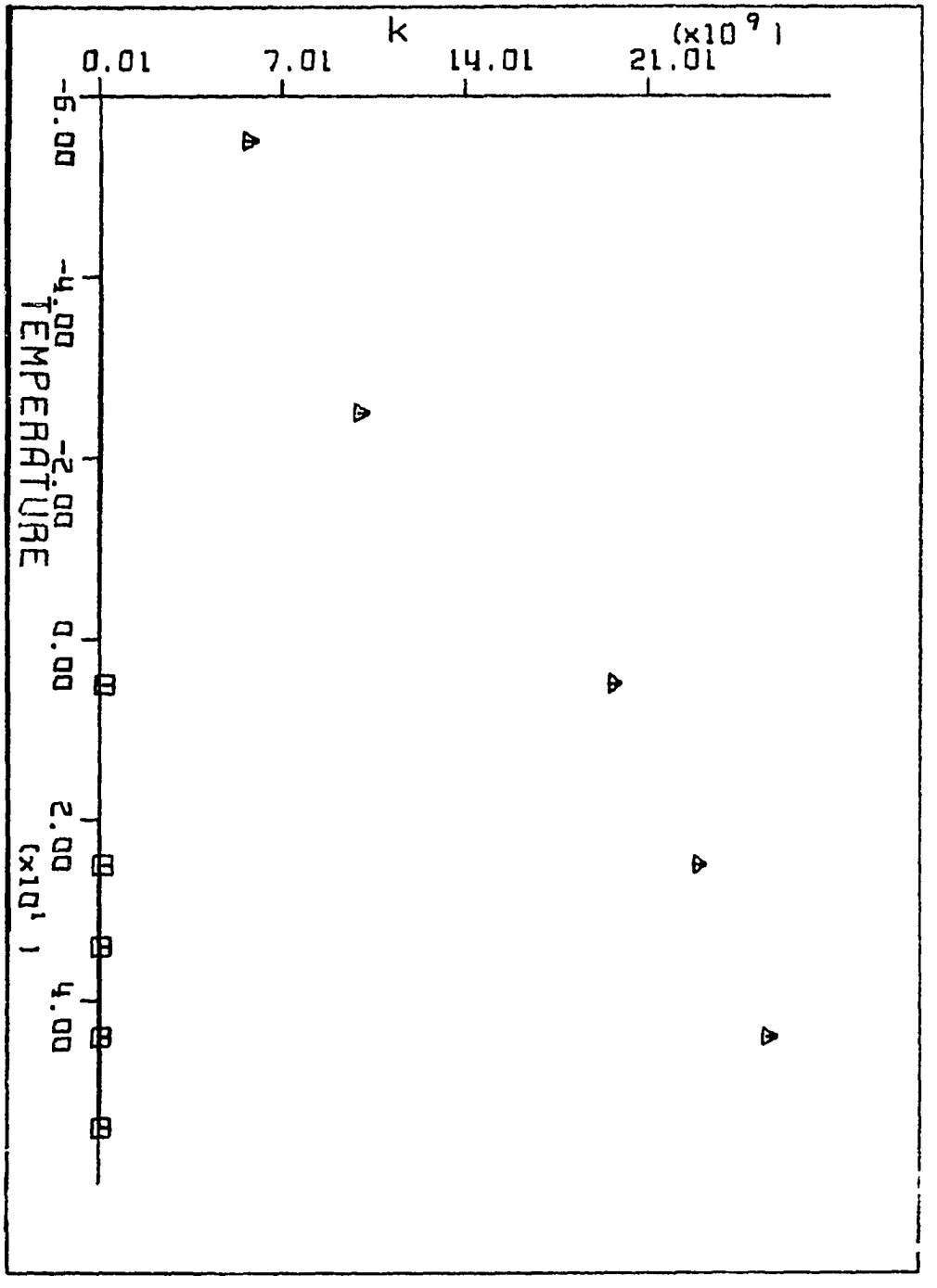
k
(x10 9)
0.01
7.01
14.01
21.01
-6.00
-4.00
-2.00
0.00
2.00
4.00
TEMPERATURE
(x10 1)

Figure 38. Plot of quantum yield of addition of 4 molar TME versus temperature

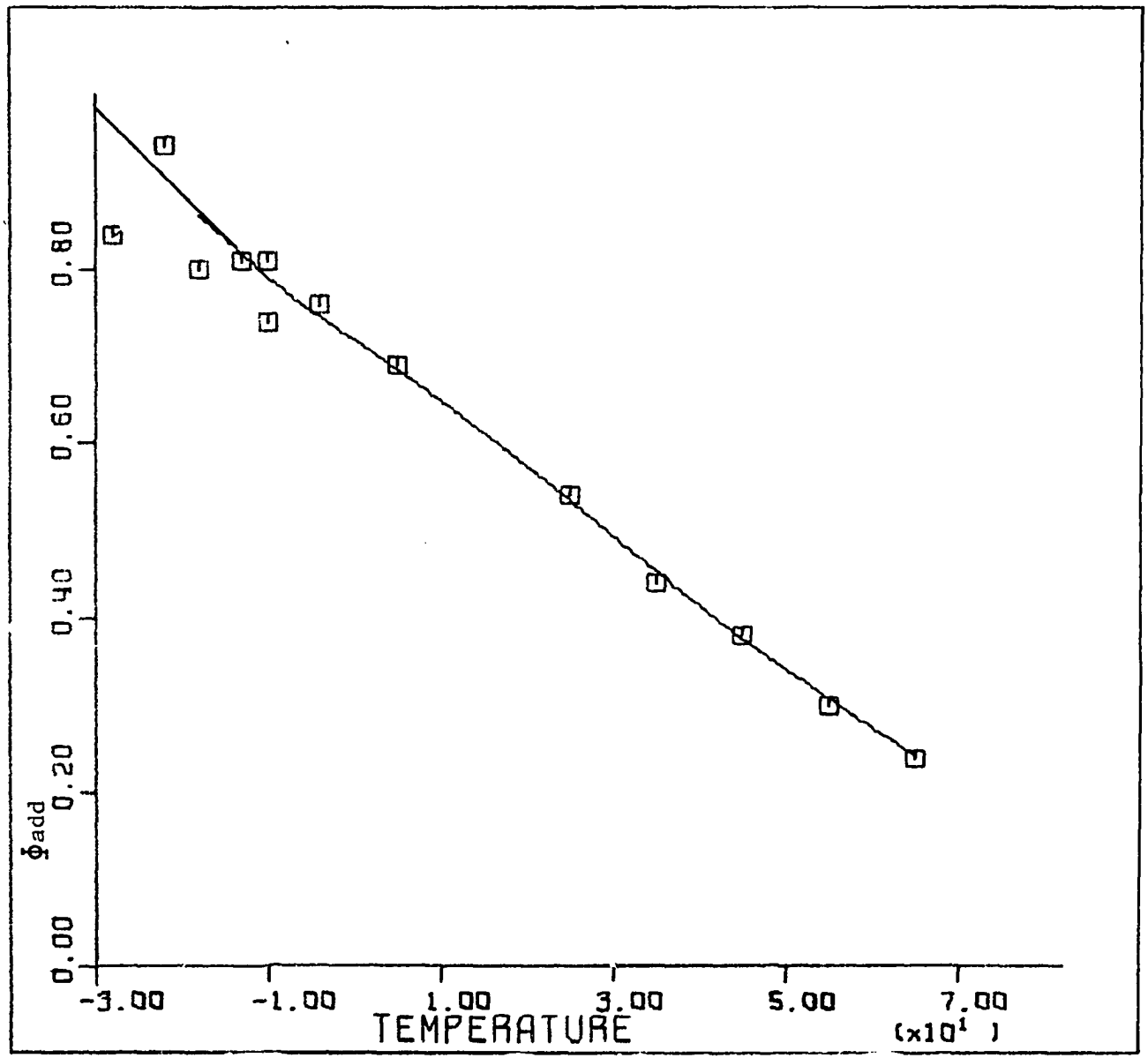
0.00
0.20
0.40
0.60
0.80
ϕ_{add}
-3.00
-1.00
1.00
3.00
5.00
7.00
TEMPERATURE
(x10^1)

verified by findings of deMayo (68). It can be assumed therefore that k_e will have the value of the diffusion controlled rate constant at any temperature.

Allowing exciplex formation to be diffusion controlled, it is possible to obtain relative ratios for k_{-e} and k_a from equation 26.

$$k_{app} = k_{diff}\left[\frac{k_a}{k_a + k_{-e}}\right] \qquad (26)$$

The results of such calculations are summarized in Table 6. It can

Table 6. Ratios of k_{-e}/k_a for TME at various temperatures

Temperature	k_{-e}/k_a
5°	79
25°	160
34°	250
44°	330
54°	400

be seen that k_{-e} is increasing rapidly with temperature. The reason for reaction inefficiency, Φ_{add} 1.0, is due to the high value of the rate constant of k_{-e}. This is shown by the fact that at 54° the exciplex has 0.25% probability of forming the adduct, while the probability is raised to 100% at -29°. Again the weak binding energy of the exciplex is reflected in this large temperature affect on k_{-e}.

The ratios in Table 6 were plotted as the natural logarithm versus the reciprocal of the absolute temperature, an Arrehenius Plot, in

in Figure 39. The straight line of negative slope is indicative for one term of the ratio being temperature independent, as the ratio of two temperature dependent rate constants would be expected to give a curve rather than a straight line. The terms k_{-e} and k_a would be expected to be drastically different with respect to temperature induced changes, as has been observed by Rappoport (95).

The value of k_{app} determined from the slope of the $1/\Phi_{add}$ plots can be counterchecked by the value obtained from fluorescence quenching data. Equation 27 represents the ratio of the quantum yield of fluo-

$$\frac{\Phi_f}{\Phi_{f_{olefin}}} = 1 + \frac{k_e k_a [0]}{(k_{-e} + k_a)} \qquad (27)$$

rescence in the absence of olefin to that in the presence of olefin. The slope of the equation is given by 28. This is the reciprocal of

$$k_{app} = \frac{k_e k_a}{(k_{-e} + k_a)} = \text{slope} \qquad (28)$$

the slope from the $1/\Phi_{add}$ vs. $1/[0]$ plot, offering a second way of determining the value for k_{app}. The value of k_{app} determined by this method from the slope of Figure 22 of 0.22 is 1.3×10^8 1 $mole^{-1}sec^{-1}$, in excellent agreement to the value of 1.4×10^8 1 $mole^{-1}sec^{-1}$ from the $1/\Phi_{add}$ data.

Values of k_{app} were determined for 1-methylcyclohexene (Figures 24, 31 and 40), 2-methyl-2-butene (Figures 23 and 32) and cyclohexene (Figure 41). The values of k_{app} determined for the olefins are summarized in Table 7.

The formation of two adducts from 2-methyl-2-butene, 52 and 53,

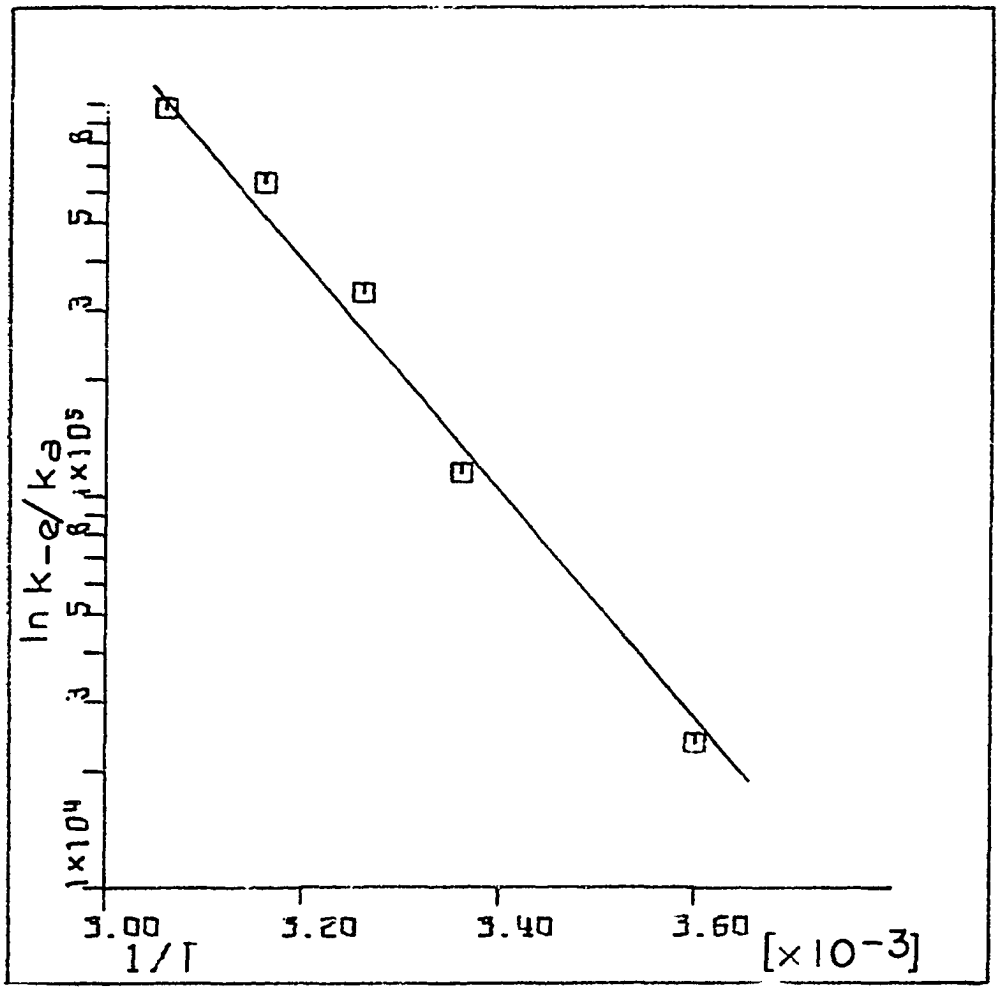

Figure 39. Plot of ln k_e/k_a versus reciprocal of absolute temperature

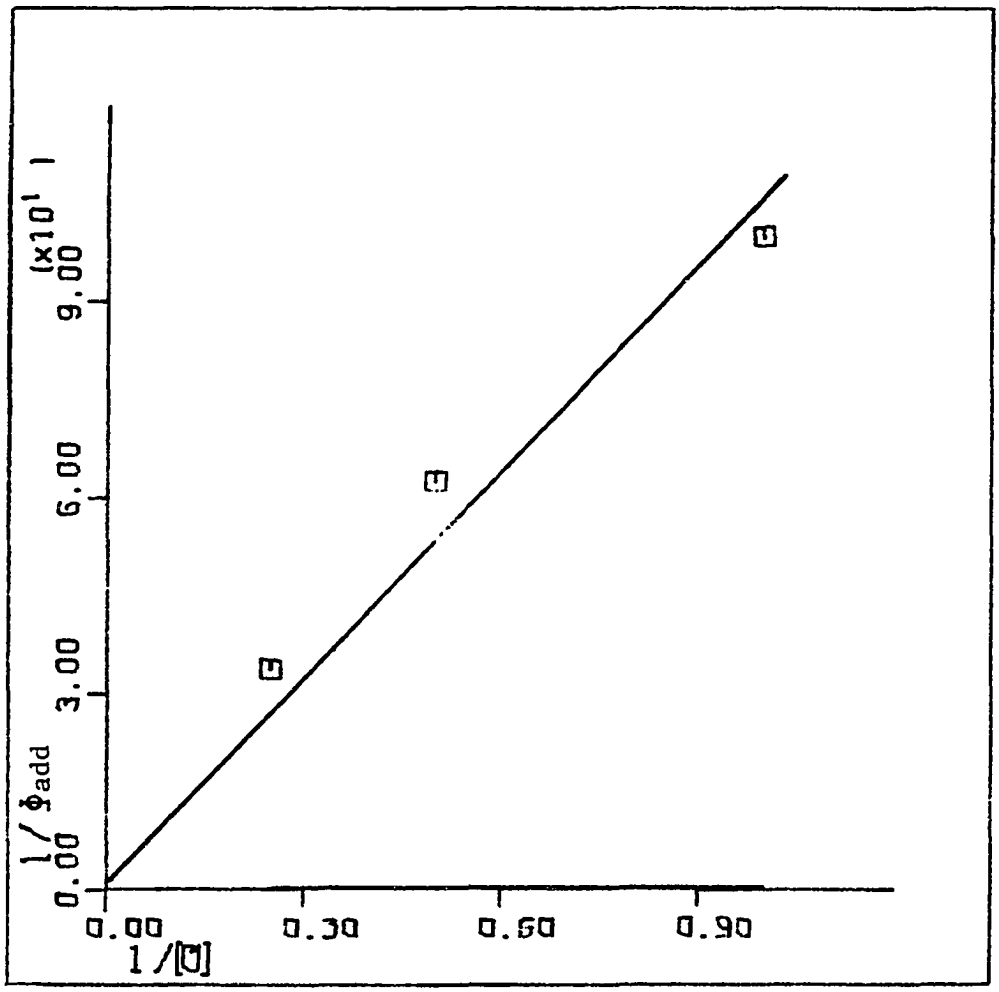

Figure 40. Plot of reciprocal of quantum yield of addition versus reciprocal of 1-methylcyclohexene concentration at 45°

Slope = 134 M

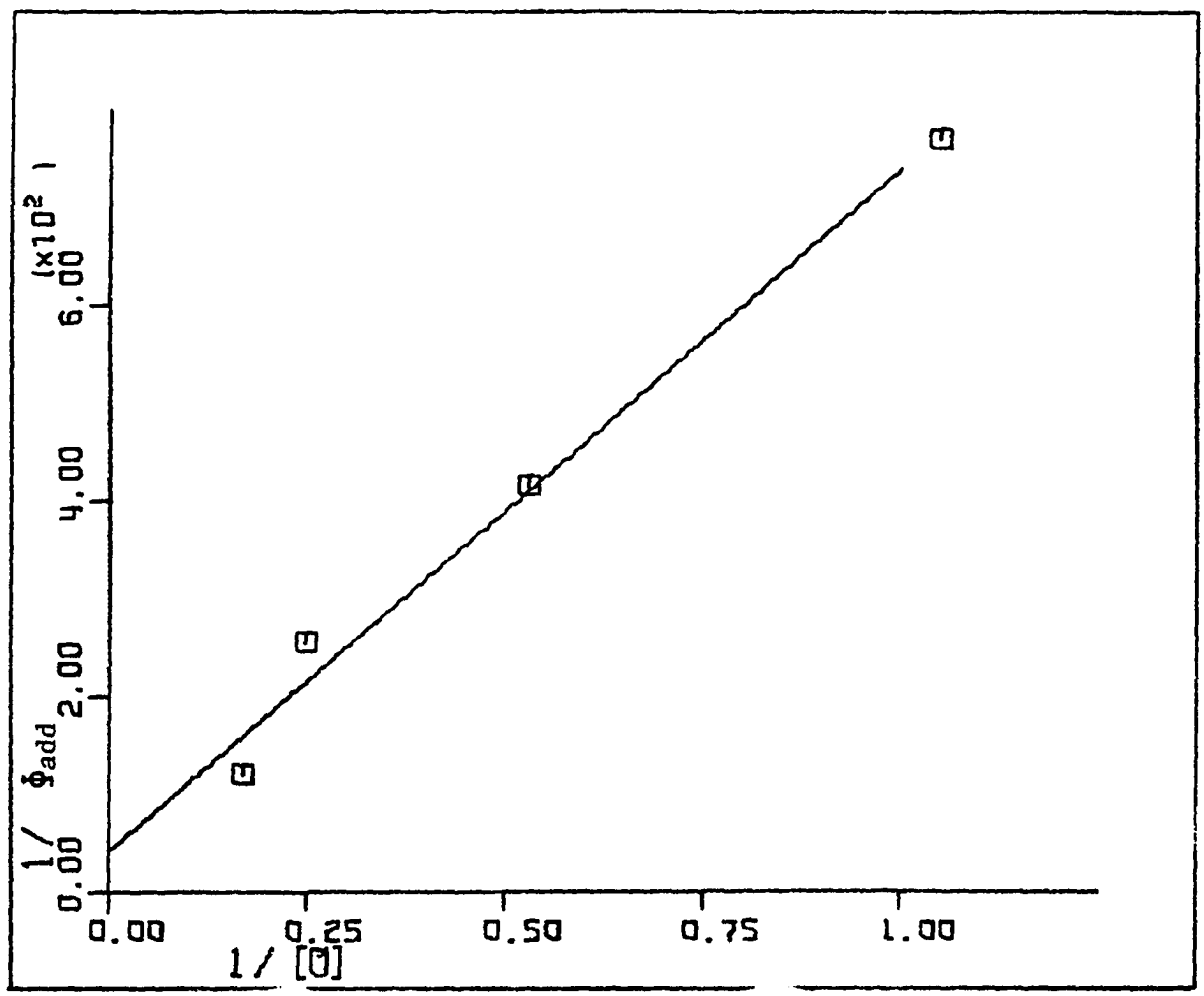

Figure 41. Plot of reciprocal of quantum yield of addition versus reciprocal of cyclohexene concentration at 25°

Slope = 699±58 M

Intercept = 41.5±35.5

Table 7. Calculated values of k_{app} for 1-methylcyclohexene, 2-methyl-2-butene and cyclohexene

Olefin	Temperature	k_{app} $1/\Phi_{add}$ method	k_{app} Φ_f/Φ_f olefin
1-methyl cyclohexene	25°	6.5×10^6	5.1×10^7
1-methyl cyclohexene	45°	4.0×10^6	
2-methyl-2-butene major adduct	25°	8.8×10^6	
minor adduct	25°	3.9×10^6	
total adduct	25°	1.3×10^7	4.5×10^7
cyclohexene	25°	8.3×10^5	

necessitates a two exciplex mechanism, as the reaction has been shown to be stereospecific and therefore each adduct must arise from a different exciplex. The two exciplexes can be pictured as 60 and 61, the two geometric arrangements of addition to trans-stilbene. The

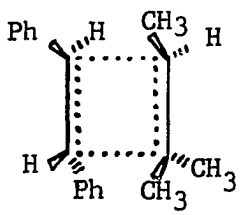

60

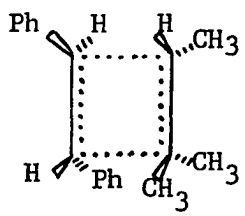

61

total mechanism is that shown in Figure 42. The mechanism is basically

$$S_t \xrightarrow{h\nu} {}^1S_t$$

$${}^1S_t \xrightarrow{k_d} S_t$$

$${}^1S_t \xrightarrow{k_f} S_t + h\nu_f$$

$${}^1S_t \xrightarrow{k_{ic}} {}^3S_t$$

$${}^1S_t \xrightarrow{k_i} S_c$$

$${}^1S_t + 0 \xrightarrow{k_{e1}} \text{Exciplex 1}$$

$${}^1S_t + 0 \xrightarrow{k_{e2}} \text{Exciplex 2}$$

$$\text{Exciplex 1} \xrightarrow{k_{-e1}} {}^1S_t + 0$$

$$\text{Exciplex 2} \xrightarrow{k_{-e2}} {}^1S_t + 0$$

$$\text{Exciplex 1} \xrightarrow{k_{a1}} \text{Adduct (Minor)}$$

$$\text{Exciplex 2} \xrightarrow{k_{a2}} \text{Adduct (Major)}$$

Figure 42. Two exciplex mechanism for 2-methyl-2-butene adduct formation

two concurrent TME mechansims. Fluorescence quenching (Figure 23) and the failure to sensitize adduct formation indicate that both adducts arise from the singlet. The decay of exciplex to ground state stilbene has not been considered due to the unity intercept of total adduct production in Figure 32. The expression for $1/\Phi_{add}$ for the major and minor adducts are equations 29 and 30 respectively. The term for the slope, $(k_{-e2} + k_{a2})/\tau k_{a2}k_{e2}$, is the same as the expression for the slope of the TME plot and therefore values of k_{app} calculated in this way are correct.

The reversibility of the exciplex is seen in the increase of the

$$1/\Phi_{add_{major}} = \frac{(k_{-e_2} + k_{a_2})}{\tau k_{a_2} k_{e_2} [0]} + 1 + \frac{(k_{-e_2} k_{e_1} + k_{a_2} k_{e_1})}{k_{a_2} k_{e_2}} - \left[\frac{(k_{-e_2} + k_{a_2})}{k_{a_2} k_{e_2}}\right] \left[\frac{k_{-e_1} k_{e_1}}{k_{-e_1} + k_{a_1}}\right] \quad (29)$$

$$1/\Phi_{add_{minor}} = \frac{(k_{-e_1} + k_{a_1})}{\tau k_{a_1} k_{e_1} [0]} + 1 + \frac{(k_{-e_1} k_{e_2} + k_{a_1} k_{e_2})}{k_{a_1} k_{e_1}} - \left[\frac{(k_{-e_1} + k_{a_1})}{k_{a_1} k_{e_1}}\right] \left[\frac{k_{-e_2} k_{e_2}}{k_{-e_2} + k_{a_2}}\right] \quad (30)$$

value for Φ_{add} at 4 molar olefin as a function of temperature for each adduct (Table 25) shown in Figure 43. At -22° the quantum yield of the major adduct is raised to 0.15 from the value of 0.040 at 55°, while the minor adduct is raised from 0.018 at 55° to 0.058 at -22°. From these high values for Φ_{add} at 4 molar olefin it is possible to calculate the value of k_{app} at that temperature by preparing a two point $1/\Phi_{add}$ vs. $1/[0]$ plot from the value of unity at infinite concentration, though the value is not unity this is sufficiently accurate to allow a reasonable calculation, as the intercept for total adduct is known to be unity, and the value for Φ_{add} at 4 molar olefin is sufficiently small to produce a large slope. From this plot the slope for the major and minor adduct can be determined, 24.4 and 72.3 respectively, and k_{app} calculated from it as per the method of TME. The values for k_{app} at -22°

Figure 43. Plot of quantum yield of addition of 4 molar 2-methyl-2-butene versus temperature

□- major adduct

Δ- minor adduct

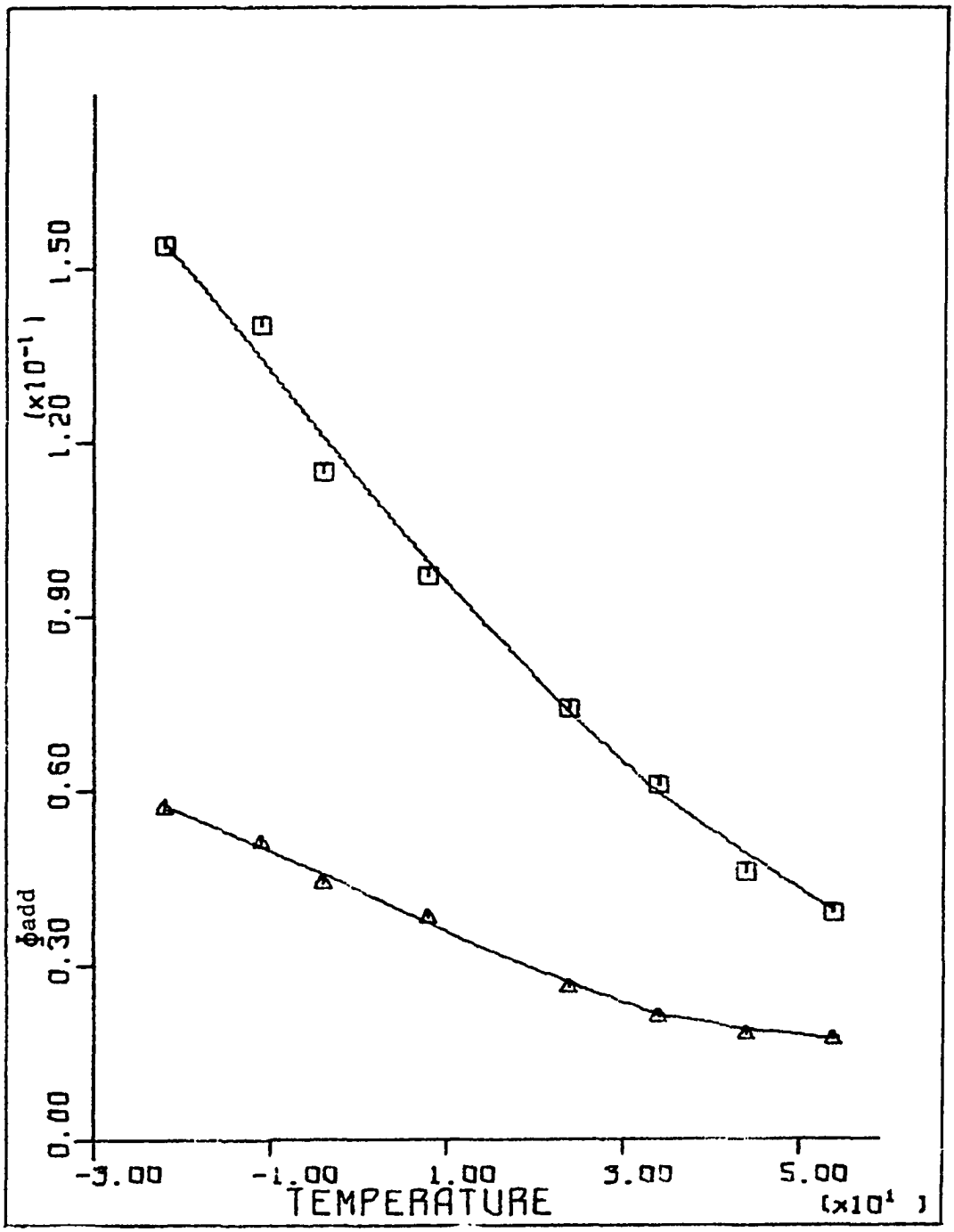
0.00
0.30
0.60
0.90
1.20
1.50
(x10⁻¹)
ϕadd
-3.00
-1.00
1.00
3.00
5.00
TEMPERATURE
(x10¹)

for the major and minor adduct are 2.5×10^7 and 8.2×10^6 l mole^{-1} sec^{-1}, nearly triple the values at 25° in Table 7. The value for $k_{e_{1 \text{ and } 2}}$ is larger than the value calculated at 25° but the maximum value has not been reached as the quantum yield is still increasing at the limits of the experimental determinations.

The formation of the exciplexes in this reaction is, as for TME, a bimolecular process governed by diffusion of two species together. The rate of the diffusion of 2-methyl-2-butene molecules to trans-stilbene and vice-versa should proceed at the same rate as for TME and trans-stilbene as there are no hindering factors, in fact 2-methyl-2-butene is less hindered than TME, which would slow down the diffusion. Once the molecules have diffused together actual interaction rate constant would not be expected to be any different as the energy levels of the two molecules, TME and 2-methyl-2-butene, are almost identical (86). Therefore, the exciplexes should form with equal ease. Thus it can be argued that the value of $k_{e_{1 \text{ and } 2}}$ should be the diffusion controlled rate constant at any temperature, as has been shown to be the case for TME.

The reason for the lower quantum yield of formation of 2-methyl-2-butene compared to TME is therefore due to a weaker binding energy of the exciplex, reflected by a higher value for k_{-e} and the much decreased temperature dependence of k_{-e} with respect to k_a. This is seen in the fact that the quantum yield is still quite low, $\Phi_{add_{total}} = 0.20$ at -22°, k_{-e} is decreasing much slower than in the TME case. The ratios of k_{-e}/k_a at 25° for the two adducts are 2650, major, and 5600 minor,

while at -22°, the ratios are 400, major, and 1200 for the minor. At -22° k_{-e} is still the dominant term in the fraction of exciplex to product portion of the slope expression, $k_a/(k_a + k_{-e})$. This is reasonable if the exciplex has a weaker binding energy, driving the equilibrium, k_e/k_{-e}, to the left. As the temperature is lowered, these exciplexes are stabilized less than the TME exciplex with respect to dissociation.

The reason for the decrease in exciplex stability is attributed to the substitution pattern on the ground state olefin. The only change from TME to 2-methyl-2-butene is the substitution of a hydrogen for a methyl group. Therefore the greater the number of alkyl substituents, the greater the stability of the exciplex. The reason for this may be due to the electronic stabilization of the charge transfer contribution to exciplex binding, as charge transfer complexes are known to be stabilized by increased alkyl substitution (98).

Based on the assumption of $k_{e_1} = k_{e_2}$, equations 29 and 30 can be reduced to 31 and 32. It can be seen that at the temperature where

$$1/\Phi_{add_{major}} = \frac{(k_{-e_2} + k_{a_2})}{\tau k_{a_2} k_{e_2} [0]} + 2 + \frac{k_{-e_2}}{k_{a_2}} - \frac{(k_{e_2} + k_{a_2})}{k_{a_2}} \left[\frac{k_{-e_1}}{(k_{-e_1} + k_{a_1})}\right] \tag{31}$$

$$1/\Phi_{add_{minor}} = \frac{(k_{-e_1} + k_{a_1})}{\tau k_{a_1} k_{e_1} [0]} + 2 + \frac{k_{-e_1}}{k_{a_1}} - \frac{(k_{e_1} + k)_{a_1}}{k_{a_1}} \left[\frac{k_{-e_2}}{(k_{-e_2} + k_{a_2})}\right] \tag{32}$$

k_{-e_1} and k_{-e_2} are negligible compared to k_{a_1} and k_{a_2} both plots should intercept at 2.0, indicating that each adduct would be formed equally, $\Phi_{add_{major}} = \Phi_{add_{minor}} = 0.50$. At the temperatures studied, the two adducts are not formed at equal rates, again indicating a difference between the two exciplexes involved. From the lower rate of the minor adduct the value of k_{-e} must be higher for this exciplex than for the exciplex for the major adduct, indicating lower binding energy in this exciplex. It is somewhat peculiar that the sterically more hindered exciplex should be the more stable. This may be due to participation of the cis methyl group restricting rotation of the adjacent phenyl, thus increasing the overlap of the aromatic system into the exciplex, increasing the effective system of the exciplex.

The values of k_{app} calculated for 1-methylcyclohexene are 6.5×10^6 and 5.1×10^7 1 $mole^{-1}sec^{-1}$. The value from the fluorescence quenching, 5.1×10^7 1 $mole^{-1}sec^{-1}$, is less reliable as these measurements are based on small differences. As with the previously mentioned olefins, 1-methycyclohexene exhibits enhanced quantum yield upon lowering the temperature (Table 30) as is seen in Figure 44, therefore the value of k_{app} at 25^o is the minimum value for k_e. The maximum measured value, obtained for Φ_{add} at -28^o is 2.4×10^7 1 $mole^{-1}sec^{-1}$, four times the value at 25^o. The value of I_{add} is increasing at -28^o, indicating the maximum value for k_e has not been reached. Therefore, by analogy to the other olefins, it can be argued that the rate constant for exciplex formation should be very near to the diffusion controlled rate constant.

The inefficiency in this cycloaddition then must again be attributed to a high value of k_{-e} with respect to k_a. The ratio of k_{-e}/k_a at 25^o

Figure 44. Plot of quantum yield of addition of 4 molar 1-methylcyclohexene versus temperature

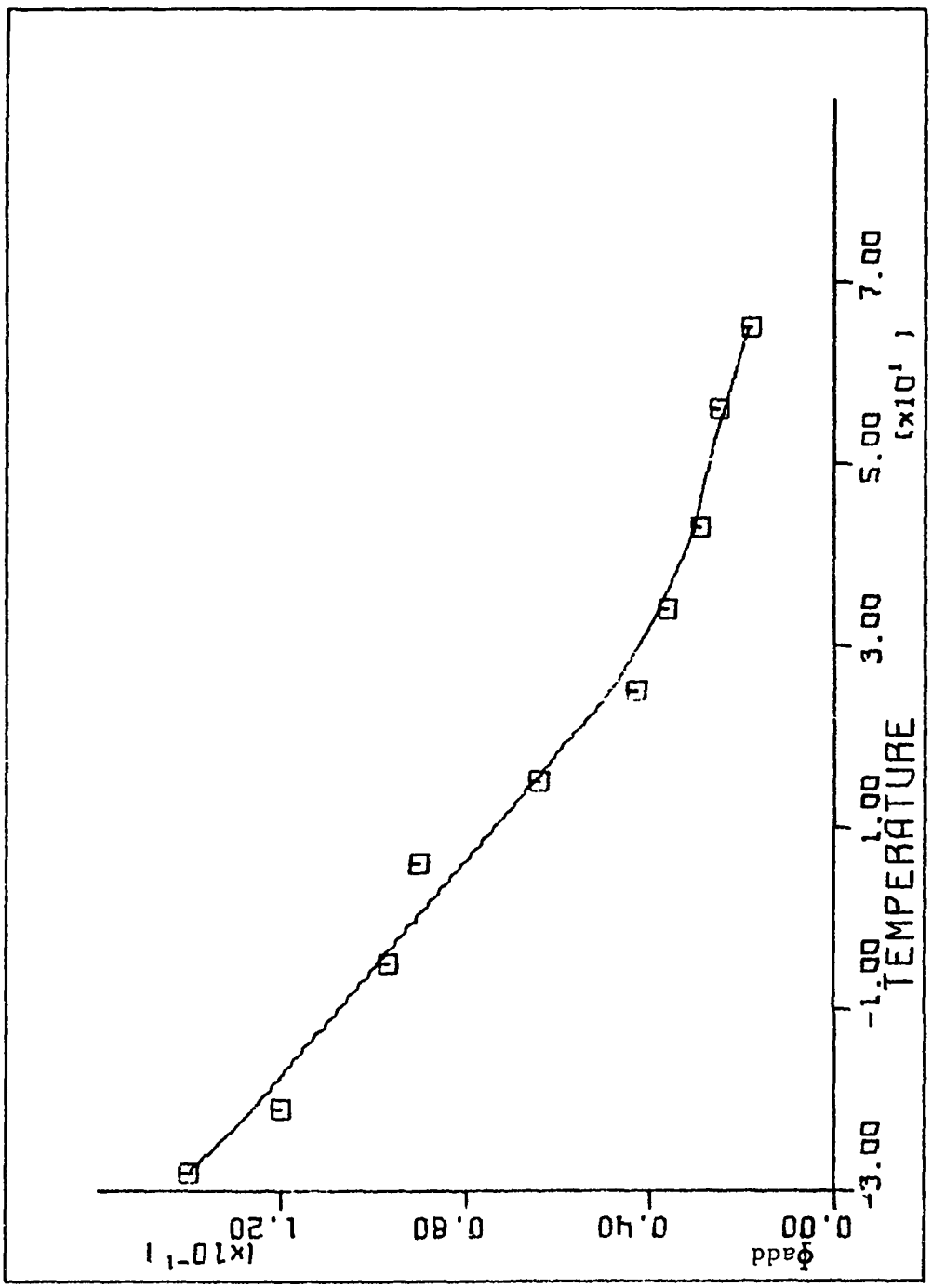
0.00
0.40
0.80
1.20
(x10⁻¹)
Φadd
-3.00
-1.00
1.00
3.00
5.00
7.00
(x10¹)
TEMPERATURE

is calculated to be 3600 which is reduced to 400 at -28°. The same k_{-e}/k_a ratio is obtained for the major adduct of 2-methyl-2-butene at -22°, indicating that the 1-methylcyclohexene exciplex 62 has an added degree of destabilization over the other syn tri-substituted exciplex 60. This added degree of destabilization is due to the six

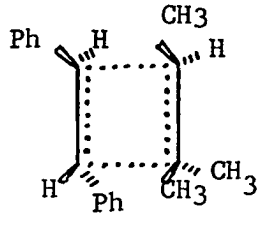

60

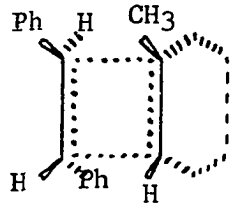

62

membered ring. The ring is seen as little barrier to exciplex formation as it is somewhat conformational locked, but in the exciplex the double bond strength is reduced with the net result being increased rotational freedom in the ring. This increased ring motion increases the torsional strain on the exciplex, facilitating its reversibility.

The calculated value of k_{app} for cyclohexene of 8.3×10^5 1 $mole^{-1}$ sec^{-1} again reflects the increase of k_{-e} with decreased alkyl substitution as k_{-e}/k_a = 26,000 at 25°. Cyclohexene addition is also temperature dependent (Table 34) as presented in Figure 45. The quantum yield could not be determined at lower temperatures due to operational difficulties. The low efficiency of this addition is therefore attributed not to a low value to k_e but a high value for exciplex dissociation.

Part of the decreased stability of the exciplexes of 1-methylcyclohexene and cyclohexene addition has been attributed to increased

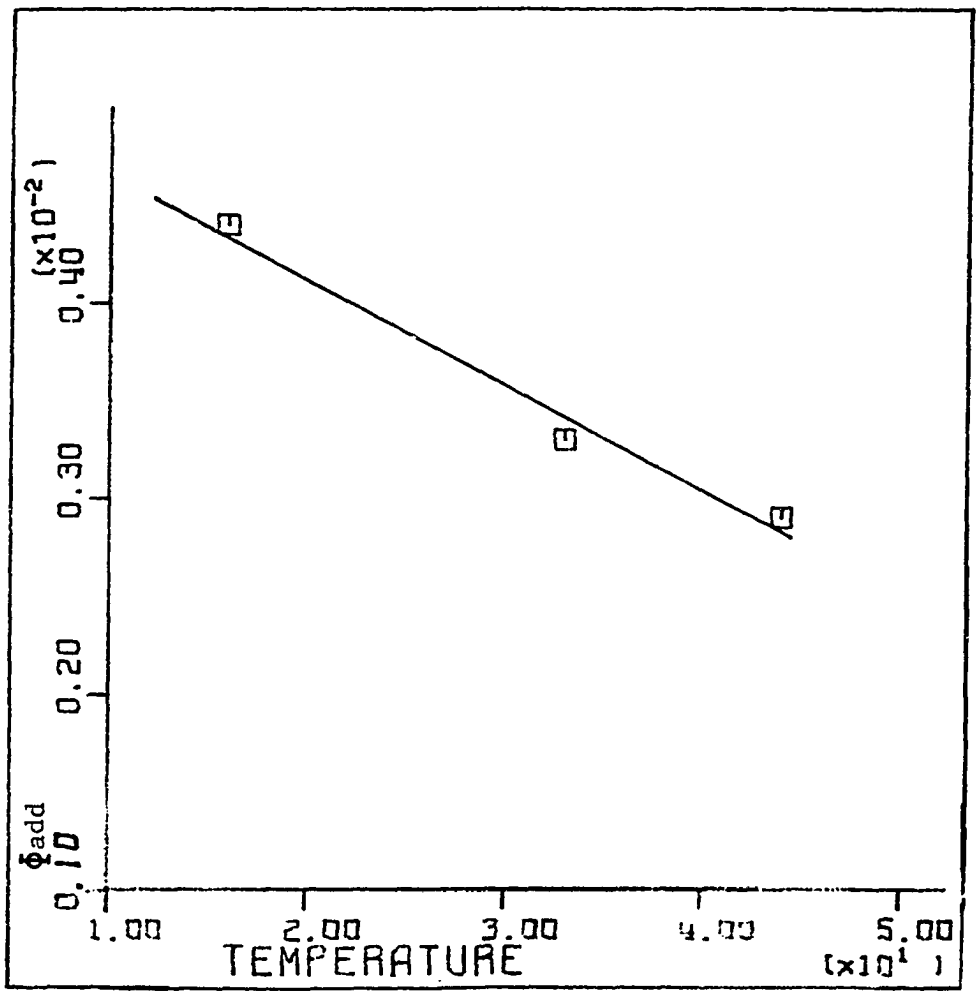

Figure 45. Plot of quantum yield of addition of 4 molar cyclohexene versus temperature

strain on the exciplex from conformational flipping. This can be shown to be correct on the basis of values of quantum yields for 1-methylcyclopentene, cyclopentene, and cycloheptene at 4 molar olefin.

The adduct from 1-methylcyclopentene and trans-stilbene has been identified as 1-methyl-6-endo-7-exo-diphenyl-cis-bicyclo [3.2.0] heptane 63 on the basis of spectral data. The infrared spectrum (Figure 46) reveals absorptions at 3.32, 3.34, 3.36, 5.15, 5.35, 5.55, 5.75, 6.21,

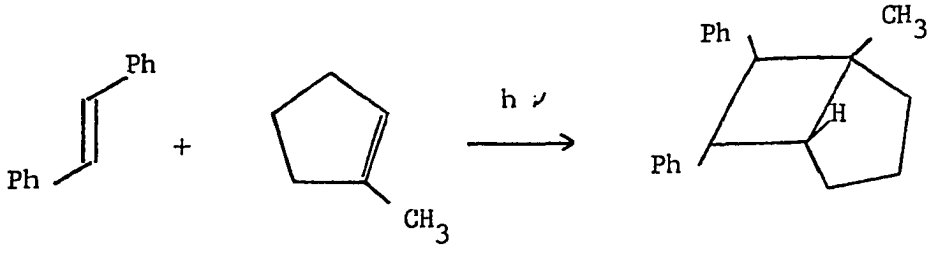

63

6.90, 9.70, 12.4, 13.6 and 14.4μ. The mass spectrum (Table 8) shows a 1:1 adduct m/e 262, 16%. A trace peak at m/e 247 results from the loss of the methyl group. The base peak m/e 180 is that from elimination of stilbene. The nmr spectrum (Figure 47) reveals a singlet at 7.11δ, integrating for 10 aromatic protons. The benzylic signal exists as a multiplet from 3.20-4.20δ, integrating for 2 protons. A broad resonance from 2.20-2.65δ, integrates for 1 methine proton. The ring methylene protons appear as a broad pattern 0.80-2.00δ, with the methyl singlet at 0.90δ, integrating for a total of 9 protons. The methyl group is considered to be cis to the adjacent phenyl group on the basis of the high field position.

Figure 46. Infrared spectra

Top: 1-methyl-6-endo-7-exo-diphenyl-cis-bicyclo [3.2.0] heptane

Middle: 6-endo-7-exo-diphenyl-cis-bicyclo-[3.2.0] heptane

Bottom: 8-endo-9-exo-diphenyl-cis-bicyclo-[5.2.0] nonane

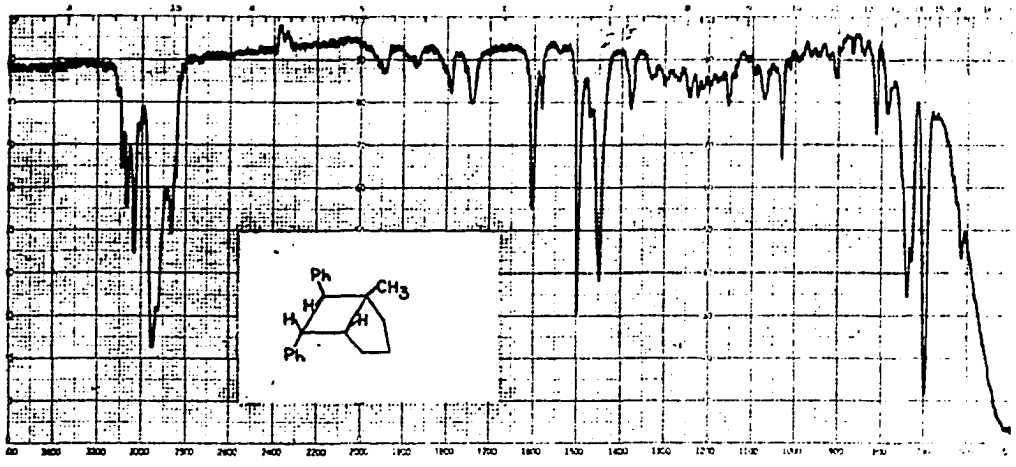
Ph
CH3
H
H
H
Ph

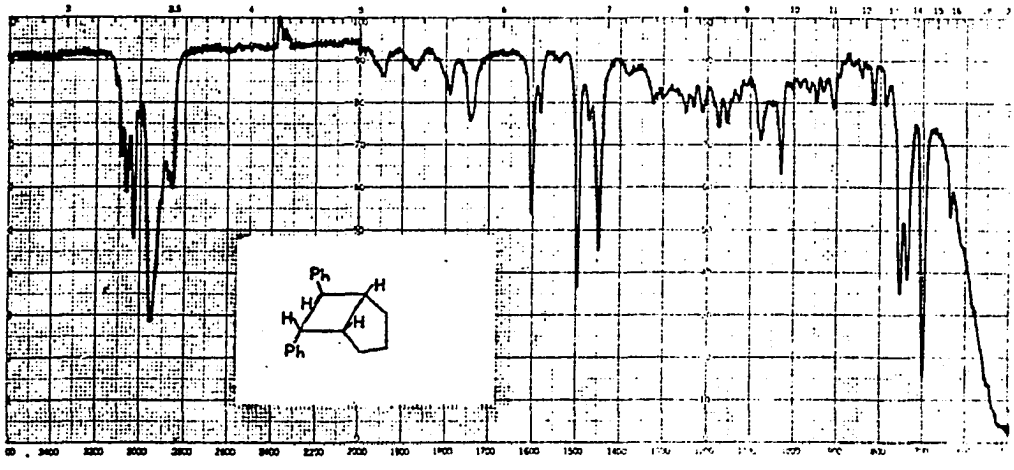
Ph
H
H
H
H
Ph

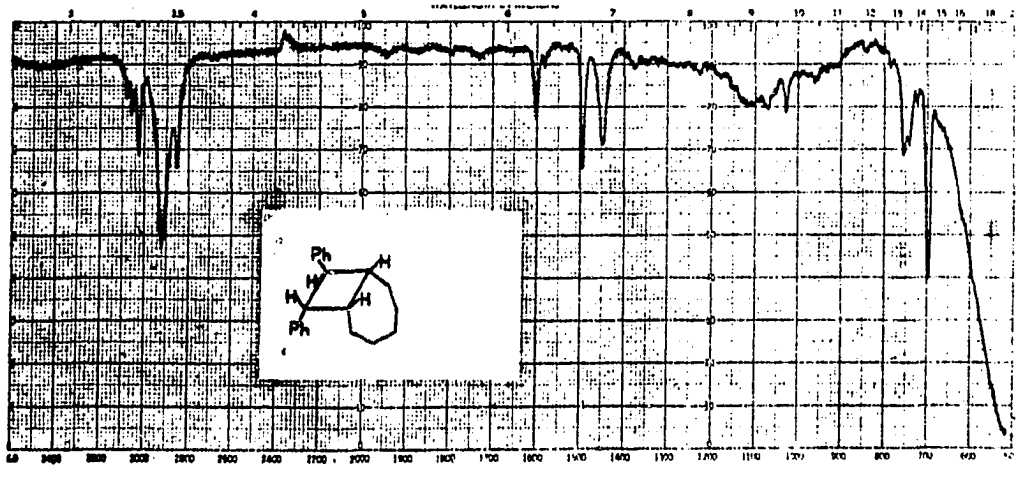
Ph
H
H
H
H
Ph

Figure 47. Nuclear magnetic resonance spectra

Top: 1-methyl-6-endo-7-exo-diphenyl-cis-bicyclo [3.2.0] heptane

Middle: 6-endo-7-exo-diphenyl-cis-bicyclo-[3.2.0] heptane

Bottom: 8-endo-9-exo-diphenyl-cis-bicyclo-[3.2.0]nonane

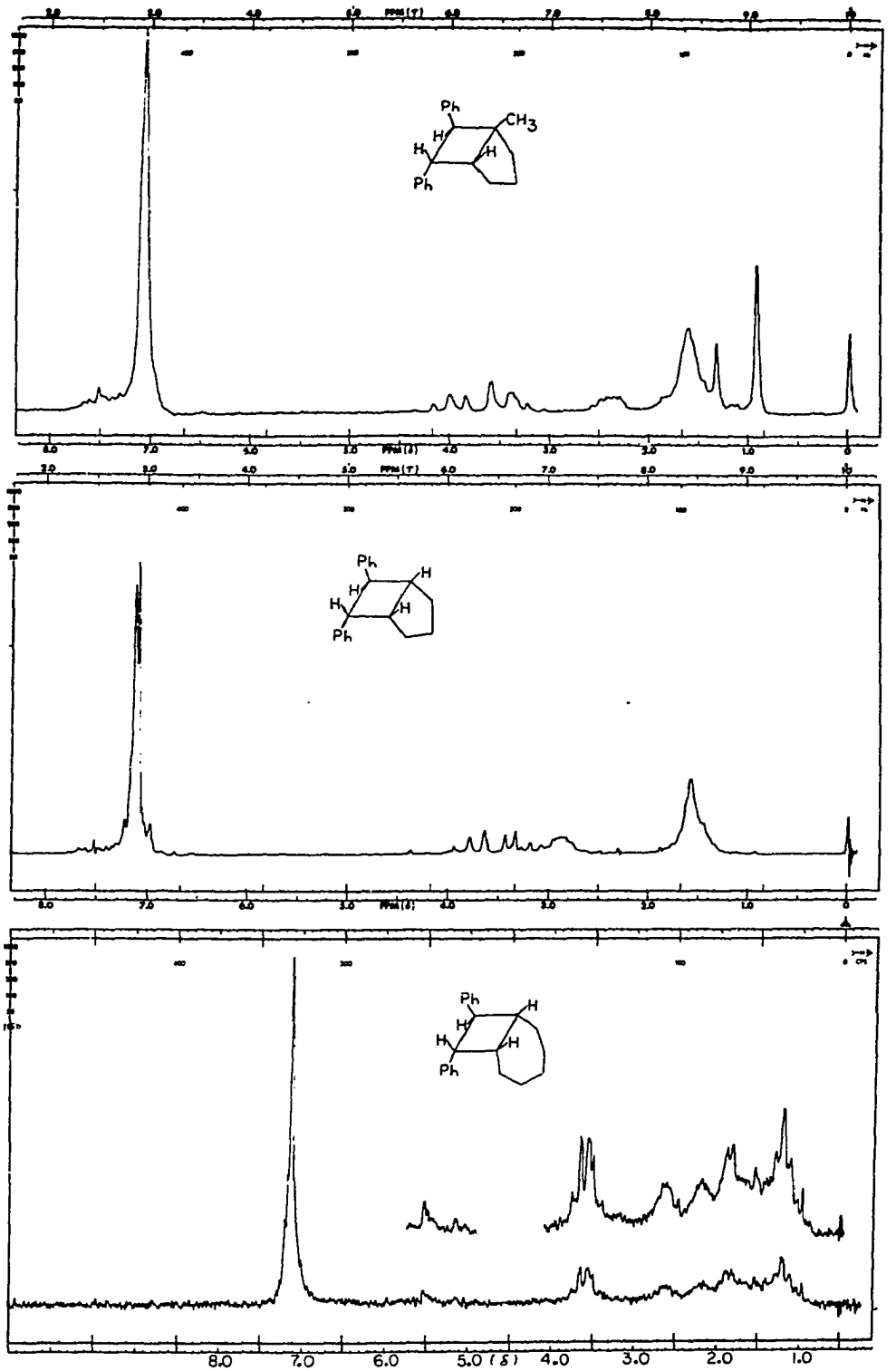
Ph
CH3
H
H
H
Ph
Ph
H
H
H
H
Ph
Ph
H
H
H
H
Ph
8.0
7.0
6.0
5.0 (δ)
4.0
3.0
2.0
1.0

Table 8. Mass spectra of adducts 63, 64 and 65

63		64		65	
m/e	rel. int.	m/e	rel. int.	m/e	rel. int
262	16.0	248	25.0	277	8.8
247	trace	181	16.0	276	37.7
181	14.0	180	100.0	181	10.0
180	100.0	179	50.0	180	100.0
179	42.2	178	40.0	179	68.5
178	35.5	177	3.4	178	40.5
177	7.6	176	3.4	177	7.0
176	3.4	91	3.0	176	5.6
91	6.5			91	3.8
				77	4.2

Irradiating trans-stilbene in the presence of cyclopentene produced 6-endo-7-exo-diphenyl-cis-bicyclo[3.2.0] heptane 64. The product was

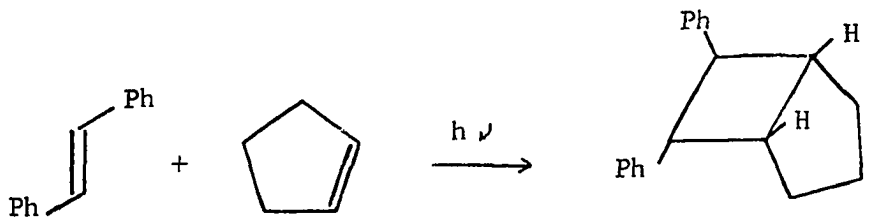

64

so identified on the basis of spectral evidence. The infrared spectrum (Figure 46) reveals absorptions at 3.32, 3.34, 3.36, 3.40, 3.44, 5.15,

5.35, 5.55, 5.75, 6.21, 6.65, 6.90, 9.70, 13.4, 13.6 and 14.3μ. The mass spectrum (Table 8) reveals a 1:1 adduct m/e 248, 25%. The base peak is that from the molecular ion of stilbene m/e 180. The nmr spectrum (Figure 47) reveals aromatic resonances at 7.10 and 7.16δ, integrating for 10 protons. A broad resonance from 2.70-2.10 and 3.10-3.95δ integrates for 4 protons, methine and benzylic. The methylene protons appear as a broad peak at 1.30-1.85δ which integrates for 6 protons.

The adduct from cycloheptene and trans-stilbene was identified as 8-endo-9-exo-diphenyl-cis-bicyclo [5.2.0] nonane 65 on the spectral data.

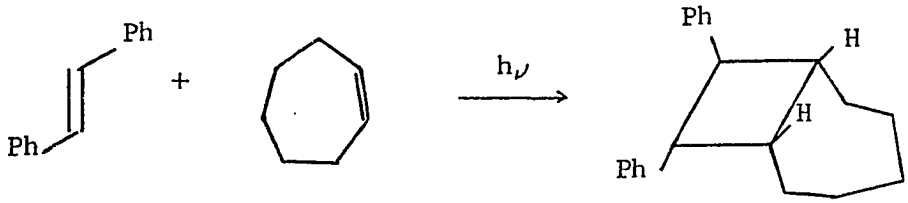

65

The infrared spectrum (Figure 46) shows absorptions at 3.32, 3.34, 3.36, 3.40, 3.45, 6.21, 6.70, 6.90 and 14.3μ. The mass spectrum (Table 8) shows a 1: 1 adduct m/e 276, 38%. The base peak is the molecular ion of trans-stilbene m/e 180. The nmr spectrum (Figure 47) shows a singlet at 7.13δ which integrates for 10 protons. A multiplet centered at 3.55δ integrates for 2 benzylic protons. A complex broad pattern from 0.80-2.70δ integrates for 12 protons, methine and methylene.

The values of the quantum yield of addition of various olefins are summarized in Table 9. The effect of ring size on destabilizing

Table 9. Quantum yield of addition of various olefins at 4 molar concentration to trans-stilbene

Olefin	Φ_{add}
1,2-dimethyl-cyclopentene	0.33
1-methyl-cyclopentene	0.11
cyclopentene	0.0075
1,2-dimethyl-cyclohexene	0.17
1-methyl-cyclohexene	0.043
cyclohexene	0.003
cycloheptene	0.0006

the exciplex is seen in the series cycloheptene Φ_{add} = 0.0006, cyclohexene Φ_{add} = 0.003 and cyclopentene, Φ_{add} = 0.0075. This increase in quantum yield with decreasing ring size is consistent to the idea of conformational flipping or steric interaction decreasing the overall forward reaction. As the ring size increases, both the steric interaction and ability of the molecule to undergo greater degrees of conformational rotations, which would increase the torsional strain on the exciplex, increases. This same effect is seen in the efficient tetra-substituted olefins, 1,2-dimethylcyclohexene and 1,2-dimethylcyclopentene. The five membered ring is twice as reactive as the six membered ring, 0.33 to 0.17.

The change in quantum yield with change in the number of substituents

from four to three is approximately a factor of 4; TME Φ_{add} 0.54, 2-methyl-2-butene $\Phi_{add_{total}}$ 0.10; 1,2-dimethylcyclohexene Φ_{add} 0.17, 1-methylcyclohexene Φ_{add} 0.043; 1,2-dimethylcyclopentene Φ_{add} 0.33, 1-methylcyclopentene Φ_{add} 0.11. It is interesting to note that the change in quantum yield in progressing from tri- to di-substituted olefins: 1-methylcyclohexene Φ_{add} 0.043, cyclohexene Φ_{add} 0.003; 1-methylcyclopentene Φ_{add} 0.11, cyclopentene Φ_{add} 0.0075; 2-methyl-2-butene $\Phi_{add_{total}}$ 0.10, cis or trans-2-butene $\Phi_{add_{cis}}$ 0.002 $\Phi_{add_{trans}}$ 0.006, is now a reduction by a factor of 15 to 60.

The negative temperature dependence of the measured rate constant, increase with decreasing temperature, has been explained in terms of an exciplex reversibility step incorporated into the mechanism. The temperature dependence may also be due to a dependence of excited state lifetime with temperature, increase of singlet lifetime with decreasing temperature. Dyck and McClure have determined that singlet trans-stilbene lifetime can be expressed by $1/(k_f + k_c + Ae^{-E/kT})$, the reciprocal of the sums of the temperature independent fluorescence rate constant, k_f, which has been determined to be 4×10^8 sec^{-1}; a temperature independent rate constant k_c, $.16 \times 10^8$ sec^{-1}; and a thermal quenching term $Ae^{-E/kT}$, E 1070 cm^{-1} (14), A 5.6×10^{11} sec^{-1} (94). From this equation, lifetimes of trans-stilbene singlet can be calculated at any temperature.

Equation 33 can be derived for a mechanism which does not involve

$$1/\Phi_{add} = \frac{k_a + k_{cd}}{k_a} + \frac{1}{\tau k_e [0]} \qquad (33)$$

exciplex reversibility. The slope of a $1/\Phi_{add}$ plot is given by $1/\tau k_e$. The values for k_e, calculated from the measured slopes and lifetimes calculated from the Dyck and McClure equation, are presented in Table 10 for TME. The values for k_e are seen to increase with decreasing

Table 10. Calculated singlet lifetimes and values of k_e derived from the calculated lifetimes

Temperature	τ ($\times 10^{-10}$ sec)	Slope	k_e ($\times 10^{9}$ l mole^{-1} sec^{-1})
54	1.33	8.06	0.93
44	1.52	7.00	0.94
34	1.74	5.88	0.98
25	1.98	4.20	1.20
5	2.70	2.94	1.33
-5	3.23	1.34	2.52
-10	3.50	0.98	4.47
-22	4.42	0.28	8.10

temperature, an increase which would not be expected if the temperature effect were solely dependent on lifetime changes, as k_e must be temperature independent. Therefore, an additional effect must be operating in conjunction with any lifetime change, exciplex reversibility.

This can be further demonstrated by the fact that 1-methylcyclohexene and the two adducts from 2-methyl-2-butene do not exhibit the same temperature dependence as TME and each other, as shown in Table 11. In all cases the values for k_e are seen to increase with decreasing temperature. Each olefin exhibits a different rate of temperature enhancement as seen by comparing the ratios of the slopes at the extremes of the temperature range, TME 28.5, 1-methylcyclohexene 5.3; over the range 54 to -10°, TME 8.2, major adduct of 2-methyl-

Table 11. Values for k_e for 1-methylcyclohexene and 2-methyl-2-butene from calculated singlet lifetimes

	1-methylcyclohexene		2-methyl-2-butene			
			Major		Minor	
Temp	Slope	$k_e(x10^7)$	Slope	$k_e(x10^7)$	Slope	$k_e(x10^7)$
56	156	4.74				
54			103	7.25	223	3.25
43	134	4.86	83.3	7.98	213	3.02
34	108	5.37	61.7	9.30	184	3.08
25	89.4	5.67	53.9	9.20	151	3.36
-4			29.4	10.6	87	3.60
-11			24.5	11.6	75	3.76
-22	29.4	8.14				

2-butene 4.2 and the minor adduct of 2-methyl-2-butene 3.0. The two adducts from 2-methyl-2-butene have different temperature dependences which can not be explained on the basis of lifetime effects and further supports the reverse exiplex participation.

The lifetime effect is seen as the dominant factor in TME at higher temperatures and the minor adduct of 2-methyl-2-butene at all temperatures. This reflects, in the case of TME, the slow change in k_{-e}/k_a ratio at high temperatures where k_{-e} is the dominant factor and the values of the ratio change little with temperature. At lower temperatures the ratio is changing rapidly as k_{-e} and k_a are changing roles of dominance in the fraction, and the apparent rate constant for addition rises rapidly. The slight change in the 2-methyl-2-butene minor adduct is attributed to the fact that over the entire measureable temperature range k_{-e} is the dominant term in the fraction and subsequently the small enhancement of the addition is observed. The major

adduct of 2-methyl-2-butene and 1-methylcyclohexene are intermediate cases in that the ratio of k_{-e}/k_a is not as large as in the minor adduct and a steady increase is seen in the temperature range and yet not as small as for TME which exhibits the rapid rise where the terms change roles of dominance.

This method of calculating k_e does not take into account the change in the diffusion controlled rate for a bimolecular process. As the temperature is lowered, the rate at which two molecules can diffuse together decreases as the viscosity of the solution increases. This effect acts in opposition to enhancement effects expected from lifetime changes. The decrease in the diffusion rate is slight in the high temperature range, but on cooling from 25 to -22° the diffusion rate decreases by 108%. The lifetime increase over this range is 125% and a net effect enhancement effect of 17% could be expected if the lifetime increase is opposed by the decrease in diffusion rates. The values of k_e, allowing a 17% net lifetime increase, at the lowest temperatures are 1.5×10^{10}, and 1.5×10^{8}, 1 $mole^{-1}sec^{-1}$ for TME and 1-methylcyclohexene respectively. These values are nearly double the values neglecting any diffusion effects in Table 11. If diffusion effects are considered, the contribution from reverse exciplex increases over that already evident from the previous treatment.

A ground state trans-stilbene molecule is excited to the first excited singlet state with each quanta of light absorbed. The singlets then deactivate to ground state species through various reaction modes. In the case of trans-stilbene and TME it is possible to account for virtually all of the singlet decay on the basis of three processes,

isomerization, fluorescence and addition (equation 34). Quantum yields

$$\Phi_{Total} = \Phi_{Add} + \Phi_{Fluor} + \Phi_{Isom} \qquad (34)$$

of isomerization were determined at 4 molar TME at various temperatures (Table 18). The quantum yield of fluorescence can be approximated from the known value for $\Phi_{Fluor} = 0.08$ (29) and the fluorescence quenching ratio at 4 molar of near two. The value for total isomerization is the measured Φ_c, quantum yield for formation of cis-stilbene, divided by the known partition ratio of 0.55 obtained from studies of the photostationary state by Fischer (29). The results of the calculation of I_{Total} are summarized in Table 12. The three processes are seen to

Table 12. Total quantum yield of reaction for TME at 4 molar at various temperatures

Temperature	Φ_{Add}	Φ_{Fluor}	Φ_{Isom}	Φ_{Total}
55°	0.30	0.04	0.49	0.83
45°	0.38	0.04	0.42	0.84
25°	0.54	0.04	0.35	0.93
-4°	0.76	0.02	0.14	0.92

account for virtually all the light, indicating that the value contributed from radiationless decay is relatively small.

Photocycloaddition of cis-Stilbene to TME

In the course of mechanistic studies of trans-stilbene and TME, it was discovered that cis-stilbene irradiated in the presence of TME gave rise to the same adduct as from trans-stilbene. It was therefore undertaken to study the reaction in the light of the apparent inversion of the stilbene portion of the molecule. Irradiating cis-stilbene at 254 nm in the presence of TME has, as the prime process, production of trans-stilbene and therefore values for the quantum yield from cis-stilbene must be corrected for the amount of adduct which is produced from the trans-stilbene. As a result the reaction can only be taken to a low percent completion and combined with the subsequent correction factor the errors in the measurements are greater than those for trans-stilbene.

The stereospecificity with respect to the ground state partner cannot be determined at this time as TME is the only olefin reacting rapidly enough for addition to cis-stilbene to be measureable. The inversion of stereochemistry of the stilbene portion is based on identical gas chromatographic retention times on column C and D (see EXPERIMENTAL section) with authentic TME adduct. In light of the retention time difference of the two adducts from 2-methyl-2-butene, which differ only in the change of a methyl group, the structure of the photoadduct with cis-diphenyl would certainly be expected to have a different retention time than the trans isomer.

The assignment of the multiplicity of the reactive state of

cis-stilbene is hampered by the fact that cis-stilbene does not emit. Sensitization data (Table 38) points to the singlet state. The apparent sensitization by thioxanthone is again a mystery, as in the 1-methylcyclohexene and trans-stilbene case. Michler's ketone has presented consistent data for trans-stilbene and it is assumed that triplet sensitization of adduct formation is not operating, therefore a singlet mechanism is favored.

The stereochemical results are in disagreement with the normal stereo-retention properties of singlet reactions (see REVIEW OF LITERATURE section). The key to the problem may lie in the potential energy level diagram for stilbenes (Figure 3). For singlet trans-stilbene there is a plateau for the first 60° of rotation around the central bond, while for cis-stilbene there is an immediate decrease in energy of the singlet with respect to rotation. It is therefore possible that cis-stilbene may immediately, upon being excited to the singlet, rotate to the twisted singlet energy minimum, a rotation of 60° from cis. The exciplex may therefore form with this twisted singlet and undergo decay to the trans-product, possibly on steric grounds equation 35 .

The evidence for an exciplex is, in the case of cis-stilbene, much less secure. An exiplex is favored on the basis of the endothermic quenching of the singlet by TME and the negative temperature effect.

There are two possible mechanisms for such a process one of which is shown in Figure 48. This mechanism is quite similar to that proposed for trans-stilbene. Singlet cis can undergo internal cyclization to

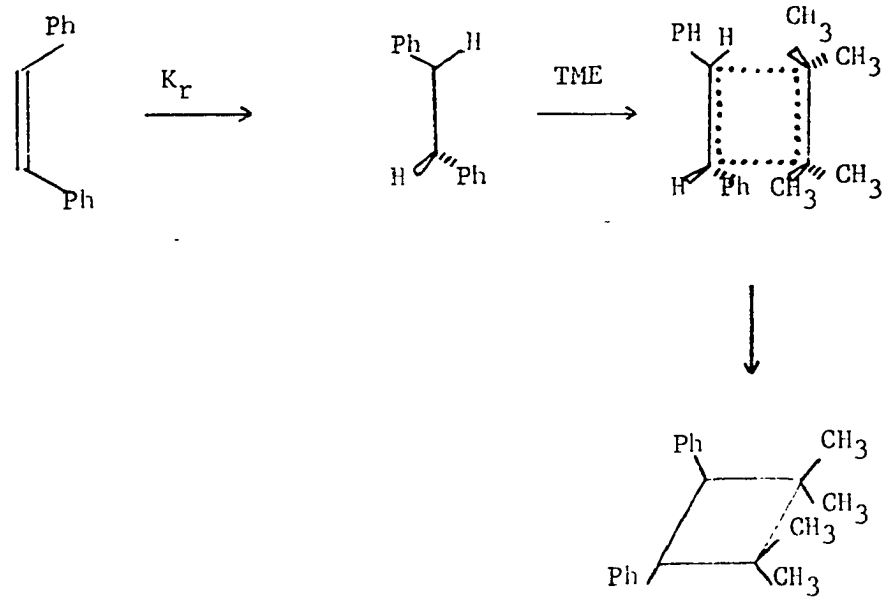

(35)

form the dihydrophenthrene. Upon formation of the phantom singlet, it can partition between ground state cis and trans-stilbene and exciplex formation. Once the exciplex is formed, it has the same type decay modes as the exciplex from trans-stilbene. The reversible mode for the exciplex produces phantom singlet and ground state olefin.

The expression for $1/\Phi_{add}$ is given by equation 36 . This equation

$$1/\Phi_{add} = \frac{(k_d + k_{ic} + k_{dhp} + k_r)(k_{pt} + k_{pc})(k_a + k_{cdt} + k_{cd_c} + k_{-e})}{k_r k_e k_a [0]} + \frac{(k_d + k_{ic} + k_{dhp} + k_r)(k_a + k_{cd_t} + k_{cd_c})}{k_r k_a} \quad (36)$$

can be simplified to equation 37 by substituting $1/\tau_c$, the reciprocal of cis-singlet lifetime, for $(k_d + k_{ic} + k_{dhp} + k_r)$ and $1/\tau_p$, the reciprocal of phantom singlet lifetime, for $(k_{p_c} + k_{p_t})$.

$$S_c \longrightarrow {}^1S_c$$

$${}^1S \xrightarrow{k_d} S_c$$

$${}^1S_c \xrightarrow{k_{ic}} {}^3S_c$$

$${}^1S_c \xrightarrow{k_{dhp}} \text{Dihydrophenanthrene}$$

$${}^1S_c \xrightarrow{k_r} {}^1S_p$$

$${}^1S_p \xrightarrow{k_{pdt}} S_t$$

$${}^1S_p \xrightarrow{k_{pdc}} S_c$$

$${}^1S_p + 0 \xrightarrow{k_e} \text{Exciplex}$$

$$\text{Exciplex} \xrightarrow{k_{-e}} {}^1S_p + 0$$

$$\text{Exciplex} \xrightarrow{k_{cd_t}} S_t + 0$$

$$\text{Exciplex} \xrightarrow{k_{cd_c}} S_c + 0$$

$$\text{Exciplex} \xrightarrow{k_a} \text{Adduct}$$

Figure 48. Possible mechanism for addition of cis-stilbene to TME

$$1/\Phi_{add} = \frac{(k_a + k_{cd_t} + k_{cd_c} + k_{-e})}{\tau_c \tau_p k_r k_e k_a [0]} + \frac{(k_a + k_{cdt} + k_{cd_c})}{k_r k_a} \qquad (37)$$

The values for $1/\Phi_{add}$ vs. $1/[0]$ (Table 36) are shown in Figure 49, slope 67.5 $\pm$ 14.5, intercept 6.47 $\pm$ 5.14. Due to the higher error in the values for Φ_{add}, the intercept value may be within experimental error of unity. For this value to be true two conditions must be met, $k_r = 1/\tau_c$ and $k_a = (k_a + k_{cd_t} + k_{cd_c})$.

The first conditions requires the conversion quantum yield to the phantom singlet to be 1.0. In view of the known production of dihydrophenanthrene (I_{DHP} = 0.10) from singlet cis-stilbene, the maximum value of the conversion to phantom singlet is 0.90. This value is within error limits to satisfy the condition. The conversion quantum yield of 0.90 assumes the isomerization of cis-stilbene proceeds solely via the singlet, as is the contention of Saltiel (32). In light of the potential energy diagram, it is possible that the mechanism for cis-stilbene isomerization may differ from that of trans-stilbene, cis via singlet, trans via triplet. However, should cis isomerize from the triplet the value for the conversion to phantom singlet would be lowered to 0.32. The total isomerization quantum yield is given by Φ_t/α, quantum yield for production of cis divided by the partition factor α leading to cis-stilbene, 0.26/0.45 = 0.58. The value for production of dihydrophenanthrene is 0.10, for a total of 0.68 for other processes. The second condition for an intercept of unity, k_{cd_t} and k_{cd_c} being negligible compared to k_a, would be compatible with the results from trans-stilbene exciplexes. For further analysis of the kinetic studies

Figure 49. Reciprocal of plot of quantum yield of addition of cis-stilbene versus reciprocal of TME concentration

Slope = 67.8 ± 14.6 M

Intercept = 6.48 ± 5.15

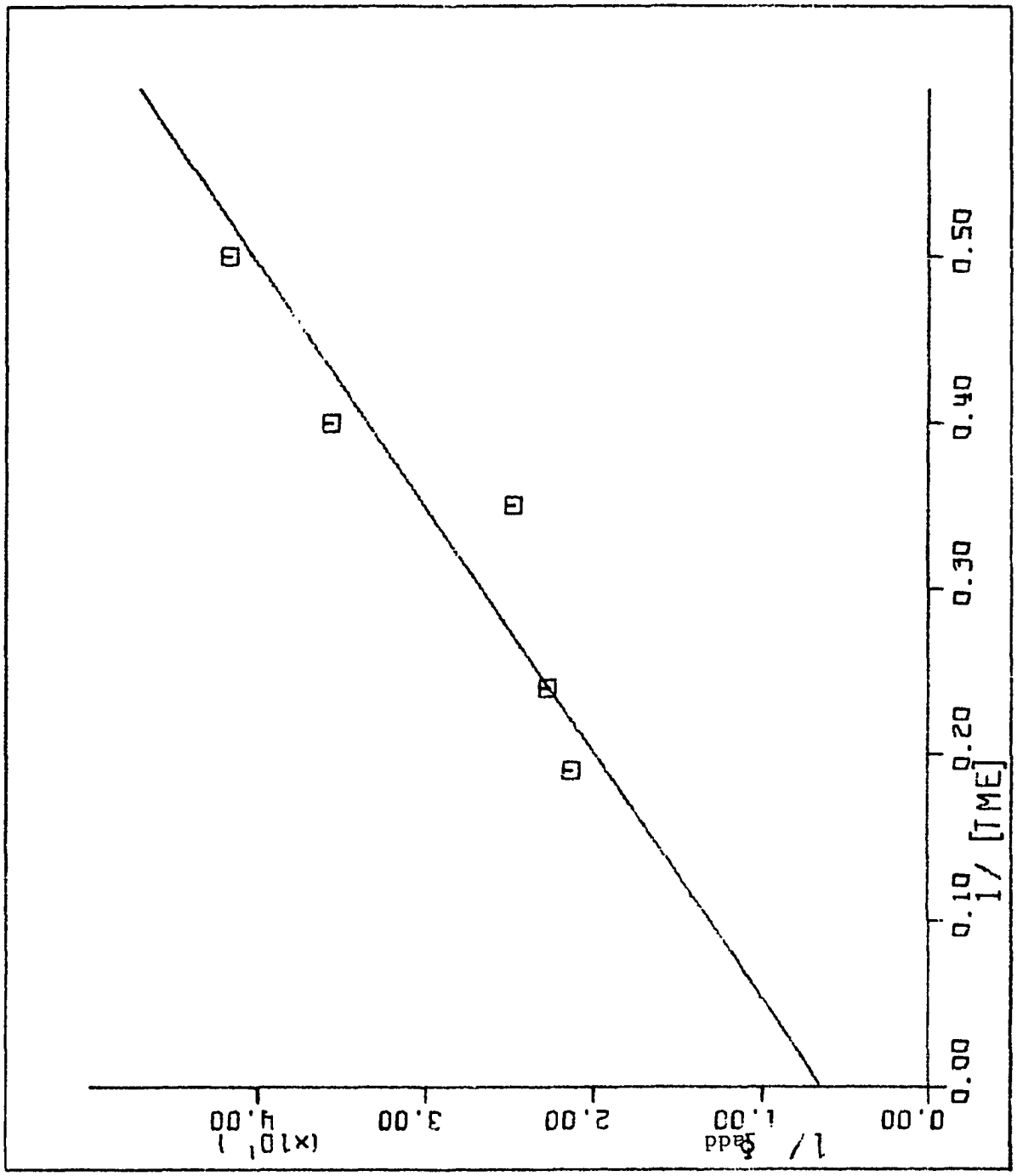
0.00
0.10
0.20
0.30
0.40
0.50
1/ [TME]
0.00
1.00
2.00
3.00
4.00
(x10¹)
1/ δadd

k_{cd_t} and k_{cd_c} will be assumed to be negligible. An intercept of unity would, according to this mechanism, require isomerization not to be a triplet process.

The value of Φ_{add} exhibits a temperature dependence (Table 37) shown in Figure 50. The increase in quantum yield with decrease in temperature serves to verify the necessity for including exciplex reversibility in the mechanism. Due to the lack of lifetime data for cis-stilbene singlet, no value can be calculated for k_{app} according to equation 38.

$$\frac{(k_a + k_{-e})}{\tau_c \tau_p k_r k_e k_a} = \frac{1}{\tau_c \tau_p k_r k_{app}} = \text{slope} \qquad (38)$$

The second mechanism is seen in Figure 51. This mechanism differs from the first in that the only processes involving singlet cis are conversion to dihydrophenanthrene and slide down the potential curve of Borrell and Greenwood (20). The formation of DHP from cis is presumed to involve an interaction of the tilted phenyl rings from ground state through the excitation process and subsequent closure from the excited state. Once singlet cis is produced, it immediately assumes the path of least resistance, rotation around the central bond to lower the energy of the system. The other processes, including intersystem crossing, result from the phantom singlet. The other steps of the mechanism are the same as the mechanism in Figure 48.

The expression for $1/\Phi_{add}$ is given by equation 39. The term $(k_{DHP}\ k_r)/k_r$ is the reciprocal of the conversion efficiency to the phantom which has a value of 1.10, as I_{DHP} is known to be 0.10. The

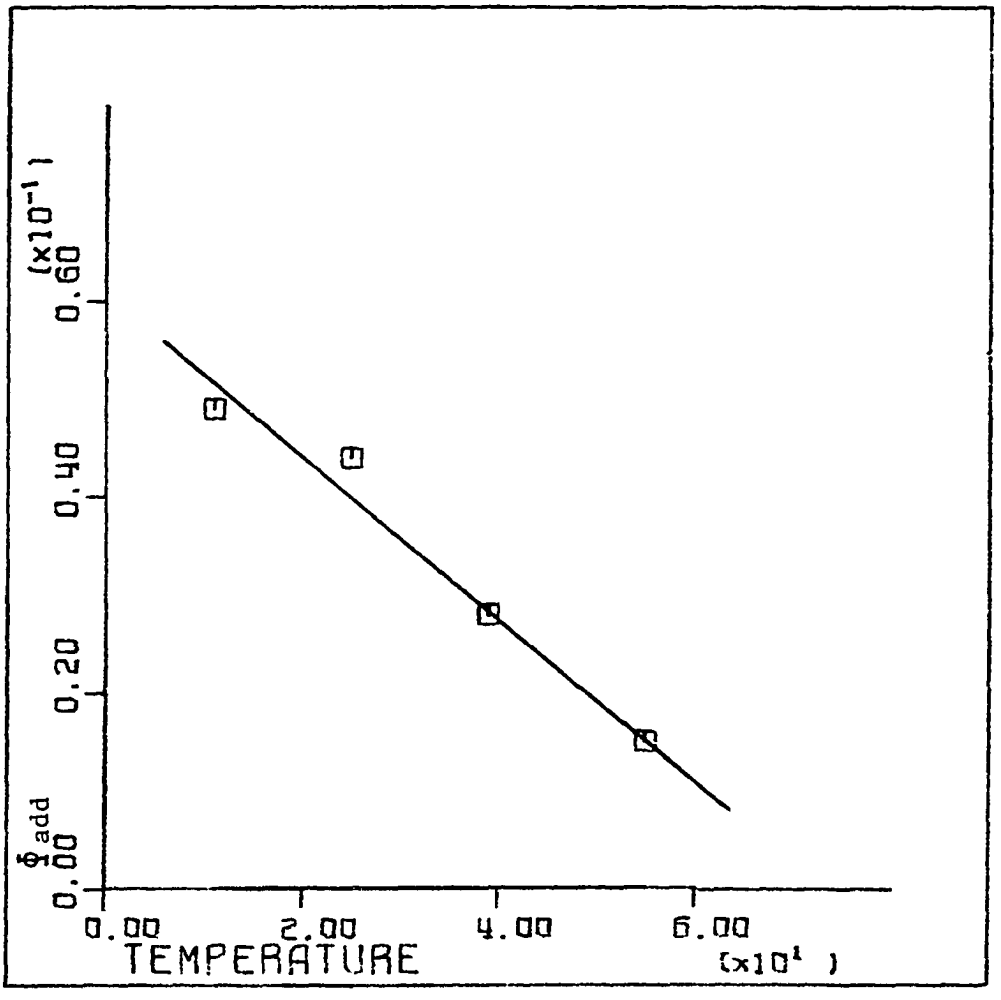

Figure 50. Plot of quantum yield of addition of cis-stilbene to 4 molar TME versus temperature

$$S_c \xrightarrow{h\nu} {}^1S_c$$

$${}^1S_c \xrightarrow{k_{DHP}} \text{Dihydrophenanthrene}$$

$${}^1S_c \xrightarrow{k_r} {}^1S_p$$

$${}^1S_p \xrightarrow{k_{pt}} S_t$$

$${}^1S_p \xrightarrow{k_{p_c}} S_c$$

$${}^1S_p \xrightarrow{k_{ic}} {}^3S_p$$

$${}^1S_p + 0 \xrightarrow{k_e} \text{Exciplex}$$

$$\text{Exciplex} \xrightarrow{k_{-e}} {}^1S_p + 0$$

$$\text{Exciplex} \xrightarrow{k_a} \text{Adduct}$$

$$\text{Exciplex} \xrightarrow{k_{cd_t}} S_t + 0$$

$$\text{Exciplex} \xrightarrow{k_{cd_c}} S_c + 0$$

Figure 51. Mechanism for addition of cis-stilbene to TME involving immediate conversion to phantom singlet

$$1/\Phi_{add} = \frac{(k_{DHP} + k_r)(k_{p_t} + k_{p_c} + k_{i_c})(k_a + k_{cd_t} + k_{cd_c} + k_{-e})}{k_r k_e k_a [0]} \quad (39)$$

$$+ \frac{(k_{DHP} + k_r)(k_a + k_{cd_t} + k_{cd_c})}{k_r k_a}$$

term $(k_{p_t} + k_{p_c} + k_{ic})$ can be substituted by $1/\tau p$. This reduces the expression to equation 40. A value of 1.10 for the intercept would then again

$$1/\Phi_{add} = \frac{(k_a + k_{cd_t} + k_{cd_c} + k_{-e})}{\tau_p \quad k_e k_a \quad 0} \quad 1.10 + \quad 1.10 \frac{(k_a + k_{cd_t} + k_{cd_c})}{k_a} \quad (40)$$

require k_{cd_t} and k_{cd_c} be negligible compared to k_a.

Of the two mechanisms, the first would require the quantum yield of isomerization be independent of olefin, at high concentrations, as there is no competition for a common species in the two processes. The second mechanism would have the value of Φ_{isom} decrease with high olefin concentration as both isomerization and addition involve the same species. The values for Φ_{isom} in the presence of olefin (Table 36) show no change with increasing olefin concentration, 2.0 to 5.3 molar. This is not conclusive data, due to the low value for Φ_{add} as the effect on Φ_{isom} would be very small, if detectable in mechanism of Figure 51. To conclusively eliminate one mechanism the effect on Φ_{isom} must be studied at lower temperatures where the addition reaction is expected to be moderately efficient.

The increased value for k_{-e}, reflected in the low efficiency of TME adduct formation from this source, is due to the decreased stability

of the phantom singlet exciplex. This is due to the decreased orbital overlap in the exciplex, as would be expected from the twisted nature of the excited partner.

EXPERIMENTAL

Photocycloaddition of trans-Stilbene to Olefins

General instruments and methods

Infrared spectra were recorded on a Beckman IR-9. Nuclear Magnetic Resonance specta were recorded on a Varian Associates Model A-60 or HA-100, or a Perkin-Elmer Hitachi Model R-20B, and the values are for solutions in carbontetrachloride. Mass spectra were recorded on an Atlas CH-4 mass spectrometer. High resolution mass spectra were recorded on an AEI MS-902. Microanalyses were performed by Spang Microanalytical Laboratories, Ann Arbor, Michigan. Preparative gas chromatography was performed on an Aerograph Model 1520-A using; column A, 12 ft. x 3/8 in., 10% polyalkylene glycol (Ucon water soluble) on Chromosorb W, 60/80 mesh or column B, 12 ft. x 3/8 in., 15% silicone gum rubber (SE 30) on Chromosorb W, 60/80 mesh.

Rotating and linear quantum yield apparatus

A rotating photochemical apparatus (referred to as the wheel) similar to that described by Moses et al., (99) was used for simultaneous irradiations of samples. A closed-loop water circulating system was employed to cool the lamp housing (100). The temperature of the water in which the wheel was immersed was controlled by a Tecan Tempunit, range 15-90°C. The lamp jacket was placed within a quartz filter-solution cell, having two concentric solution compartments of 1 cm solution thickness. The inner solution compartment was filled with 250 ml of potassium chromate solution, 132 mg potassium chromate in 250 ml

of 1% aqueous sodium carbonate, which is known to transmit light of wavelength 310 ± 20 nm, becoming transparent past 470 nm (101). The outer compartment contained 250 ml of a solution of 65 g cobalt sulfate in 250 ml distilled water (101). The cobalt sulfate solution was employed to filter out light of wavelength 440 nm.

A linear quantum yield apparatus was used for irradiation of single samples and for temperature dependence studies (100).

Variable temperature quantum yield apparatus

Variable temperature quantum yields were determined using the linear apparatus and a variable temperature sample holder. For temperatures of +10 to +65°C. a hollow aluminum block, through which thermostatically controlled water was circulated, was used. The temperature was controlled by a Tecan Tempunit, range 15 to 90°C. in an external reservoir.

For temperatures below 10°C. the apparatus in Figure 52 was used. The stainless steel sample holder block was encased in a stainless steel vacuum shroud to prevent condensation on the quartz sample compartment window. The sample block was equipped with a nitrogen bleed line at the bottom of the sample compartment. Dried nitrogen was bled into the sample compartment prior to opening to the atmosphere to create a positive pressure with intent of preventing moisture from entering and condensing in the sample compartment. The sample block was cooled by passing cooled-compressed air through the air flow channels surrounding the sample compartment. The air was first dried in a two foot drying column packed with Drierite. The dried air was then cooled by passing through

Figure 52. Low temperature apparatus

Top: Stainless steel sample block

Bottom: Stainless steel vacuum shroud

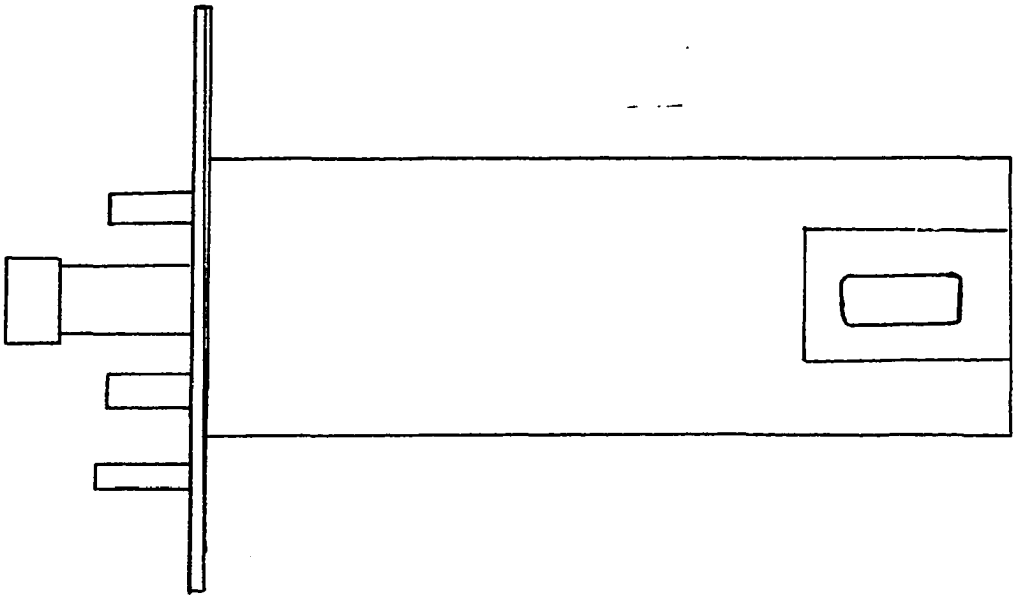

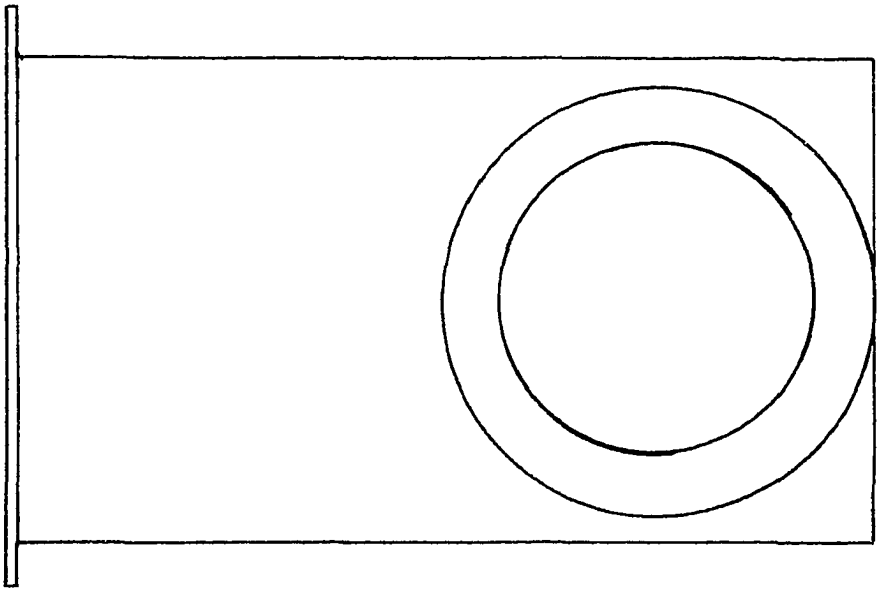

coils of 3/8 in. copper tubing in Dewar flasks containing Dry Ice-ethanol. The temperature was controlled by regulating the flow rate of the air and the size and number of cooling coils used. The internal block temperature was measured by a iron-Constantin thermocouple imbedded in the block at the level of the sample.

Cells used for quantum yield measurements

For irradiations at 313 and 366 nm, rounds cells (5.0 cm long) constructed from 13 x 100 mm Pyrex culture tubes and equipped with standard taper 10/30 joints, were used. For irradiations at 254 nm, cells were constructed from quartz tubing (13 mm) to the same dimensions as the Pyrex tubes. The quartz tubes were equipped with quartz to Pyrex graded-seals for ease in sealing and reconstructing the tubes.

Actinometry

Potassium ferrioxalate actinometry was used for measuring light intensities (102). Cells containing 3.0 ml of 0.013M potassium ferrioxalate solution were irradiated for a known length of time. A 1.0 ml aliquot of the irradiated solution was added to a 50 ml volumetric flask containing 8.0 ml of 0.10% 1, 10-phenanthroline solution and 1.0 ml of sodium acetate-sulfuric acid buffer which had been diluted to 40 ml with distilled water. After diluting to 50 ml, the solutions were stored in the dark for a minimum of one hour. The optical density was then measured at 510 nm with a Beckman DU spectrophotometer equipped with a Model 205 Gilford power supply, Model 220 Gilford optical density

converter and Model 209 Gilford automatic absorbance meter. Actinometers were run in duplicate before and after each irradiation.

Preparation and irradiation of samples

For all quantum yield measurements a 3.0 ml sample was used. Samples were prepared from volumetric solutions of the respective components and were measured into the cells using Becton Dickinson syringes equipped with Teflon needles. The solvent for quantum yield studies was n-hexane and for sensitization experiments benzene was used. Samples were degassed by four freeze-pump-thaw cycles at liquid nitrogen temperatures to 10^{-4} mm and were sealed with a torch under vacuum. Samples were shielded from light during preparation and degassing by wrapping with aluminum foil, and were kept in the dark before and after irradiation. The samples, except the time dependent studies, were irradiated to 6% or less completion in the wheel or linear apparatus.

Analytical procedures

Analysis of products were performed on an Aerograph Model 1520 A and B gas chromatograph using a thermal conductivity detector and a disc integrator for measurement of peak areas. Product ratios were analyzed relative to an external standard added after irradiation and were corrected for differences in thermal conductivity. Benzophenone, methyl trans-cinnamate and fluoren-9-one were used as external standards in the quantum yield studies.

The data reported in the tables is the average of two or more chromatographic analyses which agreed within ±4%. The quantum yield samples were concentrated to 1/4 original volume prior to analysis. Evaporation of solvent was found to have no effect on the composition of the sample. The columns were eluted with helium at 96 cc/minute. The colums referred to in the experimental section are: column C, 6 ft. x 1/4 in., 7% poylalkylene glycol (Ucon water soluble) on Chromosorb W, acid washed, 60/80 mesh, maintained at 180-190°; column D, 8 ft. x 1/4 in., 10% Silicone gum rubber (SE 30) on Chromosorb W, acid washed, 60/80 mesh, maintained at 190-205°.

Fluorescence equipment

Fluorescence emission spectra were recorded on an Aminco-Bowman Spectrophotofluorometer Model 4-48202 (American Instrument Co., Inc.) equipped with a 150 watt Hanovia Xenon lamp source and a RCA R136 photomultiplier tube. The instrument was connected to an Aminco-Bowman Microphotometer Model 10-267 and an Aminco X-Y-T recorder Model 1620-838. Samples were analyzed in 1 cm x 1 cm four-face quartz fluorescence cells.

Plots of quantum yield data

Least-squares plots were drawn by a simplotter from a program plot computer program which calculated least-squares slopes, intercepts, and error limits in terms of standard deviation.

Format and symbols used in the tables of data

The format for the listing of experimental results of quantum yield and sensitization measurements consists of a statement of instrument used, irradiation conditions and analytical procedure used. This is followed by a table listing the pertinent experimental details and results. The symbols used in the tables of experimental data refer to the following: $[S_t]$, concentration of trans-stilbene in moles/liter; $[S_c]$, concentration of cis-stilbene in moles/liter; $[O]$, concentration of olefin in moles/liter; $[Sens]$, concentration of sensitizer in moles/liter; Φ_{add}, quantum yield of cycloaddition; Φ_{isom}, quantum yield of isomerization of stilbene; $(\Phi_f/\Phi_f)_{olefin}$, ratio of the quantum yield of fluorescence in the absence of olefin to the quantum yield of fluorescence in the presence of olefin.

Preparation and purification of reagents

trans-Stilbene (Scintillation Grade, Aldrich Chemical Co.) was twice recrystallized from n-hexane (Spectragrade, Fischer) for quantum yield measurements. For preparative reaction the commercial trans-stilbene was used without further purification. cis-Stilbene (Aldrich) was twice distilled through a 50 cm spinning band column under vacuum. Spectragrade n-hexane (Fischer) was used with no further purification. Reagent grade benzene was stirred with concentrated sulfuric acid for 24 hours, followed by extraction with water and sodium bicarbonate solution. After drying over anhydrous calcium chloride, it was distilled

through a 30 cm Vigreaux column and analyzed by nmr for purity. For preparative reactions the olefins were distilled once. Thioxanthone and Michler's ketone were recrystallized from suitable solvents and had melting points consistent with literature values.

Irradiation of trans-stilbene in the presence of cis-2-butene

trans-Stilbene (3.0 g, 0.017 mole) was added to a solution of cis-2-butene (20 ml, 0.36 mole) and absolute ether (20 ml) in a quartz tube immersed in a Dry Ice-ethanol filled quartz Dewar flask. The solution, continually kept at Dry Ice-ethanol temperature, was irradiated external to a Pyrex immersion well using a 450 watt Hanovia lamp for 48 hours. The solvent was removed under reduced pressure to yield a yellow oil. The nmr spectrum of the oil revealed the presence of stilbene, cis and trans, and an adduct of stilbene with cis-2-butene. The adduct was isolated in pure form by preparative gas chromatography using column A. The adduct was identified as trans-1,2-diphenyl-cis-3,4-dimethylcyclobutane from the infrared spectrum (Figure 12), nmr spectrum (Figure 13) and mass spectrum (Table 2).

High resolution mass spectrum, in lieu of microanalysis

Theoretical for $C_{18}H20$: 236.1564920 (M^+). Found : 236.1565014 (M^+).

Irradiation of trans-stilbene in the presence of trans-2-butene

trans-Stilbene (3.0 g, 0.017 mole) was added to a solution of trans-2-butene (20 ml, 0.36 mole) and absolute ether (20 ml) in a quartz

tube immersed in a Dry Ice-ethanol filled quartz Dewar flask. The solution, continually kept at Dry Ice-ethanol temperature, was irradiated external to a Pyrex immersion well for 48 hours. The solvent was removed under reduced pressure to yield a yellow oil. The nmr spectrum of the oil revealed the presence of stilbene, cis and trans, and an adduct of stilbene with trans-2-butene. The adduct was isolated in pure form by preparative gas chromatography using column A. The adduct was identified as either trans-1,2-diphenyl-syn-trans-3,4-dimethylcyclobutane or trans-1,2-diphenyl-anti-trans-3,4-dimethylcyclobutane from the infrared spectrum (Figure 12), nmr spectrum (Figure 13) and mass spectrum (Table 2).

High resolution mass spectrum, in lieu of microanalysis

Theoretical for $C_{18}H_{20}$: 236.1564920 (M^+). Found : 236.155407 (M^+).

Attempted sensitization of cis and trans-2-butene adduct formation

Samples in Pyrex tubes were irradiated in the wheel at 25°. Analysis using column D gave the results shown in Table 13.

Attempted sensitization of TME adduct formation

Samples were irradiated in Pyrex cells in the linear apparatus. Samples were analyzed for TME adduct by gas chromatography using column C. The results are presented in Table 14.

Table 13. Attempted sensitization of cis and trans-2-butene adduct formation

Sensitizer	[Sens] [a]	[S_t]	[O]	λ nm	Irrad. time	cis	trans	adduct
Blank	--	0.054	trans 5.33	366	7 days	15	19	1
Thioxanthone	sat'd in benzene	0.054	trans 5.33	366	7 days	1.4	1	-
Michler's ketone	sat'd in benzene	0.054	trans 5.33	366	7 days	1.5	1	-
Blank	--	0.054	cis 5.59	366	9 days	11	10	1
Thioxanthone	sat'd in benzene	0.054	cis 5.59	366	9 days	3	1	-
Michler's ketone	sat'd in benzene	0.054	cis 5.59	366	9 days	1.8	1	-

[a]Sensitizer absorbed > 99% of light.

Table 14. Attempted sensitization of TME adduct formation

Sensitizer	[Sens][a]	[S_t]	[0]	λ nm	Irrad. time	cis	trans	adduct
Blank	--	0.06	0.74	366	6 hr	9.8	43	1
Thioxanthone	0.05	0.06	0.74	366	6 hr	1.1	1	-
Michler's ketone	0.08	0.06	0.74	366	6 hr	1.1	1	-
Michler's ketone	0.09	0.06	0.74	366	24 hr	1.4	1	-
Michler's ketone	0.09	0.06	0.74	366	33 hr	1.7	1	-

[a]Sensitizer absorbed 99% of light.

Quenching of trans-stilbene fluorescence by TME

Volumetrically prepared samples were transferred to quartz fluorescence cells. Fluorescence intensities were measured using exciting light of 310 nm wavelength. Spectragrade n-hexane was used as solvent. The results are presented in Table 15.

Table 15. Quenching of trans-stilbene fluorescence by TME[a]

[O]	$\Phi_f/\Phi_{f_{olefin}}$ [b]
1.09	1.44
2.95	1.76
4.32	2.13
8.27	2.86

[a] $[S_t] = 1 \times 10^{-5}$M, 27-30°.
[b] λ_{max} of emission 360 nm, no new emission peak appeared upon adding olfin.

Quantum yield of adduct formation as a function of TME concentration

Samples in Pyrex cells were irradiated in the wheel at 25° using 313 nm light of 40 nm bandwidth. trans-Stilbene, 0.054M, absorbed greater than 99% of the light. Analysis on column C gave the results shown in Table 16.

Quantum yield of TME adduct formation as a function of percent conversion

Samples in Pyrex tubes were irradiated in the linear apparatus at 25° using 313 nm light of 44 nm bandwidth. The olefin concentration

Table 16. Quantum yield of adduct formation as a function of TME concentration

[O]	1/[O]	Φ_{add}	$1/\Phi_{add}$
4.0	0.25	0.54	1.85
2.0	0.50	0.35	2.86
1.0	1.00	0.19	5.26
0.7	1.33	0.14	7.15
0.5	2.00	0.11	9.09

was 4.0M and trans-stilbene 0.054M. Analysis on column C gave the results shown in Table 17.

Table 17. Quantum yield of TME adduct formation as a function of percent conversion

% Conversion	Φ_{add}
0.85	0.49
2.31	0.62
4.42	0.55
9.20	0.54
19.80	0.54

Quantum yield of adduct formation and quantum yield of isomerization of trans-stilbene to cis-stilbene at 4 molar TME as a function of temperature

Samples in Pyrex cells were irradiated in the linear apparatus. Analysis on column C gave the results in Table 18.

Table 18. Quantum yield of adduct formation and quantum yield of isomerization of trans-stilbene to cis-stilbene at 4 molar TME as a function of temperature

Temperature	Φ_{add} relative	Φ_{add} [a]	Φ_{isom}
65	0.24	0.24	
55	0.30	0.30	0.27
45	0.38	0.38	0.23
35	0.44	0.44	
25	0.54	0.54	0.19
5	0.69	0.69	
5	0.46	0.69	0.19
-4	0.53	0.76	0.08
-10	0.51	0.74	
-10	0.58	0.81	
-13	0.58	0.81	
-18	0.57	0.80	0.05
-22	0.70	0.93	
-28	0.61	0.84	

[a] Quantum yields at low temperatures were adjusted by factor to equate the two 5° quantum yields obtained from the two different pieces of variable temperature apparatus. The cause of error may be due to condensation on the quartz window or clouding of the window itself from an oil film as in the case of the apparatus in Figure 52.

Quantum yield of adduct formation as a function of TME concentration at a series of temperatures

Samples in Pyrex cells were irradiated in the linear apparatus using the aluminum block temperature apparatus. Light of 313 nm with a 44 nm bandwidth was used. The trans-stilbene concentration in all samples was 0.054M. Analysis on column C gave the results in Table 19.

Table 19. Quantum yield of adduct formation as a function of TME concentration at a series of temperatures

[0]	1/[0]	Temperature	Φ_{add}	$1/\Phi_{add}$
4.10	0.24	5	0.69	1.45
2.10	0.48	5	0.46	2.18
0.70	1.43	5	0.20	5.00
4.04	0.25	34	0.40	2.50
1.97	0.50	34	0.28	3.57
0.71	1.43	34	0.10	10.00
4.02	0.25	44	0.37	2.70
2.09	0.48	44	0.24	4.17
0.60	1.67	44	0.082	12.20
4.02	0.25	54	0.32	3.13
2.09	0.48	54	0.21	4.76
0.60	1.67	54	0.066	15.00

Irradiation of trans-stilbene in the presence of 2-methyl-2-butene

trans-Stilbene (5.0 g, 0.028 mole) and 2-methyl-2-butene (25 g, 0.36 mole) in 150 ml n-hexane were irradiated in a Pyrex immersion well for 30 hours. The solvent was removed under reduced pressure to yield

a yellow oil. Gas chromatography revealed the absence of stilbene and presence of two partially overlapping new peaks in a 1:3 ratio. Preparative gas chromatography using column B afforded purification of the major adduct and a 1:1 mixture of the minor and major adducts. The infrared spectrum (Figure 12), nmr spectrum (Figure 13) and mass spectrum (Table 2) of the major adduct are consistent with the structure trans-1,2-diphenyl-cis-3-methyl-4,4-dimethylcyclobutane. The structure of the minor adduct was deduced to be the other geometric addition isomer trans-1,2-diphenyl-trans-3-methyl-4,4-dimethylcyclobutane on the basis of the infrared spectrum of the mixture (Figure 15), the nmr spectrum of the mixture (Figure 16), the nmr spectrum of the minor adduct (Figure 16) obtained by substracting the peaks of the major isomer from the nmr spectrum of the mixture, and from the mass spectrum of the mixture (Table 3).

Analysis: Major adduct: Calculated $C_{19}H_{22}$: C, 91.20; H, 8.80. Found: C, 91.21; H, 8.81. Mixture: Calculated $C_{19}H_{22}$: C, 91.20; H, 8.80. Found: C, 91.06; H, 8.84.

Irradiation of diphenylacetylene in the presence of 2-methyl-2-butene

Diphenylacetylene (4.0 g, 0.025 mole) and 2-methyl-2-butene (80 g, 1.14 mole) in a Pyrex vessel were irradiated for 48 hours. The solution had become a bright green by the end of the irradiation. The solvent was removed under reduced pressure to yield a greenish solid.

The solid was dissolved in a small volume of chloroform and chromatographed on an Alumina column, and 75 ml fractions were collected. The column was eluted with 2% ether-hexane. Fractions 32-55 contained 750 mg of a clear oil. The oil was identified as 1,2-diphenyl-3,4,4-trimethyl-1-cyclobutene from the infrared spectrum (Figure 15), nmr spectrum (Figure 16) and mass spectrum (Table 3).

Reduction of 1,2-diphenyl-3,4,4-trimethyl-1-cyclobutene

The cyclobutene was reduced by the method of Johnson (77) The cyclobutene (460 mg, 0.0046 mole) in 20 ml anhydrous ether was added to liquid ammonia to a total volume of 100 ml. Over a period of five minutes, potassium (600 mg, 0.015 mole) was added. The solution was stirred for 20 minutes after which the ammonia was allowed to evaporate. Ethanol, 10 ml, and anhydrous ether, 7 ml, were added over 20 minutes. The solution was then added to ice water-benzene. The water layer was extracted with benzene, and the combined benzene layers were dried over anhydrous magnesium sulfate and concentrated under reduced pressure to yield a clear oil. The oil was analyzed by gas chromatography using column B revealing three products. Two of the peaks overlapped partially and were collected. The nmr spectrum of the mixture (Figure 18) and retention times on column C were identical to that of the mixture of the two adducts from trans-stilbene and 2-methyl-2-butene. The third product was identified as a ring opened compound on the basis of the infrared spectrum, nmr spectrum and mass spectrum. No further work was done to characterize the ring open compound.

Irradiation of 2-methyl-2-butene photoadducts

A 1:1 mixture of the two photoadducts was obtained by gas chromatography using column B. Samples in Pyrex cells were irradiated in the linear apparatus at 25°. Light of 313 nm with a 44 nm bandwidth was used. Analysis using column D gave the results in Table 20.

Table 20. Irradiation of 2-methyl-2-butene photoadducts

[photoadducts]	$[S_t]$	product ratio before irrad.	product ratio after irrad.
0.009	--	1:1	1:1
0.009	0.054	1:1	1:1

Attempted sensitization of 2-methyl-2-butene adduct formation

Samples in Pyrex cells were irradiated in the linear apparatus at 25°. Light of 313 nm with a 44 nm bandwidth was used. Analysis using column D gave the results in Table 21.

Table 21. Attempted sensitization of 2-methyl-2-butene adduct formation

Sensitizer	[Sens][a]	$[S_t]$	[0]	λ nm	Irrad. time	cis	trans	adduct
Blank	--	0.054	4.0	366	14 hr	3.6	4.4	1
Michler's ketone	sat'd in benzene	0.054	4.0	366	12 hr	1.7	1	--
Thioxanthone	sat'd in benzene	0.054	4.0	366	18 hr	1.3	1	--

[a]Sensitizer absorbed > 99% of light.

Quenching of trans-stilbene fluorescence by 2-methyl-2-butene

Volumetrically prepared samples were transferred to the fluorescence cells. The emission was measured using 310 nm exciting light. The results are given in Table 22.

Table 22. Quenching of trans-stilbene fluorescence by 2-methyl-2-butene[a]

[O]	$\Phi_f/\Phi_{f_{olefin}}$ [b]
0.62	1.01
2.31	1.18
3.92	1.26
6.24	1.47

[a] $[S_t] = 1 \times 10^{-5}$M, 27-30°.

[b] λ_{max} of emission 360 nm, no new emission peak appeared upon adding the olefin.

Quantum yield of formation of 2-methyl-2-butene adducts as a function of olefin concentration

Samples in Pyrex cells were irradiated in the linear apparatus at 25°. Light of 313 nm with 44 nm bandwidth was used. The stilbene concentration was 0.054M. Analysis using column D gave the results in Table 23.

Quantum yield of formation of 2-methyl-2-butene adducts at 4 molar olefin concentration as a function of percent conversion

Samples in Pyrex cells were irradiated in the linear apparatus at

Table 23. Quantum yield of formation of 2-methyl-2-butene adducts as a function of olefin concentration

[O]	1/[O]	Φ_{add} minor	Φ_{add} major	$1/\Phi_{add}$ minor	$1/\Phi_{add}$ major
4.0	0.25	0.025	0.075	40.0	13.4
2.5	0.40	0.015	0.040	66.7	25.0
1.7	0.59	0.010	0.028	100	35.7
1.0	1.00	0.0064	0.015	157	66.7
0.64	1.56	0.0042	0.010	238	100
0.38	2.63	0.0020	0.0049	500	204

25°. Light of 313 nm with 44 nm bandwidth was used. trans-Stilbene concentration was 0.054M. Analysis using column D gave the results in Table 24.

Table 24. Quantum yield of formation of 2-methyl-2-butene adducts at 4 molar olefin concentration as a function of percent conversion

% conversion[a]	Φ_{add} minor	Φ_{add} major
1.2		0.077
3.5		0.076
4.9	0.025	0.078
12.3	0.025	0.075

[a]Based on total adduct formation.

Quantum yield of formation of 2-methyl-2-butene adducts at 4 molar olefin concentration as a function of temperature

Samples in Pyrex cells were irradiated in the linear apparatus. Light of 313 nm with 44 nm bandwidth was used. trans-Stilbene concentration was 0.054M. Analysis using column D gave the results in Table 25.

Table 25. Quantum yield of formation of 2-methyl-2-butene adducts at 4 molar olefin concentration as a function of temperature

Temperature[a]	Φ_{add} minor	Φ_{add} major
54	0.017	0.037
44	0.018	0.046
34	0.021	0.061
24	0.026	0.074
8	0.038	0.097
-4	0.044	0.12
-11	0.051	0.14
-22	0.057	0.16

[a]Duplicate determinations.

Irradiation of trans-stilbene in the presence of 1-methylcyclohexene

trans-Stilbene (3.0 g, 0.016 mole) and 1-methylcyclohexene (60 g, 0.62 mole) in 150 ml n-hexane were irradiated in a Pyrex immersion well for 27 hours. The solvent was removed under recuced

pressure to yield a yellow oil. The nmr spectrum of the oil showed no stilbene present. Preparative gas chromatography using column A afforded separation of a clear oil. The oil was identified as 1-methyl-7-endo-8-exo-diphenyl-cis-bicyclo [4.2.0] octane from the infrared spectrum (Figure 20), nmr spectrum (Figure 21) and mass spectrum (Table 4).

Analysis: Calcd. for $C_{21}H_{24}$: C, 91.30; H, 8.70. Found: C, 91.25; H, 8.53.

Attempted sensitization of 1-methylcyclohexene adduct formation

Samples in Pyrex cells were irradiated in the linear apparatus at 25°. Analysis using column C gave the results in Table 26.

Quenching of trans-stilbene fluorescence by 1-methylcyclohexene

Volumetrically prepared samples were transferred to the fluorescence cells. The emission was measured using 310 nm exciting light. The results are given in Table 27.

Quantum yield of formation of 1-methylcyclohexene adduct as a function of olefin concentration

Samples in Pyrex cells were irradiated in the wheel at 26°. Light of 313 nm with 40 nm bandwidth was used. trans-Stilbene concentration was 0.054M. Analysis using column C gave the results in Table 28.

Table 26. Attempted sensitization of 1-methylcyclohexene adduct formation

Sensitizer	[Sens][a]	[S_t]	[0]	λ nm	irrad. time	cis	trans	adduct
Blank	--	0.054	4.0	366	24 hr	3.2	4.6	1
Thioxanthone	Sat'd in benzene	0.054	4.0	366	24 hr	34	24	1
Michler's ketone	Sat'd in benzene	0.054	4.0	366	36 hr	1.8	1	-

[a]Sensitizer absorbed > 99% of light.

Table 27. Quenching of trans-stilbene fluorescence by 1-methylcyclohexene[a]

[O]	$\Phi_f/\Phi_{f_{olefin}}$[b]
0.31	1.10
1.21	1.16
1.53	1.14
2.19	1.25
3.16	1.30

[a] $[S_t] = 1 \times 10^{-5}$M, 27-30°.

[b] λ_{max} of emission was 360 nm, no new emission peak appeared on increasing olefin concentration.

Table 28. Quantum yield of formation of 1-methylcyclohexene adduct as a function of olefin concentration

[O]	1/[O]	Φ_{add}	$1/\Phi_{add}$
5.08	0.19	0.057	17.6
3.48	0.29	0.038	26.3
2.02	0.50	0.022	45.5
1.12	0.89	0.013	77.0
0.91	1.10	0.0096	104
0.63	1.59	0.0069	145

Quantum yield of formation of 1-methylcyclohexene adduct at 4 molar olefin concentration as a function of percent conversion

Samples in Pyrex cells were irradiated in the linear apparatus at 25°. Light of 313 nm with 44 nm bandwidth was used. trans-Stilbene concentration was 0.054M. Analysis using column C gave the results in Table 29.

Table 29. Quantum yield of formation of 1-methylcyclohexene adduct at 4 molar olefin concentration as a function of percent conversion

% conversion	Φ_{add}
1.5	0.063
3.2	0.049
6.5	0.053
10.6	0.048

Quantum yield of formation of 1-methylcyclohexene adduct at 4 molar olefin concentration as a function of temperature

Samples in Pyrex cells were irradiated in the linear apparatus. Light of 313 nm with 44 nm bandwidth was used. trans-Stilbene concentration was 0.054M. Analysis using column C gave the results in Table 30.

Table 30. Quantum yield of formation of 1-methylcyclohexene adduct at 4 molar olefin concentration as a function of temperature

Temperature[a]	Φ_{add}
65	0.018
56	0.025
43	0.029
34	0.036
25	0.043
15	0.064
6	0.090
-5	0.097
-21	0.12
-28	0.14

[a]Duplicate determinations.

Quantum yield of formation of 1-methylcyclohexene adduct as a function of olefin concentration at 45°

Samples in Pyrex cells were irradiated in the linear apparatus at 45°. Light of 313 nm with 44 nm bandwidth was used. trans-Stilbene concentration was 0.054M. Analysis using column C gave the results in Table 31.

Irradiation of trans-stilbene in the presence of cyclohexene

trans-Stilbene (3.0 g, 0.017 mole) and cyclohexene (60 g, 0.72

Table 31. Quantum yield of formation of 1-methylcyclohexene adduct as a function of olefin concentration at 45°

[O]	1/[O]	Φ_{add}	$1/\Phi_{add}$
4.0	0.25	0.029	33.5
2.0	0.50	0.016	62.5
1.0	1.00	0.011	91.0

mole) were irradiated in a Pyrex immersion well for 14 days. The solvent was removed under reduced pressure yielding a yellow oil. Preparative gas chromatography using column B afforded separation of a clear oil. The oil was identified as 7-endo-8-exo-diphenyl-cis-bicyclo[4.2.0]octane from the infrared spectrum (Figure 20), nmr spectrum (Figure 21) and mass spectrum (Table 4).

Analysis: Calcd. for $C_{20}H_{22}$: C, 91.60; H, 8.40. Found: C, 91.45; H, 8.32.

Attempted sensitization of cyclohexene adduct formation

Samples in Pyrex cells were irradiated in the wheel at 25°. Analysis using column C gave the results in Table 32.

Quantum yield of formation of cyclohexene adduct as a function of olefin concentration

Samples in Pyrex cells were irradiated in the linear apparatus at 25°. Light of 313 nm with 44 nm bandwidth was used. trans-Stilbene

Table 32. Attempted sensitization of cyclohexene adduct formation

Sensitizer	[Sens] [a]	[S_t]	[0]	λ nm	Irrad. time	cis	trans	adduct
Blank	-	0.054	4.0	366	10 days	13	9	1
Thioxanthone	sat'd in benzene	0.054	4.0	366	10 days	88	16	1
Michler's ketone	sat'd in benzene	0.054	4.0	366	10 days	65	25	1

[a]Sensitizer absorbed > 99% of light.

concentration was 0.054M. Analysis using column C gave the results in Table 33.

Table 33. Quantum yield of formation of cyclohexene adduct as a function of olefin concentration

[O]	1/[O]	Φ_{add}	$1/\Phi_{add}$
5.99	0.17	0.0083	121
3.91	0.25	0.0039	257
1.88	0.53	0.0024	416
0.95	1.05	0.0013	770

Quantum yield of formation of cyclohexene adduct at 4 molar olefin concentration as a function of temperature

Samples in Pyrex cells were irradiated in the linear apparatus using the aluminum block temperature apparatus. Light of 313 nm with 44 nm bandwidth was used. trans-Stilbene concentration was 0.054M. Analysis using column C gave the results in Table 34.

Table 34. Quantum yield of formation of cyclohexene adduct at 4 molar olefin concentration as a function of temperature

Temperature	Φ_{add}
44	0.0029
33	0.0033
16	0.0044

Irradiation of trans-stilbene in the presence of 1,2-dimethylcyclohexene

trans-Stilbene (3.0 g, 0.017 mole) and 1,2-dimethylcyclohexene (10 g, 0.091 mole) in 150 ml n-hexane were irradiated in a Pyrex immersion well for 18 hours. The solvent was removed under reduced pressure yielding a yellow waxy-solid. Preparative gas chromatography using column A afforded a slightly yellow solid. The solid was identified as cis-1,6-dimethyl-7-endo-8-exo diphenyl-cis-bicyclo-[4.2.0]octane from the infrared spectrum (Figure 17), nmr spectrum (Figure 18) and mass spectrum (Table 3).

Analysis: Calcd. for $C_{22}H_{26}$; C, 91.03; H, 8.97. Found: C, 90.89; H, 8.99.

Irradiation of trans-stilbene in the presence of 1,2-dimethylcyclopentene

trans-Stilbene (3.0 g, 0.017 mole) and 1,2-dimethylcyclopentene (10 g, 0.11 mole) in a Pyrex tube were irradiated in a Rayonet Photochemical Reactor, using 300 nm lamps, for 7 days. The solution was concentrated under reduced pressure to yield a yellow waxy-solid. Preparative gas chromatography, using column A, yielded a white waxy solid. The solid was identified as cis-1,5-methyl-6-endo-7-exo-diphenyl-cis-bicyclo [3.2.0] heptane from the infrared spectrum (Figure 17) nmr spectrum (Figure 18) and mass spectrum (Table 4).

Analysis: Calcd. for $C_{20}H_{22}$; C, 91.60; H, 8.40. Found: C, 91.45; H, 8.34.

Irradiation of trans-stilbene in the presence of cyclopentene

trans-Stilbene (3.0 g, 0.017 mole) and cyclopentene (25 g, 0.37 mole) in 100 ml n-hexane were irradiated in a Pyrex immersion well for 72 hours. The solution was concentrated under reduced pressure yielding a yellow oil. Preparative gas chromatography, using column A, yielded a clear oil. The oil was identified as 6-endo-7-exo-diphenyl-cis-bicyclo [3.2.0] heptane from the infrared spectrum (Figure 46), nmr spectrum (Figure 47) and mass spectrum (Table 8).

Analysis: Calcd. for $C_{19}H_{20}$: C, 91.94; H, 8.08. Found: C, 91.76; H, 7.86.

Irradiation of trans-stilbene in the presence of cycloheptene

trans-Stilbene (3.0 g, 0.017 mole) in cycloheptene (100 g, 1.05 mole) was irradiated in a Pyrex immersion well for 14 days. The cycloheptene was removed under reduced pressure to yield a yellow waxy-solid, which was shown by nmr to be mainly stilbene. Preparative gas chromatography, using column A, yielded a yellow oil. The oil was identified as 8-endo-9-exo-diphenyl-cis-bicyclo [5.2.0] nonane by the infrared spectrum (Figure 46), nmr spectrum (Figure 47) and mass spectrum (Table 8).

High resolution mass spectrum, in lieu of microanalysis

Theoretical for $C_{21}H_{24}$: 276.1877904 (M^+). Found: 276.191014 (M^+).

Quantum yield of formation of various adducts at 4 molar olefin concentration

Samples in Pyrex cells were irradiated in the linear apparatus at 25°. Light of 313 nm with 44nm bandwidth was used. trans-Stilbene concentration was 0.054M. Analysis using column C gave the results in Table 35.

Table 35. Quantum yield of formation of various adducts at 4 molar olefin concentration

Olefin	Φ_{add}
trans-2-butene	0.009 (5.59M)
cis-2-butene	0.002 (5.33M)
1,2-dimethyl-cyclohexene	0.17
1,2-dimethyl-cyclopentene	0.33
1-methyl-cyclopentene	0.11
cyclopentene	0.0075
cycloheptene	0.0006

Photocycloaddition of cis-Stilbene to TME

Quantum yield of TME adduct formation from cis-stilbene and quantum yield of isomerization as a function of olefin concentration

Samples in quartz cells were irradiated in the linear apparatus at 25°. Light of 254 nm with a 44 nm bandwidth was used. cis-Stilbene concentration was 0.054M. Analysis on column C gave the results in Table 36.

Table 36. Quantum yield of TME adduct formation from cis-stilbene and quantum yield of isomerization as a function of olefin concentration

[O]	1/[O]	% t-stilbene at completion	$\Phi_{add_{total}}$	$\Phi_{add_{corr}}$ [a]	$1/\Phi_{add_{corr}}$	Φ_{isom}
5.30	0.19	3.30	0.054	0.047	21.3	0.30
4.10	0.24	4.90	0.054	0.044	22.7	0.29
2.90	0.35	5.60	0.051	0.042	24.8	0.31
2.50	0.40	5.63	0.036	0.028	35.7	
2.00	0.50	5.94	0.031	0.024	41.7	0.32

[a] $\Phi_{add_{corr}}$ was obtained by substracting from $\Phi_{add_{total}}$ the amount corresponding to the adduct which was produced by the average amount of trans-stilbene present from the known quantum yields of trans-stilbene at the conditions of the experiment.

Quantum yield of TME adduct from cis-stilbene at 4 molar olefin as a function of temperature

Samples in quartz cells were irradiated in the linear apparatus using the aluminum temperature apparatus. Light of 254 nm with a bandwidth of 44 nm was used. cis-Stilbene concentration was 0.054M. Analysis on column C gave the results in Table 37.

Table 37. Quantum yield of TME adduct formation from cis-stilbene at 4 molar olefin as a function of temperature

Temperature[a]	% t-stilbene at completion	$\Phi_{add_{total}}$	$\Phi_{add_{corr}}$
55	4.90	0.022	0.015
39	4.00	0.035	0.028
25	4.90	0.054	0.044
11	3.20	0.056	0.049

[a]Duplicate determinations.

Attempted sensitization of TME adduct formation from cis-stilbene

Samples in quartz cells were irradiated in the linear apparatus at 25°. Analysis on column C gave the results in Table 38.

Table 38. Attempted sensitization of TME adduct formation from cis-stilbene

Sensitizer	[Sens] [a]	[S_0]	[O]	λ nm	Irrad. time	cis	trans	adduct
Blank		0.054	4.0	366	24 hr	.85	.70	1
Thioxanthone	Sat'd in benzene	0.054	4.0	366	25 hr	.85	.46	1
Thioxanthone	0.002	0.054	4.0	366	23 hr	1.5	1.1	1
Michler's ketone	Sat'd in benzene	0.054	4.0	366	36 hr	1.5	1.1	-

[a]Sensitizer absorbed >99% of light.

SUMMARY

The photocyloaddition of trans-stilbene with various olefins has been shown to proceed with retention of stereochemistry with respect to stilbene and the ground state partner, as can be seen from the

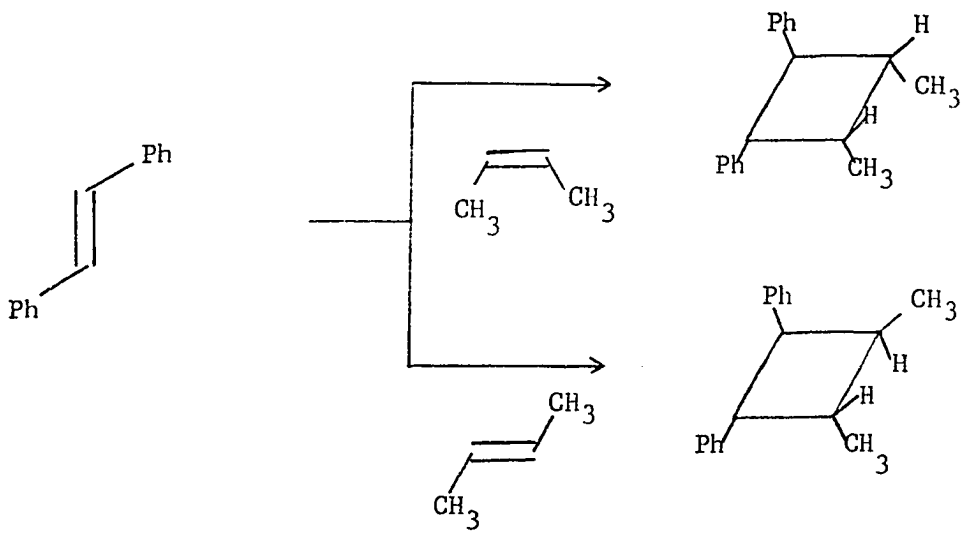

addition products from cis and trans-2-butene. The addition was shown to involve initial formation of an exciplex, which partitions between

$$^1S_t + 0 \xrightarrow{k_e} \text{Exciplex}$$

$$\text{Exciplex} \xrightarrow{k_{-e}} {}^1S_t + 0$$

$$\text{Exciplex} \xrightarrow{k_a} \text{Adduct}$$

adduct formation and dissociation to singlet trans-stilbene and ground state olefin. The exciplex was shown to be formed at a rate close to diffusion controlled.

The inefficiency of the addition is attributed to a high value of k_{-e} relative to k_a. The addition was shown to be dependent on

alkyl substitution, efficiency decreasing with decreasing substitution, TME>2-methyl-2-butene>cis or trans-2-butene. The same trend is observed upon increasing ring size, cyclopentene>cyclohexene>cycloheptene.

BIBLIOGRAPHY

1. P. deMayo, Accounts Chem. Res., in print

2. N. C. Yang, M. Nussim, M. J. Jorgenson and S. Murov, Tetrahedron Lett., 3657 (1964)

3. N. C. Yang, Pure Appl. Chem., 9, 591 (1964)

4. N. J. Turro, P. Wriede, J. C. Dalton, D. Arnold and A. Glick, J. Amer. Chem. Soc., 89, 3950 (1967)

5. N. J. Turro, P. Wriede and J. C. Dalton, J. Amer. Chem. Soc., 90, 3274 (1968)

6. J. C. Dalton, P. Wriede and N. J. Turro, J. Amer. Chem. Soc., 92, 1318 (1970)

7. E. J. Corey, J. D. Buss, R. LeMahieu and R. B. Mitra, J. Amer. Chem. Soc., 86, 5570 (1964)

8. P. Robson, P. W. Grubb and J. A. Barltrop, J. Chem. Soc., (London), 2153 (1964)

9. P. deMayo, Pure Appl. Chem., 9, 597 (1964)

10. H. Yamazaki and R. J. Cvetanovic, J. Amer. Chem. Soc., 91, 520 (1969)

11. R. S. H. Liu, N. J. Turro and G. S. Hammond, J. Amer. Chem. Soc., 87, 3406 (1965)

12. G. N. Lewis, T. T. Magel and D. Lipkin, J. Amer. Chem. Soc., 62, 2973 (1940)

13. H. Skinner, Modern Aspects of Thermochemistry, Royal Institute of Chemistry Lecture, 3, 1958

14. R. H. Dyck and D. S. McClure, J. Chem. Phys., 36, 2326 (1962)

15. D. F. Evans, J. Chem. Soc. (London), 1351 (1957)

16. W. G. Herkstroeter and D. S. McClure, J. Amer. Chem. Soc., 90, 4522 (1968)

17. H. Suziki, Bull. Chem. Soc. Japan, 33, 381 (1960)

18. D. L. Beveridge and H. H. Jaffe, J. Amer. Chem. Soc., 87, 5340 (1965)

19. C. A. Coulson, Steric effects in conjugated systems, London, England, Butterworth, 1958, p 56.

20. P. Borrell and H. H. Greenwood, Proc. Roy. Soc. (London), A298, 453 (1967)

21. G. S. Hammond, et al, J. Amer. Chem. Soc., 86, 3197 (1964)

22. S. Malkin and E. Fischer, J. Phys. Chem., 68, 1153 (1964)

23. R. Searle, J. L. R. Williams, D. E. DeMeyer and J. C. Doty, Chem. Comm., 1165 (1967)

24. R. S. H. Liu, J. Amer. Chem. Soc., 90, 1899 (1968)

25. G. S. Hammond and J. Saltiel, J. Amer. Chem. Soc., 84, 4983 (1962)

26. J. Saltiel, J. Amer. Chem. Soc., 90, 6394 (1968)

27. K. A. Muszkat, D. Gegiou and E. Fischer, J. Amer. Chem. Soc., 89, 4814 (1967)

28. D. Gegiou, K. A. Muszkat and E. Fischer, J. Amer. Chem. Soc., 90, 3907 (1968)

29. D. Gegiou, K. A. Muszkat and E. Fischer, J. Amer. Chem. Soc., 90, 12 (1968)

30. J. Saltiel, E. D. Megarity and K. G. Knupp, J. Amer. Chem. Soc., 88, 2336 (1966)

31. J. Saltiel, J. Amer. Chem. Soc., 89, 1036 (1967)

32. J. Saltiel and E. D. Megarity, J. Amer. Chem. Soc., 91, 1265 (1969)

33. C. O. Parker and P. E. Spoerri, Nature, 166, 603 (1950)

34. F. B. Mallory, C. S. Wood, J. T. Gordon, L. C. Lindquist and M. L. Savitz, J. Amer. Chem. Soc., 84, 4361 (1962)

35. K. A. Muszkat and E. Fischer, J. Chem. Soc. (London), B, 662 (1967)

36. H. Shecter, W. J. Link and G. V. D. Tiers, J. Amer. Chem. Soc., 85, 1601 (1963)

37. M. Pailer and J. Muller, Monatsh., 79, 615 (1948)

38. H. M. Rosenberg, R. Rondeau and R. Serve, J. Org. Chem., 34, 471 (1969)

39. S. Farid, Chem. Comm., 1268 (1967)

40. D. Bryce-Smith and A. Gilbert, Chem. Comm., 1318 (1968)

41. D. Bryce-Smith and A. Gilbert, Chem. Comm., 1319 (1968)

42. V. L. Levschen, Acta Physiochem., 1, 685 (1935)

43. B. Stevens and E. Hutton, Nature (London), 186, 1045 (1960)

44. Th. Forster, Angew. Chem. Int. Ed., Engl., 8, 333 (1969)

45. Th. Forster and K. Kasper, Z. Elektrochem., Ber. Bunsenges. Physik. Chem., 59, 776 (1955)

46. J. B. Birks and L. G. Christophorou, Proc. Roy. Soc. (London), A274, 552 (1963)

47. E. Doller and Th. Forster, Z. Physik. Chem., N. F., 31, 274 (1962)

48. T. V. Ivanova, G. A. Mohuva and B. Y. Sveshehov, Optics and Spectroscopy, 12, 325 (1962)

49. A. K. Chandra and E. C. Lim, J. Chem. Phys., 48, 2589 (1968)

50. J. B. Birks and L. G. Christophorou, Nature (London), 196 33 (1962)

51. J. B. Birks, D. J. Dyson and I. H. Munro, Proc. Roy. Soc., (London), A275, 575 (1963)

52. E. A. Chandross and J. Ferguson, J. Chem. Phys., 47, 2557 (1967)

53. N. Matago, K. Ezumi and T. Okada, Mol. Phys., 10, 201 (1966)

54. Th. Forster and K. Kasper, Z. Physik. Chem., N. F., 1, 275 (1954)

55. G. Castro and R. M. Hochstrasser, J. Chem. Phys., 45, 4352 (1966)

56. E. C. Lim and S. K. Chakrabarti, Mol. Phys., 13, 293 (1967)

57. S. K. Chakrabarti, Mol. Phys., 16, 417 (1969)

58. O. L. Chapman and G. L. Wampfler, J. Amer. Chem. Soc., 91, 5390 (1969)

59. P. J. Wagner and D. J. Bucheck, J. Amer. Chem. Soc., 90, 6530 (1968)

60. C. DeBoer, J. Amer. Chem. Soc., 91, 1855 (1969)

61. P. J. Wagner and D. J. Bucheck, Can. J. Chem., 47, 713 (1969)

62. A. K. Chandra and E. C. Lim, J. Chem. Phys., 49, 5066 (1968)

63. S. L. Murov, R. S. Cole and G. S. Hammond, J. Amer. Chem. Soc., 90, 2957 (1968)

64. G. O. Schenk and R. Steinmetz, Bull. Soc. Chim. Belges, 71, 781 (1962)

65. L. A. Singer and G. A. Davis, J. Amer. Chem. Soc., 89, 598 (1967)

66. L. A. Singer and G. A. Davis, J. Amer. Chem. Soc., 89, 158 (1967)

67. L. A. Singer, G. A. Davis and V. P. Muralidharan, J. Amer. Chem. Soc., 91, 897 (1969)

68. R. O. Loutfy, P. deMayo and M. F. Tchir, J. Amer. Chem. Soc., 91, 3984 (1969)

69. R. J. McDonald and B. K. Selinger, Tetrahedron Lett. 4791 (1968)

70. L. M. Stephenson, D. G. Whitten, G. F. Vesley and G. S. Hammond, J. Amer. Chem. Soc., 88, 3665 (1966)

71. R. S. Cooke and G. S. Hammond, J. Amer. Chem. Soc., 90 2958 (1968)

72. O. L. Chapman and W. R. Adams, J. Amer. Chem. Soc., 90, 2333 (1968)

73. R. M. Dodson and A. G. Zielski, J. Org. Chem., 32, 28 (1967)

74. D. Y. Curtin, H. Gruen and B. A. Shoulders, Chem. and Ind., 1205 (1968)

75. I. Fleming and D. H. Williams, Tetrahedron, 23, 2747 (1967)

76. W. G. Brown and R. L. Markezick, Abst. 153rd A. C. S. Meeting, Miami, Fla., April 1967, p 139.

77. W. Johnson, A. D. Kemp, R. Pappo, T. Ackerman and W. F. Jones, J. Amer. Chem. Soc., 78, 6312 (1956)

78. R. B. Woodward and R. Hoffman, Angew. Chem. Intern. Ed. Engl., 8, 781 (1969)

79. L. Salem, J. Amer. Chem. Soc., 90, 553 (1968)

80. A. A. Lamola and G. S. Hammond, J. Chem. Phys., 43, 2129 (1965)

81. R. Wilson, J. Chem. Soc. (London), B, 1581 (1968)

82. R. S. H. Liu and J. R. Edman, J. Amer. Chem. Soc., 90, 213 (1968)

83. R. S. H. Liu and D. M. Gale, J. Amer. Chem. Soc., 90, 1897 (1968)

84. N. C. Yang and R. L. Loeschen, Tetrahedron Lett. 2571 (1968)

85. W. J. Potts, Jr., J. Chem. Phys., 23, 65 (1955)

86. J. B. Birks and W. A. Little, Proc. Phys. Soc., 66, 921 (1953)

87. S. H. Liebson, M. E. Bishop and J. O. Elliot, Phys. Rev., 80, 907 (1950)

88. H. Kallman and G. J. Brucker, Phys. Rev., 108, 1122 (1957)

89. J. O. Elliot, S. H. Liebson and C. F. Raviloius, Phys. Rev., 79, 393 (1950)

90. J. B. Birks, T. A. King and I. H. Munro, Proc. Phys. Soc., 80, 355 (1962)

91. T. D. S. Hamilton, Proc. Phys. Soc., 78, 743 (1961)

92. V. R. Priimachek and A. N. Faidysh, Izv. Vyssh. Ucheb. Zaved. Fiz., 10, 32 (1967); Original not available; abstracted in Chemical Abstracts 68:73790 w (1968)

93. S. Arrhenius, Z. Physik. Chem., 1, 110 (1887)

94. J. Saltiel, J. D'Agostino, O. L. Chapman and R. Lura, to be submitted to J. Amer. Chem. Soc., ca 1971.

95. Zvi Rappoport, J. Chem. Soc., 4498 (1963)

96. D. Bryce-Smith and A. Gilbert, Chem. Comm., 19 (1968)

97. P. Debye, Trans. Electrochem. Soc., 82, 265 (1942)

98. H. Yada, J. Tanaka and S. Nagakura, Bull. Chem. Soc. Japan, 33, 1660 (1960)

99. F. G. Moses, R. S. H. Liu and B. M. Monroe, Mol. Photochem., 1, 245 (1969)

100. G. L. Wamfler, Photochemical studies of some 2-cyclohexenones, Unpublished Ph.D. thesis, Library, Iowa State University, Ames, Iowa, 1970.

101. J. G. Calvert and J. N. Pitts, Jr., Photochemistry, J. Wiley and Sons, New York, New York, 1967, Pp 732.

102. C. G. Hatchard and C. A. Parker, Proc. Roy. Soc., A235, 518 (1956)

ACKNOWLEDGMENTS

The author wishes to thank his wife and parents for their encouragement and understanding in the pre and post-ulcerous days of his education. The author expresses special thanks to his wife for conspicuous unselfishness in the three o'clock feedings of certain Dry Ice cooled reactions. Also special thanks are due the author's sister for finding him a job.

The author expresses his gratitude and appreciation to Professor O. L. Chapman for the advice, guidance and encouragement given him during his course of graduate study and allowing the premature departure from Iowa State to accept the previously mentioned job.

Financial support from the National Defense Education Act Title IV Fellowship is gratefully acknowledged.

A publication originating in part from the research presented here is:

O. L. Chapman and R. D. Lura, J. Amer. Chem. Soc., 92 6352 (1970)